DETERMINATION OF INTERACTION CURVES FOR

THE STABILITY OF A THREE DEGREE OF FREEDOM,

SHALLOW ARCH MODEL UNDER MULTIPLE DYNAMIC LOADS

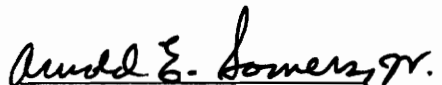by

Jay M. Fitzgerald

Thesis submitted to the Graduate Faculty of the

Virginia Polytechnic Institute and State University

in partial fulfillment for the degree of

MASTER OF SCIENCE

in

Civil Engineering

APPROVED:

R. H. Plaut, Chairman

S. M. Holzer

A. E. Somers, Jr.

August, 1978

Blacksburg, Virginia

ACKNOWLEDGMENTS

TABLE OF CONTENTS

iv

LIST OF FIGURES

LIST OF TABLES

NOTATION

[A]   3x3 matrix that depends on the θ's only; replace the θ's by α's for Eqs. 3.41 thru 3.45 only

B_i damping coefficients, i = 1, 2, 3

[B]   inverse of the [A] matrix

c   number of constraint equations or conditions

C_i rotational spring coefficients, i = 1, 2, 3

d_i see Eqs. 4.4 and 4.8

{D}   3x1 vector that depends on the θ's, the $\dot{\theta}$'s, and the P's

[DD]   3x3 "stiffness" matrix

F   Rayleigh's dissipation function

$\vec{F}_j$ force vectors of the system

I_i mass moment of interia of the ith member about its centroid

K   translational spring coefficient

L   Lagrangian of the system

L_i length of the ith member

m_i mass of the ith member

n   number of degrees of freedom of the system

N   number of rigid bars in the system

P_i applied loads, i = 1, 2, 3

$\hat{P}_i$ impulse loads, i = 1, 2, 3

q_i generalized coordinates of the system

$\dot{q}_k$ first time derivatives of the generalized coordinates q_k of the system

$\ddot{q}_k$ second time derivatives of the generalized coordinates q_k of the system

q_{i+1} a generalized coordinate at the i+1 time step

$\dot{q}_{i+1}$ first time derivative of q_{i+1}

$\ddot{q}_{i+1}$ second time derivative of q_{i+1}

$\ddot{q}$ see Eq. 4.9

Q_k generalized forces of the system

$\vec{r}_j$ position vectors corresponding to the force vectors $\vec{F}_j$ of the system

R function not dependent on $\ddot{q}$ (see Eq. 4.9)

R_{i+1} R at the i+1 time step (see Eq. 4.10)

$\{R\}$ 3x1 vector (see Eq. 4.13)

Δt magnitude of the time step for the numerical integration procedure

t time

T kinetic energy of the system; period of vibration for Eq. 4.14 only

T_i kinetic energy of the ith member; i^{th} period, i = 1, 2, 3, for Eqs. 3.49, 3.50, 3.51, and 3.52 only

v_i velocity of the mass center (centroid) of the ith member; see Eqs. 4.3 and 4.7 for different definition used in Chapter 4 only

V potential energy of the system

x horizontal position of any point along the bar

y vertical position of any point along the bar

α_i initial angle of the ith bar (radians)

β see Eqs. 4.2 and 4.4

x

ϵ	error tolerance (see Eq. 4.10)
θ	angle of the bar with the horizontal
θ_i	angle (radians) of the ith bar with the horizontal at any time t
$\dot{\theta}_i$	first time derivative of θ_i
$\ddot{\theta}_i$	second time derivative of θ_i
$\{\ddot{\theta}\}$	3x1 "acceleration" vector
ϕ_i	time dependent change in the angle's value from its initial value α_i
$\dot{\phi}_i$	first derivative of ϕ_i
$\ddot{\phi}_i$	second time derivative of ϕ_i
$\{\phi\}$	3x1 "displacement" vector
$\{\ddot{\phi}\}$	3x1 "acceleration" vector
ω_i	angular velocity of the ith member for Eq. 3.23 only; i^{th} natural frequency, i = 1, 2, 3

CHAPTER 1

INTRODUCTION

This chapter contains the purpose and scope of this study. Also contained is a review of the current literature regarding the dynamic stability and buckling of arches.

1.1 Purpose and Scope

The primary purpose of this study is to determine stability boundaries (interaction curves) for a three degree of freedom, shallow arch model under multiple dynamic loads. The loads are either all step loads, or all impulse loads.

To accomplish the purpose of this study, first the arch model is described. Then, the model's equations of motion are derived from Lagrange's equations of motion. Finally, the stability boundaries are shown as plots of the "failure" or buckling loads (non-dimensional). These loads are determined by comparing the results from the numerical integration of the model's non-dimensional nonlinear equations of motion to the buckling criteria used in this study. If the results exceed the buckling criteria, then the arch has "buckled" and the loads which produce those results are the "failure" or buckling loads.

1.2 Literature Review: Dynamic Stability and Buckling of Arches

A brief review of the current literature regarding the dynamic stability and buckling of arches is presented.

a. Stability Criteria

The dynamic stability of arches, with a search for practical and useful stability criteria, has been studied by many authors. One of the first studies was conducted by Hoff and Bruce [8], regarding laterally loaded flat arches. They presented a failure or buckling criterion based on the plot of the potential energy of the arch. Their criterion states that failure or buckling can occur only if the energy applied to the arch is sufficient to cause the motion of the arch on the energy plot to follow the "path of steepest decent," which takes the arch from a valley (stable equilibrium position), over a ridge, through a saddle point, to another valley. Their study includes results from both step and impulse loading. Next, Budiansky and Roth [4], in their study of clamped shallow spherical shells, presented a stability criterion based on a response parameter, which is defined as the "ratio of the average downward deflection to the average value of the initial shell height." Their criterion states that, for step loads applied to "shell geometries for which axisymmetric, rather than unsymmetric, deformations control the buckling phenomenon," a "jump" in the response parameter occurs at the buckling load for a small increase in the load. This "qualitative criterion ... has a physically significant basis, and analogous criteria, based on the rapid change of response with loading parameters, may be useful in other dynamic buckling problems." Finally, Hsu [11], in his study of elastic bodies with prescribed initial conditions subjected to impulsive loading, presented a rigorous

definition of dynamic stability, the necessary and sufficient stability criteria, and a more practical sufficiency condition for stability. These concepts and criteria are based on the total energy of the initial state of the elastic bodies, and the total energy of the stable equilibrium positions of the elastic bodies. They are discussed in terms of trajectories in a functional phase space (continuous system) or a phase space of finite dimension (discrete system). These concepts are similar to the Hoff and Bruce [8] criterion, but they are more general and rigorously derived. And, if care is taken, the Budiansky and Roth [4] criterion can be obtained from the above criteria. Also, the practical sufficiency condition for stability, as presented in the study, represents a lower bound for the determination of the failure or buckling loads.

Using the above articles as a basis, many authors proceeded to determine stability criteria for specific problems. Hsu [12] studied the effects of the amplitudes of the higher harmonics in the arch shape, the initial thrust, and the stiffness of the elastic supports at the arch ends on the dynamic stability of shallow arches against snap-through when subjected to impulsive loads. The results were "expressed in terms of sufficiency regions of stability in a phase space of infinite dimensions, which, in turn, lead to simple and practical energy criteria." Following this article, Hsu [13] studied the effects of timewise step loads on the dynamic stability of simply supported, shallow arches. He presented a general method to treat arches of arbitrary shape and loads of arbitrary spatial

distribution, specifically studying sinusoidal arches under sinusoidal loads, the effects of the second harmonics in the arch shape and in the load distribution, and sinusoidal arches subjected to uniform loads or concentrated and eccentric loads. The results were "expressed in the form of sufficiency conditions for stability and sufficiency conditions for instability," which represent lower and upper bounds, respectively, for the determination of the failure or buckling loads. As a generalization of the treatment given in ref. [12], Hsu [14] presented an exact and complete analysis which allows for the determination of all the possible equilibrium configurations and their dynamic stability character for an arch of arbitrary shape, with either simply-supported or clamped end conditions. "The results have immediate application to the snap-through stability of arches when subjected to impulsive loads or time-varying loads of finite duration." Finally, as an extension of ref. [13], Hsu, Kuo, and Plaut [15] studied the effects of timewise step loads on the dynamic stability of clamped shallow arches, specifically studying "simple" clamped arches under "simple" loads, clamped sinusoidal arches under uniformly distributed loads, clamped parabolic arches under uniformly distributed loads and clamped sinusoidal arches under concentrated loads which may be located eccentrically. The results were expressed as separate sufficient conditions for stability and for instability.

Authors other than Hsu have determined stability criteria for specific problems. Popelar and Abraham [30] studied the dynamic

stability of a simply supported, shallow sinusoidal arch subjected to a nearly symmetric impulsive load. The results were expressed as upper and lower bounds for the critical initial velocity for snap-through and the initial velocity necessary to parametrically excite the unsymmetric modes. These results were compared with the critical initial velocity obtained from direct numerical integration of the equations of motion. Cheung and Babcock [5] studied the dynamic stability of clamped circular arches subjected to step loading. The results were expressed as upper and lower bounds for the critical step load. These results were determined by an energy approach presented in the study, and were compared to experimental results. Ovenshire and McIvor [27] studied the dynamic stability of a shallow cylindrical shell subjected to an initial velocity distribution imparted by a nearly symmetric impulsive pressure. The results were expressed as a sufficient condition for stability. Also determined was that either immediate or delayed snap-through may occur, the latter caused by nonlinear coupling of the modes. Ovenshire and McIvor [28] also studied the dynamic stability of a shallow cylindrical shell with the supports elastically restrained against rotation subjected to impulsive loading. The results were expressed as a sufficient condition for stability. Finally, Johnson and McIvor [17] studied the effect of the spatial distribution of impulsive loads on the dynamic snap-through of a shallow circular arch. The results were expressed as a lower bound for the critical loads, and were compared

to the results from a numerical integration of the approximate equations of motion using the Budiansky and Roth [4] criterion. Also determined was that the lower bound was less conservative for finite-time (delayed) snap-through than for immediate snap-through.

b. Buckling

The dynamic buckling of arches, with a search for the buckling loads, has been studied by many authors. Humphreys [16] studied the dynamic buckling of a shallow circular arch subjected to initial-velocity (impulsive), step and rectangular-pulse loading. For step loading, a clear dynamic buckling point was observed in terms of a sudden change in the level of the response curve. For impulsive loading, there was no specific buckling load, but a critical region of increased response was observed. The response in the study was measured as the ratio of the average deflection to the average rise, similar to the Budiansky and Roth [4] criterion.

Lock [20] studied the dynamic buckling of a simply supported, shallow sinusoidal arch subjected to a sinusoidally distributed step pressure load. The buckling loads were determined by the occurrence of a "jump" in the maximum absolute value of the displacement. These loads were compared to the buckling loads determined by an infinitesimal stability analysis. Also determined in the study was that, for the nonlinear analysis, two types of snapping occurred, either direct (immediate) or indirect (time-delayed). The direct snapping occurred for the rapid application of the pressure load which induced sufficient displacement of the symmetric mode for an unstable

equilibrium configuration to be attained. The indirect snapping occurred for parametric excitation of the antisymmetric mode by the initial motion in the symmetric mode, which in turn interacts with the symmetric motion and initiates snapping.

Reed and Broyles [32] studied the dynamic buckling of an idealized structural mechanism. A step load was applied to the apex of the four bar linkage mechanism, and the initial lateral displacement produced a two-degree-of-freedom planar motion. A one-degree-of-freedom motion was produced by restraining the apex to vertical linear motion. The buckling loads for both motions were determined by using a combination of response parameter plots, energy plots, and phase plane plots, and did not vary significantly.

Fulton and Barton [6] studied the symmetric and antisymmetric dynamic buckling of a simply supported, shallow arch subjected to uniformly distributed dynamic loadings. For symmetric buckling, under either an ideal impulse or a step load of finite or infinite duration, the buckling load was determined by a "jump" in the peak average displacement for a small increase in the load. For antisymmetric buckling, under an ideal impulse, the buckling load was determined by a significant growth in the antisymmetric response component. McIvor [22] questioned the above results for the impulsive loading, and compared the above results to the results obtained in ref. [27].

Sundararajan and Kumani [34] studied the dynamic buckling of a clamped shallow circular arch subjected to a timewise step concen-trated inclined load acting at an arbitrary point. The buckling

loads were determined when the value of the average deflection ratio became greater than unity.

Rapp, Smith, and Simitses [31] studied the dynamic buckling of shallow arches with nonuniform stiffness subjected to step, ideal impulse, and pulse loading. The buckling loads were determined by the characteristics of the total potential energy surface, as described in the study.

Lo and Masur [19] presented an alternate approach to the analysis of the dynamic symmetric and antisymmetric buckling of shallow arches. The analysis consisted of converting the equations of motion to an integral-equation-finite-element system, and then numerically integrating the equations to determine the buckling loads. For symmetric buckling, the results agreed with those of Humphreys [16] and Fulton and Barton [6]. For antisymmetric buckling, the results agreed with those of Lock [20] and Fulton and Barton [6].

The results from two final articles must be mentioned. First, Lock [21] determined that if the load attains its steady value over a short duration of time, rather than instantaneously as for step loads, the critical loads for ref. [20] increase. Secondly, Hegemier and Tzung [7] determined that, in the presence of velocity-dependent damping of any nonzero magnitude, no difference exists between the static and dynamic buckling loads for arch rises above a certain magnitude for a simply supported, shallow sinusoidal arch subjected to a sinusoidally distributed step pressure load. Below the foregoing value of arch rise, buckling is governed entirely by symmetric buckling.

CHAPTER 2

ARCH MODEL

This chapter contains the description of the arch model and its parameters. Also contained is the procedure for the determination of the number of degrees of freedom for the arch model.

2.1 Description of the Model and Its Parameters

The arch model is shown in Fig. 2.1. From the figure, one can see that the model is comprised of four uniform rigid bars (①, ②, ③, ④) connected at the joints (1, 2, 3, 4, 5) by frictionless pins. At each interior joint (2, 3, 4), there is a rotational spring, a dashpot, and an applied load. At the right hand exterior joint (5), there is a linear spring. The model's parameters are described below.

Each rigid bar has a length L_i and a mass m_i, where $i = 1, 2, 3$, or 4. The rotational springs, which have stiffnesses C_i, $i = 1, 2, 3$, supply the moment resistance for the model. The dashpots, which have damping coefficients B_i, $i = 1, 2, 3$, supply the viscous damping for the model. The translational spring, which has a stiffness K, supplies the compressibility for the model. The applied loads, which are time dependent and have magnitudes P_i, $i = 1, 2, 3$, are vertical and remain so throughout their application to the model. The angles θ_i, $i = 1, 2, 3, 4$, define the geometry or shape of the model. Also, these angles are the measure of the angular rotation for the centroids of the rigid bars [33]. The angles θ_1 and θ_2 are measured counter

9
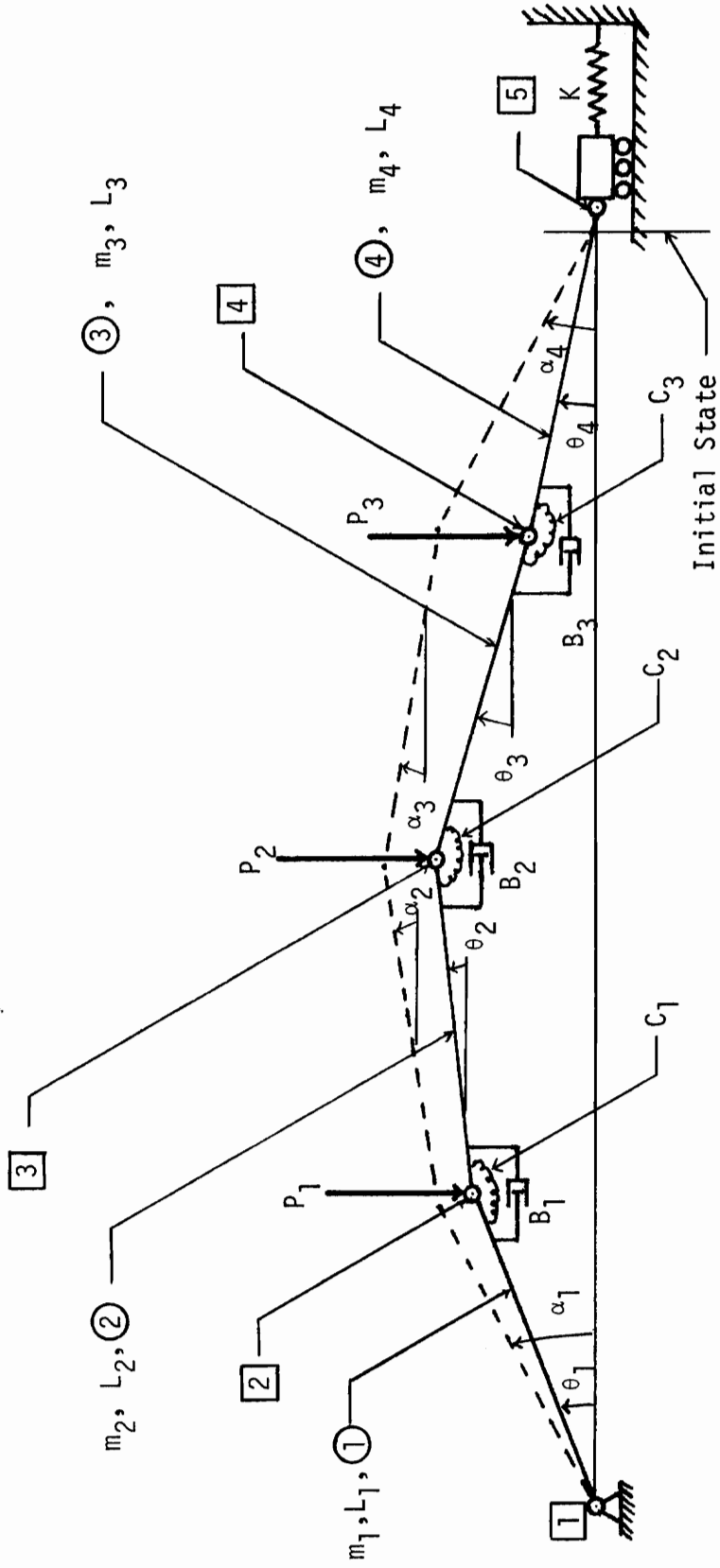
FIGURE 2.1: Three Degree of Freedom, Shallow Arch Model

clockwise and the angles θ_3 and θ_4 are measured clockwise. When no loads are applied to the model, it is in the undeformed state, and thus, the angles θ_i are equal to their initial values α_i. This is depicted in Fig. 2.1 by the dashed lines.

2.2 Determination of the Number of Degrees of Freedom

As stated earlier, the model is a three degree of freedom system. This was determined by examining the definition given by Wells [35], which states that the number of degrees of freedom is "the number of independent coordinates (not including time) required to specify completely the position of each and every ... component of the system." The four rigid bars, which are the components of the model (system), have their positions completely specified by their respective θ's, as can be seen in Fig. 2.1. And it can also be seen in the figure that any one of the θ's can be determined from the other three θ's and thus is a combination of the other three θ's. For the given model (system), θ_4 is chosen to be specified by the other three θ's, with the equation specifying θ_4 in terms of the other three θ's given in Appendix A-2. Therefore, for the given model (system), it has been shown that only three of the θ's are required to be specified to determine the position of all four rigid bars.

As demonstrated above, one can just look at the figure of this model to determine its number of degrees of freedom. But there is a more systematic and rigorous approach which can be used to determine the number of degrees of freedom of this model (system) or any other rigid bar system. This approach is described below.

The equation which determines the number of degrees of freedom for a system is given as

$$n = 3N - c \qquad (2.1)$$

where n is the number of degrees of freedom of the system, 3 is the number of degrees of freedom of a rigid bar, N is the number of rigid bars in the system, and c is the number of constraint equations or conditions. Three is the number of degrees of freedom of a rigid bar because, since the length of the bar is constant, specifying the horizontal position x and the vertical position y for any point along the bar and the angle θ of the bar with the horizontal axis completely specifies the position of any other point along the bar. The constraint equations or conditions for a rigid bar system are the joint compatibility conditions of the system. Thus, for our model (system), N equals 4, c equals 9, and the desired result of n equal 3 is given by Eq. 2.1 [23].

To obtain the value c equals 9 for our model (system), one must first choose the point at joint ☐1 on bar ① to be the point at which x, y, and θ will be specified for the bar. If this is done, one can see that x and y are defined by joint compatibility at joint ☐1, and thus are not "degrees of freedom" for our model. Since the position of any point along the bar can now be specified, the position of the point at joint ☐2 on bar ① is defined. If one now chooses the point at joint ☐2 on bar ② to be the point at which x, y, and θ will be specified for the bar, one can see that x and y will be

defined by joint compatibility at joint $\boxed{2}$, and thus will not be "degrees of freedom" for our model. One can continue this process up to joint $\boxed{5}$. At that joint, no new bar is present, thus no new x, y, and θ are specified. But there is specified the joint compatibility condition y equals 0. Thus, at joint $\boxed{5}$, no new "degrees of freedom" are specified, but one constraint condition is specified. If one now counts two constraint conditions per joint for joints $\boxed{1}$, $\boxed{2}$, $\boxed{3}$, and $\boxed{4}$, and one constraint conditon at joint $\boxed{5}$, then the desired result of c equal 9, as stated earlier, is given.

CHAPTER 3

EQUATIONS OF MOTION

This chapter contains the derivation of the model's equations of motion from Lagrange's equations of motion, prefaced by a brief description of Lagrange's equations. Also contained is the procedure for the non-dimensionalization of the model's equations of motion. Finally, the chapter contains the derivation of the linearized equations of motion for the model, which are used to determine the natural frequencies, periods, and mode shapes of the "linearized" model.

3.1 Description of Lagrange's Equations of Motion

Lagrange's equations of motion were developed to derive the equations of motion for dynamic problems. Their development was initiated by trying to extend the principle of virtual work, which is used to derive the equilibrium equations for static problems, to dynamic problems. This was accomplished by the use of D'Alembert's principle. Although D'Alembert's principle "represents the most general formulation" [23] of dynamic problems and "enables one to treat dynamic problems as if they were statical" [23], "it is not very convenient for deriving the equations of motion" [23] because "the problems are formulated in terms of the position coordinates, which, in contrast with generalized coordinates, may not all be independent." Thus, from D'Alembert's principle, Lagrange's equations of motion, which are formulated in terms of the generalized coordinates, were developed. For an easy to read and understand

14

presentation of the complete details of the development of Lagrange's equations of motion, see Meirovitch [23].

Now, following the brief outline of their development, Lagrange's equations of motion are presented, having the form

$$\frac{d}{dt} \frac{\partial L}{\partial \dot{q}_k} - \frac{\partial L}{\partial q_k} = Q_k, \qquad k = 1, 2, \ldots, n \qquad (3.1)$$

where

$$L = T - V \qquad (3.2)$$

and

$$Q_k = \sum_{j=1}^{P} \vec{F}_j \cdot \frac{\partial \vec{r}_j}{\partial q_k}, \qquad k = 1, 2, \ldots, n. \qquad (3.3)$$

As can be seen, Eqs. 3.1 are a set of n simultaneous differential equations, where L is the Lagrangian of the system, q_k are the generalized coordinates of the system, $\dot{q}_k$ are the first time derivatives of the generalized coordinates q_k of the system, Q_k are the generalized forces of the system, and t is the time. In Eq. 3.2, T is the kinetic energy of the system, and V is the potential energy of the system. In Eq. 3.3, $\vec{F}_j$ are the force vectors of the system, and $\vec{r}_j$ are the position vectors corresponding to the force vectors $\vec{F}_j$ of the system. In all three equations, n is the number of generalized coordinates. By making use of all three equations listed above, the equations of motion for any holonomic system can be derived [23].

Of course, Eqs. 3.1 are written for nonconservative systems, in which the forces of the system not derivable from a potential function, such as dissipative forces and time dependent forces, are included in the generalized forces Q_k of the system. Thus, the potential energy V of the system, given in Eq. 3.2, cannot contain any applied forces that are dependent on time. However, one exception to this condition is the applied forces that are step loads of constant magnitude, infinite duration, and applied to the system at time zero. Because of the nature of these forces, they are not actually dependent on time, and therefore can be included in the potential energy V of the system. For conservative systems, in which all the forces of the system are derivable from a potential function and thus are contained in the potential energy V of the system, Q_k equals 0. In this case, with

$$Q_k = 0, \quad k = 1, 2, \ldots, n, \tag{3.4}$$

Eqs. 3.1 become

$$\frac{d}{dt} \frac{\partial L}{\partial \dot{q}_k} - \frac{\partial L}{\partial q_k} = 0, \quad k = 1, 2, \ldots, n. \tag{3.5}$$

Finally, as previously stated, all of the above is restricted to holonomic systems, which is the only type of system considered in this study. Because of this restriction, one obtains the very useful result that the number of generalized coordinates of the system equals the number of degrees of freedom of the system [18].

Thus, the n of Eq. 2.1 equals the n of Eqs. 3.1, 3.2, 3.3, 3.4, and 3.5.

For further information concerning the material presented here, see refs. [18, 23, 33, 35].

3.2 Derivation of the Model's Equations of Motion

In section 2.2 it was determined that the model used in this study has 3 degrees of freedom, which were chosen to be θ_1, θ_2, and θ_3. Because the model is holonomic, as stated in section 3.1, it has 3 generalized coordinates, which will be chosen to be the same as the 3 degrees of freedom, namely θ_1, θ_2, and θ_3. Thus, from sections 2.2 and 3.1, it has been determined that for Eqs. 3.1 thru 3.5

$$n = 3, \tag{3.6}$$

and that

$$q_1 = \theta_1, \tag{3.7}$$

$$q_2 = \theta_2, \tag{3.8}$$

$$q_3 = \theta_3. \tag{3.9}$$

Now, the derivation of the model's equations of motion from Lagrange's equations of motion can begin by applying Eqs. 3.2, 3.6, 3.7, 3.8, and 3.9 to Eqs. 3.1. The result is a set of 3 simultaneous differential equations, which are

$$\frac{d}{dt} \frac{\partial(T-V)}{\partial \dot{\theta}_1} - \frac{\partial(T-V)}{\partial \theta_1} = Q_1, \tag{3.10}$$

$$\frac{d}{dt} \frac{\partial(T-V)}{\partial\dot{\theta}_2} - \frac{\partial(T-V)}{\partial\theta_2} = Q_2 , \tag{3.11}$$

$$\frac{d}{dt} \frac{\partial(T-V)}{\partial\dot{\theta}_3} - \frac{\partial(T-V)}{\partial\theta_3} = Q_3 . \tag{3.12}$$

If these equations are expanded, knowing that the potential energy V of the system contains no $\dot{\theta}_k$ terms, they become

$$\frac{d}{dt} \frac{\partial T}{\partial\dot{\theta}_1} - \frac{\partial T}{\partial\theta_1} + \frac{\partial V}{\partial\theta_1} = Q_1 , \tag{3.13}$$

$$\frac{d}{dt} \frac{\partial T}{\partial\dot{\theta}_2} - \frac{\partial T}{\partial\theta_2} + \frac{\partial V}{\partial\theta_2} = Q_2 , \tag{3.14}$$

$$\frac{d}{dt} \frac{\partial T}{\partial\dot{\theta}_3} - \frac{\partial T}{\partial\theta_3} + \frac{\partial V}{\partial\theta_3} = Q_3 . \tag{3.15}$$

In the above equations, the potential energy V of the system contains the applied loads P_1, P_2, and P_3, even though they are time dependent, because they are considered to be step loads for this model. (For further discussion, see section 3.1.) However, even if the applied loads P_1, P_2, and P_3 are not step loads, they could be included in the potential energy V of the system as long as they are not functions of the $\dot{\theta}_k$. If this is the case, then the applied loads P_1, P_2, and P_3 would not affect the first term in Eqs. 3.10, 3.11, and 3.12, and the results from including these loads in the potential energy V of the system or in the generalized forces Q_k of the system will be the same.

Since the applied loads P_1, P_2, and P_3 are included in the potential energy V of the system, only the dissipative forces are included in the generalized forces Q_k of the system. To represent these dissipative forces, Rayleigh's dissipation function F will be used, resulting in the generalized forces Q_k of the system having the form [23]

$$Q_1 = - \frac{\partial F}{\partial \theta_1} , \qquad (3.16)$$

$$Q_2 = - \frac{\partial F}{\partial \theta_2} , \qquad (3.17)$$

$$Q_3 = - \frac{\partial F}{\partial \theta_3} . \qquad (3.18)$$

Applying these equations to Eqs. 3.13, 3.14, and 3.15, and rearranging terms yields

$$\frac{d}{dt} \frac{\partial T}{\partial \dot{\theta}_1} - \frac{\partial T}{\partial \theta_1} + \frac{\partial V}{\partial \theta_1} + \frac{\partial F}{\partial \theta_1} = 0 , \qquad (3.19)$$

$$\frac{d}{dt} \frac{\partial T}{\partial \dot{\theta}_2} - \frac{\partial T}{\partial \theta_2} + \frac{\partial V}{\partial \theta_2} + \frac{\partial F}{\partial \theta_2} = 0 , \qquad (3.20)$$

$$\frac{d}{dt} \frac{\partial T}{\partial \dot{\theta}_3} - \frac{\partial T}{\partial \theta_3} + \frac{\partial V}{\partial \theta_3} + \frac{\partial F}{\partial \theta_3} = 0 . \qquad (3.21)$$

In the above equations, T is the kinetic energy of the system, V is the potential energy of the system, and F is Rayleigh's dissipation function of the system. Expressing these terms in equation form yields

$$T = \sum_{i=1}^{4} T_i , \tag{3.22}$$

where

$$T_i = \frac{1}{2} m_i v_i^2 + \frac{1}{2} I_i \omega_i^2 , \tag{3.23}$$

$$V = \frac{1}{2} c_1 [(\alpha_1 - \alpha_2) - (\theta_1 - \theta_2)]^2$$

$$+ \frac{1}{2} c_2 [(\alpha_3 + \alpha_2) - (\theta_3 + \theta_2)]^2$$

$$+ \frac{1}{2} c_3 [(\alpha_4 - \alpha_3) - (\theta_4 - \theta_3)]^2$$

$$+ \frac{1}{2} K [L_1 \cos \theta_1 + L_2 \cos \theta_2 + L_3 \cos \theta_3$$

$$+ L_4 \cos \theta_4 - L_1 \cos \alpha_1 - L_2 \cos \alpha_2$$

$$- L_3 \cos \alpha_3 - L_4 \cos \alpha_4]^2$$

$$- P_1 [L_1 \sin \alpha_1 - L_1 \sin \theta_1] \tag{3.24}$$

$$- P_2 [L_1 \sin \alpha_1 + L_2 \sin \alpha_2$$

$$- L_1 \sin \theta_1 - L_2 \sin \theta_2]$$

$$- P_3 [L_1 \sin \alpha_1 + L_2 \sin \alpha_2 - L_3 \sin \alpha_3$$

$$- L_1 \sin \theta_1 - L_2 \sin \theta_2$$

$$+ L_3 \sin \theta_3] ,$$

and

$$F = \frac{1}{2} B_1 \ (\dot{\theta}_1 - \dot{\theta}_2)^2 + \frac{1}{2} B_2 \ (\dot{\theta}_3 + \dot{\theta}_2)^2$$

$$+ \frac{1}{2} B_3 \ (\dot{\theta}_4 - \dot{\theta}_3)^2 . \tag{3.25}$$

In Eq. 3.23, T_i is the kinetic energy of the ith member, v_i is the velocity of the mass center (centroid) of the ith member, I_i is the mass moment of inertia of the ith member about its centroid, and ω_i is the angular velocity of the ith member.

Finally, applying Eqs. 3.22, 3.23, 3.24, and 3.25 to Eqs. 3.19, 3.20, and 3.21, rearranging terms, and expressing in matrix form yields

$$[A] \ \{\ddot{\theta}\} = \{D\} , \tag{3.26}$$

where $[A]$ is a 3 x 3 matrix that depends on the θ's only, $\{\ddot{\theta}\}$ is a 3 x 1 "acceleration" vector with $\ddot{\theta}_1$, $\ddot{\theta}_2$, and $\ddot{\theta}_3$ as its members, and $\{D\}$ is a 3 x 1 vector that depends on the θ's, the $\dot{\theta}$'s, and the P's. Eq. 3.26 represents the model's equations of motion, which are non-linear, and which will be used to determine the dynamic buckling loads of the model.

For further details of Eqs. 3.23, 3.24, and 3.25, their partial derivatives, which are needed for use in Eqs. 3.19, 3.20, and 3.21, and the expressions for the terms in Eq. 3.26, see Appendix A-2.

3.3 Non-Dimensionalization of the Model's Equations of Motion

Non-dimensionalization of the model's equations of motion is performed so that the numerical solution procedure, which is applied to the model's equations of motion, will not be involved with units

(lb, ft, sec, etc.) in the terms of Eq. 3.26. The non-dimension-
alization is to be performed with respect to the model's m_1, L_1,
and K parameters. To accomplish this, all of the model's parameters
are modified according to the following equations, which were derived
so that all of the terms of Eq. 3.26 are non-dimensional. The
equations are

$$L_1 = 1 = \frac{L_1}{L_1} \, , \tag{3.27}$$

$$m_1 = 1 = \frac{m_1}{m_1} \, , \tag{3.28}$$

$$K = 1 = \frac{K}{K} \, , \tag{3.29}$$

$$L_i = \frac{L_i}{L_1} \, , \quad i = 2, 3, 4 \, , \tag{3.30}$$

$$m_i = \frac{m_i}{m_1} \, , \quad i = 2, 3, 4 \, , \tag{3.31}$$

$$P_i = \frac{P_i}{KL_1} \, , \quad i = 1, 2, 3 \, , \tag{3.32}$$

$$C_i = \frac{C_i}{KL_1{}^2} \, , \quad i = 1, 2, 3 \, , \tag{3.33}$$

$$B_i = \frac{B_i}{L_1{}^2 \sqrt{Km_1}} \, , \quad i = 1, 2, 3 \, , \tag{3.34}$$

and

$$t = \sqrt{\frac{K}{m_1}} \; t \, , \tag{3.35}$$

where the left hand side of the equations represents the model's non-
dimensional parameters, and the right hand side of the equations
represents the model's dimensional parameters.

In Eqs. 3.27 and 3.35, it can be easily seen that there has been no change of symbols between the dimensional and non-dimensional form of the model's parameters. This is done so that both the model's dimensional and non-dimensional equations of motion have the same form, thus requiring the model's equations of motion to be written only once. Although this might create some confusion with regard to distinguishing between the two forms in the remaining sections of this study, it is hoped that this has been avoided by carefully documenting the particular form of the parameters and equations being used. Thus, the non-dimensionalization of the model's equations of motion is accomplished by applying Eqs. 3.27 thru 3.35 to Eq. 3.26.

Finally, it must be stated that if the model's equations of motion are to be non-dimensionalized with respect to dimensional parameters of the model other than m_1, L_1, and K, then relationships similar to Eqs. 3.27 thru 3.35 must be derived. These relationships can then be applied to Eq. 3.26 to accomplish the non-dimensionalization of the model's equations of motion.

3.4 Derivation of the Model's Linearized Equations of Motion

In this section, the model's linear equations of motion are derived from the model's nonlinear equations of motion. The derivation procedure applies to both the dimensional and non-dimensional form of the model's nonlinear equations of motion. Also, for the parabolic arch (see Table 5.1), the natural

frequencies, periods, and mode shapes are calculated from the model's
non-dimensional linear equations of motion.

a. Linearized Equations of Motion

The model's nonlinear equations of motion are to be linearized
about the model's initial state. This means that the definition

$$\theta_i \, (t) = \phi_i \, (t) + \alpha_i \, , \quad i = 1, \, 2, \, 3, \, 4 \tag{3.36}$$

must be used, where $\phi_i(t)$ is the time dependent change in the angle's
value from its initial value α_i. It is assumed that ϕ_i represents
a small angle value, so that the equations

$$\cos \phi_i = 1 \tag{3.37}$$

and

$$\sin \phi_i = \phi_i \tag{3.38}$$

can be used. Also, from Eq. 3.36, the equations

$$\dot{\theta}_i \, (t) = \dot{\phi}_i \, (t) \, , \quad i = 1, \, 2, \, 3, \, 4 \tag{3.39}$$

and

$$\ddot{\theta}_i \, (t) = \ddot{\phi}_i \, (t) \, , \quad i = 1, \, 2, \, 3, \, 4 \tag{3.40}$$

result. Now, with the use of Eqs. 3.36 thru 3.40, the linearization
of Eq. 3.26 can begin.

The first step in the linearization procedure is to delete all
of the $\dot{\theta}_i$, B_i, and P_i terms in Eq. 3.26. The reason for this is
Eq. 3.39 and the fact that only the undamped free vibration form of

the model's linearized equations of motion is of interest in this study. After the above has been accomplished, Eq. 3.40 is applied to the $\{\ddot{\theta}\}$ vector. This results in the $\{\ddot{\theta}\}$ vector becoming the $\{\ddot{\phi}\}$ vector with $\ddot{\phi}_1$, $\ddot{\phi}_2$, and $\ddot{\phi}_3$ as its members. Next, Eqs. 3.36, 3.37, and 3.38 are applied to the [A] matrix. However, because the [A] matrix is multiplied by the $\{\ddot{\phi}\}$ vector, all of the ϕ_i terms must be deleted in order to avoid the nonlinear terms which occur when the ϕ_i terms are multiplied by the $\ddot{\phi}_i$ terms. The result is the same as if θ_i were replaced by α_i instead of using Eq. 3.36. Thus, the linearized [A] matrix is the nonlinear [A] matrix with θ_i replaced by α_i. Finally, Eqs. 3.36, 3.37, and 3.38 are applied to the {D} vector. This results in the {D} vector becoming [DD] $\{\phi\}$ where [DD] is a 3 x 3 "stiffness" matrix and $\{\phi\}$ is a 3 x 1 "displacement" vector with ϕ_1, ϕ_2, and ϕ_3 as its members. Therefore, after the linearization procedure has been applied to the model's nonlinear equations of motion, the model's linear equations of motion have the form

$$[A] \{\ddot{\phi}\} = [DD] \{\phi\} \qquad\qquad (3.41)$$

where all the terms are as defined above.

    b. <u>Natural Frequencies and Periods</u>

The natural frequencies ω of the model's non-dimensional linear equations of motion for the parabolic arch (see Table 5.1) are found by writing Eq. 3.41 in the form

$$[A] \{\ddot{\phi}\} - [DD] \{\phi\} = 0 \; . \tag{3.42}$$

Using the substitution

$$\{\ddot{\phi}\} = - \omega^2 \{\phi\} \tag{3.43}$$

in Eq. 3.42 and rearranging terms yields

$$([DD] + \omega^2 [A]) \{\phi\} = 0 \; . \tag{3.44}$$

As can be seen, this is the characteristic-value or eigenvalue problem of the system. For a nontrivial solution of Eq. 3.44 to exist, the equation

$$\det ([DD] + \omega^2 [A]) = 0 \tag{3.45}$$

must be satisfied. Eq. 3.45 is called the characteristic equation of the system, which is a cubic polynomial in ω^2 with 3 real roots. Solving for these roots and taking their square roots yields

$$\omega_1 = 0.36848 \; , \tag{3.46}$$

$$\omega_2 = 0.15605 \; , \tag{3.47}$$

$$\omega_3 = 0.07487 \; , \tag{3.48}$$

which are the natural frequencies of the model's non-dimensional linear equations of motion for the parabolic arch. (Note: for the numerical calculations, $C_i = 0.001$, $i = 1, 2, 3$ was used.)

The periods T for the parabolic arch are determined from

$$T_i = \frac{2\pi}{\omega_i} , \qquad i = 1, 2, 3 , \tag{3.49}$$

which relates the periods to the natural frequencies. Using Eqs. 3.46, 3.47, and 3.48 in Eq. 3.49 yields

$$T_1 = 17.05163 , \tag{3.50}$$

$$T_2 = 40.26392 , \tag{3.51}$$

$$T_3 = 83.92127 , \tag{3.52}$$

which are the non-dimensional periods of the system [24].

c. Mode Shapes

The mode shapes describe the time independent relationships between the displacement parameters ϕ_1, ϕ_2, ϕ_3, and ϕ_4 for the 3 different undamped free vibration states (modes) that are defined by their natural frequencies ω_i and their corresponding periods T_i. To determine the relationships between the ϕ's , replace the ω in Eq. 3.44 by its corresponding numerical value and solve for ϕ_2 and ϕ_3 in terms of ϕ_1. (Note: ϕ_4 can be given in terms of ϕ_1 by using the relationship between θ_4 and θ_1, θ_2, and θ_3 given in Appendix A-2 and Eq. 3.36.) This is done for all 3 natural frequencies ω_i with the results being

$$\begin{Bmatrix} \phi_1 \\ \phi_2 \\ \phi_3 \\ \phi_4 \end{Bmatrix} = \begin{Bmatrix} \phi_1 \\ 2.62780 \ \phi_1 \\ 1.81157 \ \phi_1 \\ 1.84480 \ \phi_1 \end{Bmatrix} \tag{3.53}$$

for Eq. 3.46,

$$\left\{\begin{array}{c} \phi_1 \\ \phi_2 \\ \phi_3 \\ \phi_4 \end{array}\right\} = \left\{\begin{array}{c} \phi_1 \\ -1.93399 \quad \phi_1 \\ -1.94383 \quad \phi_1 \\ 1.01018 \quad \phi_1 \end{array}\right\} \tag{3.54}$$

for Eq. 3.47, and

$$\left\{\begin{array}{c} \phi_1 \\ \phi_2 \\ \phi_3 \\ \phi_4 \end{array}\right\} = \left\{\begin{array}{c} \phi_1 \\ -0.96223 \quad \phi_1 \\ 0.96388 \quad \phi_1 \\ -0.99352 \quad \phi_1 \end{array}\right\} \tag{3.55}$$

for Eq. 3.48. Eqs. 3.53, 3.54, and 3.55 represent the non-dimensional mode shapes of the system [24].

CHAPTER 4

SOLUTION TECHNIQUES

This chapter contains a brief review of the current literature regarding the direct numerical integration techniques that are presently available and being used. Also contained is the description of the particular procedure used in this study, and the reasons for its use.

4.1 Direct Numerical Integration Techniques

A brief review of the current literature regarding direct numerical integration techniques is necessary because presently many techniques are available for use. These techniques include both implicit methods and explicit methods [3], each of which has its own particular advantages and disadvantages. Because of this, a decision on which particular method to use in this study was made according to the conclusions drawn from the results of the articles listed below.

Bathe and Wilson [2] "present a systematic and fundamental procedure for the stability and accuracy analysis of direct integration methods and apply the techniques to the Newmark, the Houbolt and the Wilson θ method." They found that for linear problems, "the Newmark method with $\delta = \frac{1}{2}$ and $\alpha = \frac{1}{4}$ is most accurate and only gives period elongations." This method also "retained the response of the high frequency components."

Nickell [26] analyzed "several alternative methods for carrying out the step-by-step integration of the equations of motion of a

(linear) structural system" for "forced structural vibration"
problems, which are "dominated by low frequency components of the
response." Although the Newmark method has been found to become
unstable for some problems, it has been determined that in most cases
this can be avoided by the proper selection of the size of the time
step used. Thus, his conclusion is that "from all evidence, then,
it would seem that the trapezoidal, or Newmark, operator is the most
attractive operator for both linear and nonlinear problems."

Adeli, Gere, and Weaver [1] investigated "several competitive and
widely-used numerical integration techniques in order to determine
which is the most efficient technique for nonlinear dynamic analysis
of structures modeled by finite elements." Three implicit and three
explicit methods were investigated. "The accuracy, stability, and
efficiency of the methods were examined by comparing the results for
a plane stress sample problem." The results were that "among the
three explicit methods, it was concluded that the central difference
predictor is the best," and that among "the three implicit approaches,
the Park stiffly-stable method was found to be somewhat better than
the Newmark-Beta method.... For large time steps, the results for
the Newmark-Beta method with $\beta = \frac{1}{4}$ and $\gamma = \frac{1}{2}$ tend to be unstable."

Although the three articles described above are just a small
sample from the current literature on the subject of direct numerical
integration techniques, it is felt that they represent the general
results. For further discussion, see Horne [10].

4.2 Solution Method

In this section, the equations and procedures used in the Newmark-Beta method, which is the numerical integration technique used for the numerical integration of the model's non-dimensional nonlinear equations of motion, are described. Also, the reasons for the selection of the Newmark-Beta method and the accuracy of this method are described.

a. Description of the Method Used

The Newmark-Beta method, with $\beta = \frac{1}{4}$, has been selected as the numerical integration technique for use in this study. The basis of the Newmark-Beta method is the equations

$$\dot{q}_{i+1} = v_i + \frac{1}{2} \ddot{q}_{i+1} \, \Delta t \tag{4.1}$$

$$q_{i+1} = d_i + \beta \ddot{q}_{i+1} \, \Delta t^2 \tag{4.2}$$

where

$$v_i = \dot{q}_i + \frac{1}{2} \ddot{q}_i \, \Delta t \tag{4.3}$$

and

$$d_i = q_i + \dot{q}_i \, \Delta t + (\frac{1}{2} - \beta) \ddot{q}_i \, \Delta t^2 \; . \tag{4.4}$$

In the above equations, q represents one of the generalized coordinates, $\dot{q}$ represents the first time derivative of q, $\ddot{q}$ represents the second time derivative of q, Δt represents the magnitude of the time step for the integration procedure, and the subscript i represents the ith time step [1, 2, 3, 9, 25, 26]. Thus, for

$\beta = \frac{1}{4}$, Eqs. 4.1, 4.2, 4.3, and 4.4 become

$$\dot{q}_{i+1} = v_i + \frac{1}{2} \ddot{q}_{i+1} \Delta t , \tag{4.5}$$

$$q_{i+1} = d_i + \frac{1}{4} \ddot{q}_{i+1} \Delta t^2 , \tag{4.6}$$

$$v_i = \dot{q}_i + \frac{1}{2} \ddot{q}_i \Delta t , \tag{4.7}$$

$$d_i = q_i + \dot{q}_i \Delta t + \frac{1}{4} \ddot{q}_i \Delta t^2 . \tag{4.8}$$

The procedure used in the Newmark-Beta method is listed below, and applies only to the equations that are in the form or can be written in the form

$$\ddot{q} = R \tag{4.9}$$

where R is not a function of $\ddot{q}$. The steps of the procedure are:

1) initialize the quantities q_0, $\dot{q}_0$, $\ddot{q}_0$, v_0, and d_0 for each generalized coordinate q;

2) for each time step:

   a) assume $\ddot{q}_{i+1} = \ddot{q}_i$ for each generalized coordinate q;

   b) compute q_{i+1} and $\dot{q}_{i+1}$ from Eqs. 4.5 and 4.6 for each generalized coordinate q;

   c) compute R in Eq. 4.9 for each generalized coordinate q;

   d) test equilibrium of Eq. 4.9 for each generalized coordinate q by checking if

$$|\ddot{q}_{i+1} - R_{i+1}| < \varepsilon \qquad\qquad (4.10)$$

is satisfied, where $|\ |$ means absolute value and ε is a very small number. If Eq. 4.10 is satisfied for all of the generalized coordinates, go to 2e. If Eq. 4.10 is not satisfied for all of the generalized coordinates, let $\ddot{q}_{i+1} = R_{i+1}$ for the generalized coordinates not satisfying Eq. 4.10, but do not alter $\ddot{q}_{i+1}$ for the generalized coordinates satisfying Eq. 4.10, and then go to 2b and repeat;

e) calculate v_{i+1} and d_{i+1} from Eqs. 4.7 and 4.8 [9].

As stated above, the Newmark-Beta method applies only to equations written in the form of Eq. 4.9. Thus, Eq. 3.26 must be written in the form of Eq. 4.9. To accomplish this, let

$$[B] = [A]^{-1} \qquad\qquad (4.11)$$

where it is assumed that the inverse of the [A] matrix exists. Applying Eq. 4.11 to Eq. 3.26 and rearranging terms yields

$$\{\ddot{\theta}\} = [B]\{D\}, \qquad\qquad (4.12)$$

which can be written as

$$\{\ddot{\theta}\} = \{R\}, \qquad\qquad (4.13)$$

where $\{R\}$ is a 3 x 1 vector. Thus, Eq. 4.13 represents a form of the model's non-dimensional nonlinear equations of motion which can

be numerically integrated by using the Newmark-Beta method described above.

b. Reasons for the Selection of the Method Used

The Newmark-Beta method was selected to numerically integrate the model's non-dimensional nonlinear equations of motion for three main reasons.

The first reason for the selection is, based on the discussion of section 4.1, that the Newmark-Beta method is one of the best, if not the best, method used for numerical integration of linear and nonlinear equations. Even though some researchers have found that the method tends to be unstable for some nonlinear problems [26], most conclude that if the stability of the method can be guaranteed or proved for a problem, then it is still one of the best methods available [26].

The second reason for the selection is that the equations and procedures used in the Newmark-Beta method are easy to program. Since the user can program the method, more freedom is given in the selection of the particular programming procedures used. Also, since the user writes the algorithm for the method, it will be easier to check for errors, make changes, and follow the logic, than if a "canned" routine written by someone else is used.

Finally, the last reason for the selection is that, for our model, the Newmark-Beta method requires from 5 to 10 times less execution time than a Hamming predictor-corrector (SSP) method, with essentially no difference in the results obtained from the use of

the two methods. This was determined from a comparison of the two methods on a limited basis.

One additional influence for the selection is that the author prefers the Newmark-Beta method over the other methods because he is more familiar and more confident with this method.

c. Accuracy

In the previous section, four reasons were presented for using the Newmark-Beta method to numerically integrate the model's non-dimensional nonlinear equations of motion. But as stated earlier, the Newmark-Beta method has been determined to be unstable for some nonlinear problems. Thus, it must be determined whether or not the method is stable for our model. If the method is determined to be unstable, then the reasons stated in the previous section for its use are invalid.

It has been determined that for linear problems, the Newmark-Beta method, $\beta = \frac{1}{4}$, is unconditionally stable, and converges if the equation

$$\frac{\Delta t}{T} \leq 0.318 \tag{4.14}$$

is satisfied, where Δt is the magnitude of the time step used, and T is the magnitude of the smallest period of the linear problem. Thus Eq. 4.14 can be used to determine the "critical" time step magnitude for which the convergence of the method is guaranteed for linear problems [3, 9, 25]. Also, it has been suggested that the usual time step magnitude used in the method should be approximately

$\frac{1}{16}$ to $\frac{1}{20}$ of the smallest period of the system. Therefore, if Eq. 4.14
is applied to the smallest period calculated for the parabolic arch
from the model's non-dimensional linear equations of motion, the
critical time step magnitude is determined to be 5.4. The usual
time step magnitude for the parabolic arch, as calculated from the
criteria described above, is between 0.9 and 1.1.

Now the periods and "critical" time step magnitude for the
parabolic arch, determined from the model's non-dimensional nonlinear
equations of motion, will be examined. When a time step magnitude of
1.0 is used in the Newmark-Beta method, it is determined that for low
loads, there exists two different periods of magnitude 18 and 48 for
the system. If these periods are compared to Eqs. 3.50 and 3.51, then
it can be seen that the two lowest periods determined for the linear
and nonlinear equations of motion are similar. Also, from numerical
studies, it was determined that the "critical" time step magnitude
to "guarantee" convergence for the nonlinear equations of motion is
5.4. As can be seen, this is equal to the "critical" time step
magnitude for the linear equations of motion.

Thus, by comparison of the periods and the "critical" time step
magnitudes, there is determined to be little difference between the
model's linear and nonlinear non-dimensional equations of motion
(at least for low loads). Therefore, the author believes that by
using a time step magnitude of 1.0 in the Newmark-Beta method, the
numerical integration of the model's non-dimensional nonlinear
equations of motion is "guaranteed" to be "stable" and "convergent".

Two final comments must be made at this point. The first comment
is that the error tolerance ε in Eq. 4.10 was specified to be 1.0 x
10^{-12} for all of the above work. This number was selected arbitrarily.
Thus, for a different value of ε, the results may differ slightly from
those presented above. The last comment is that even though the above
work was done for the parabolic arch, the general result that a time
step magnitude of 1.0 used in the Newmark-Beta method will "guarantee"
the "stability" and the "convergence" of the numerical integration of
the model's non-dimensional nonlinear equations of motion should also
apply for an eccentric arch, because the periods and "critical" time
step magnitudes of the two arch types should not differ greatly.

CHAPTER 5

RESULTS

This chapter contains the results (interaction curves) for five problems, prefaced by an introduction explaining how the results are determined. All of the values listed in this chapter are non-dimensional quantities.

5.1 Introduction

In this study, the results for each type of loading, either step or impulse, are determined for two different initial shallow arch geometries or shapes, parabolic and eccentric. The parabolic arch is characterized by bars of equal lengths and equal masses, and by equal rotational springs. It is also symmetric, with α_1 equal to $2.0\,\alpha_2$. The eccentric arch is characterized by bar ④ being 2.5% less in both length and mass than the other bars, but with equal rotational springs. It is not symmetric, but α_1 equals $2.0\,\alpha_2$ and α_2 equals α_3. The values of the parameters, for both the parabolic arch and the eccentric arch, are listed in Table 5.1.

The interaction curves for the problems studied are determined by plotting the buckling loads as points in a two dimensional load space, and drawing a "smooth" curve through those points. The buckling loads are determined for the four "principal" axes, P_1, P_2, P_3, and $P_1 = P_3$, and the eighteen rays which divide the four "principal" planes. The four "principal" planes and the rays in those planes are shown in Figs. 5.1, 5.2, 5.3, and 5.4. For information

regarding interaction curves for static problems, see Plaut [29] and Welton [36].

The buckling loads are those loads for which the results obtained from the numerical integration of the model's non-dimensional non-linear equations of motion exceed the buckling criterion. For this study, it has been decided that the arch has buckled when the values of both θ_1 and θ_4 are simultaneously less than zero. Thus, the buckling criterion states that, if the values of both θ_1 and θ_4 are never negative simultaneously, then the arch has not buckled.

All of the buckling loads are determined to three digits, with the digits being determined from left to right. Thus, for example, if a buckling load has a value 245, first the 2 is determined, secondly the 4 is determined, and finally the 5 is determined. This procedure is used to determine the buckling loads because it requires from 3 to 30 times less execution time than incremental loading, incrementing the third (right most) digit by 1 beginning with zero load.

The numerical integration of the model's non-dimensional non-linear equations of motion is performed for a non-dimensional time of 300.0, which represents approximately 3 times the longest non-dimensional period of the linearized model as given by Eq. 3.52. Johnson and McIvor [17] determined that the use of 3 times the longest period as the duration of time for the numerical integration of the equations of motion to be performed is sufficient, with no effect on the buckling loads obtained for increased time. Refs.

[6, 16, 19, 20] also use 3 times the longest period as the duration of time for the numerical integration of the equations of motion to be performed, although it is not specifically stated. The linearized period is used because, as stated in section 4.2.c, the linear and non-linear models do not differ considerably.

Finally, it must be repeated that all of the values listed in this chapter are non-dimensional quantities.

TABLE 5.1

Non-Dimensional Values of the Model's
Parameters for the Parabolic and Eccentric Arches

Parameter	Parabolic	Eccentric
α_1	0.30	0.30
α_2	0.15	0.15
α_3	0.15	0.15
α_4	0.30	0.30794
m_1	1.0	1.0
m_2	1.0	1.0
m_3	1.0	1.0
m_4	1.0	0.975
L_1	1.0	1.0
L_2	1.0	1.0
L_3	1.0	1.0
L_4	1.0	0.975
C_1	0.001	0.001
C_2	0.001	0.001
C_3	0.001	0.001
K	1.0	1.0
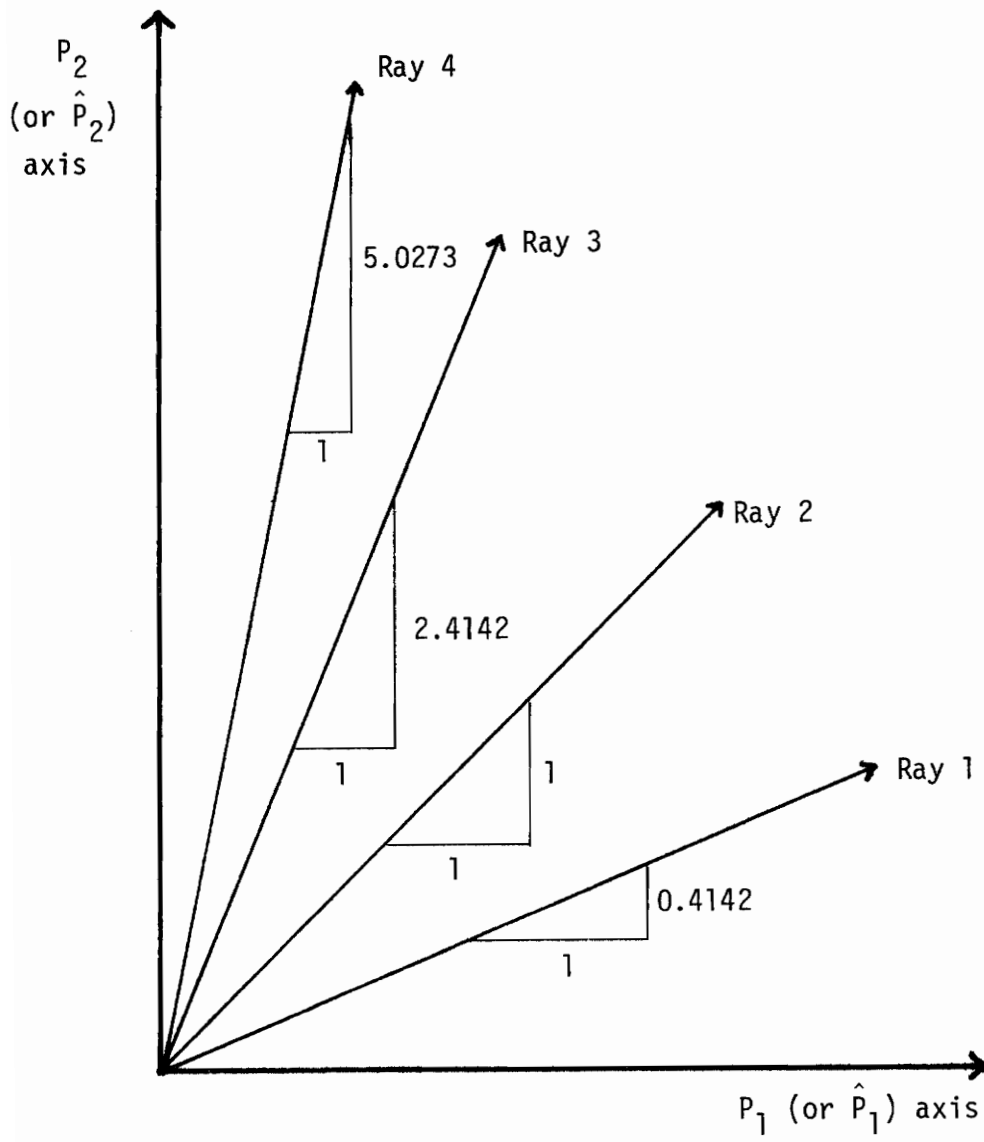
FIGURE 5.1: Rays in the P_2 vs. P_1 Plane
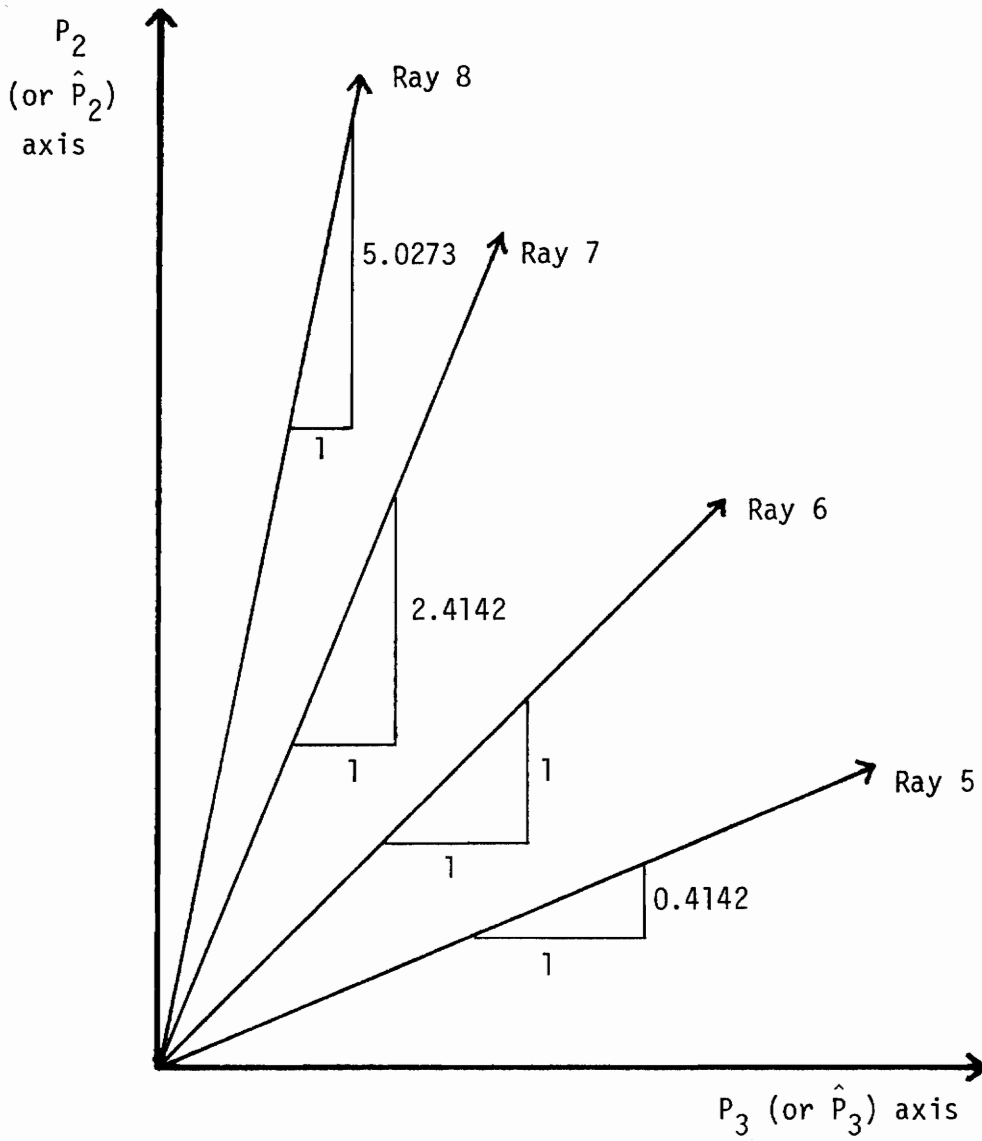
FIGURE 5.2:   Rays in the P_2 vs. P_3 Plane
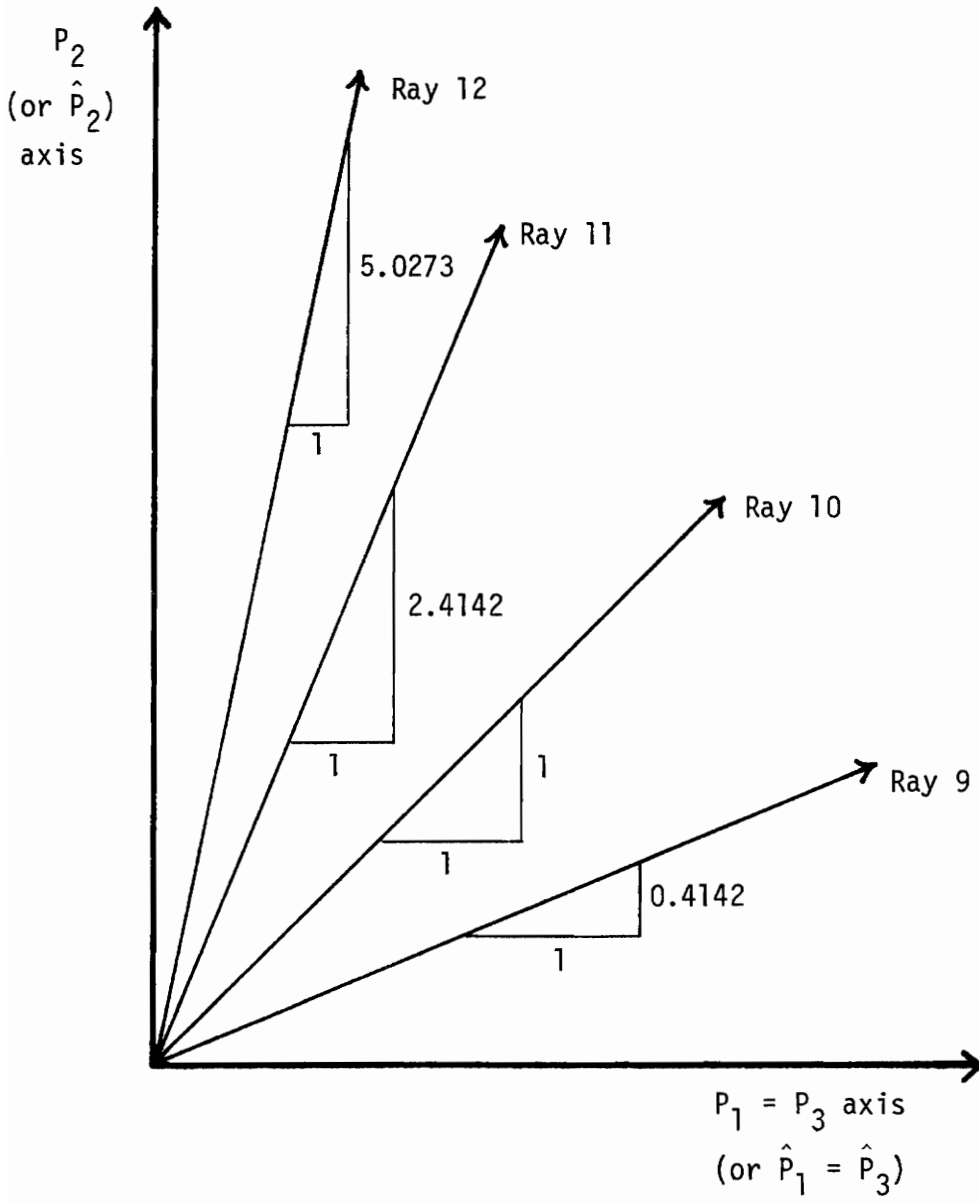
FIGURE 5.3: Rays in the P_2 vs. $P_1 = P_3$ Plane
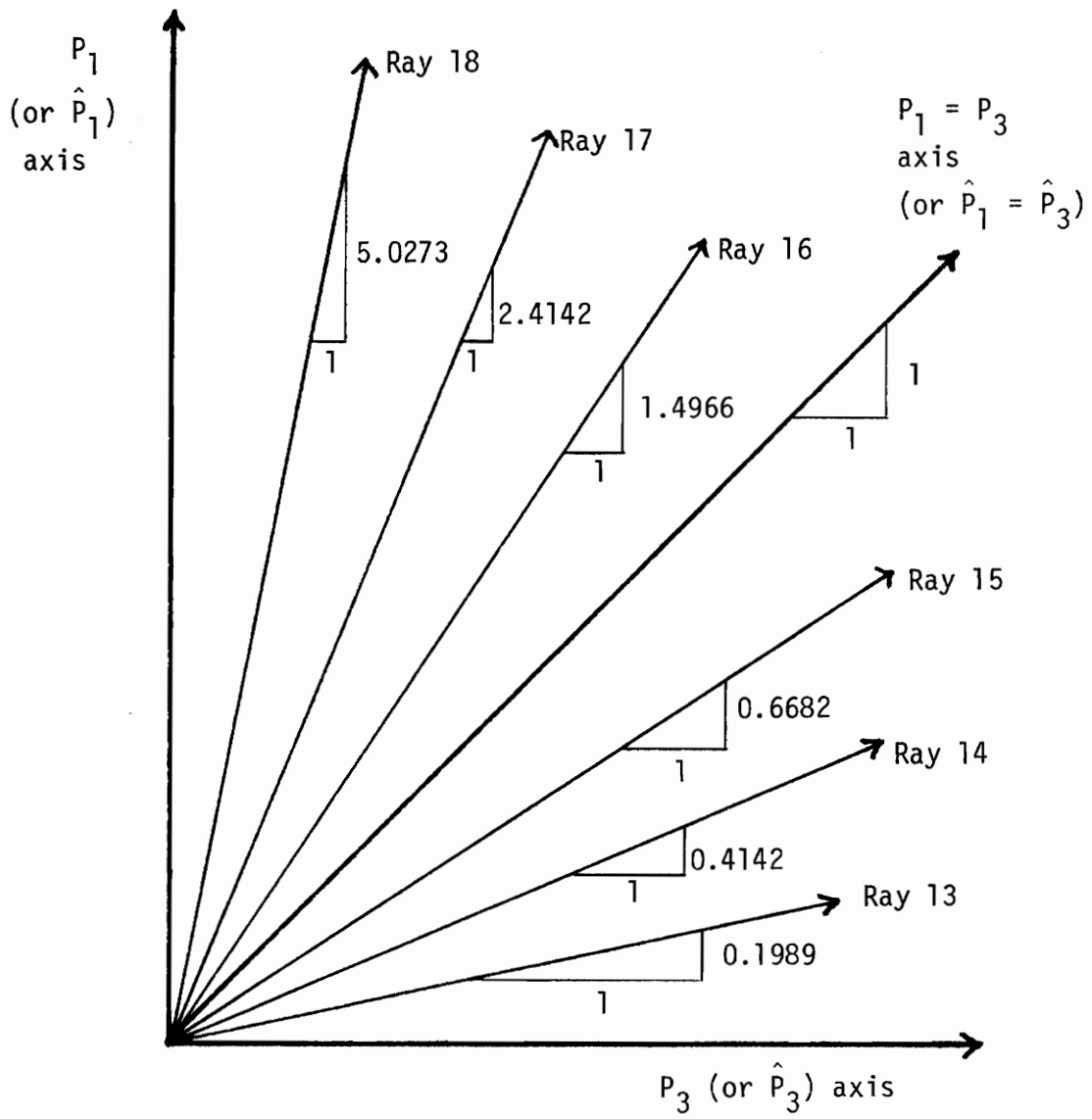
FIGURE 5.4: Rays in the P_1 vs. P_3 Plane

5.2 Step Loads

All of the loads for the three problems discussed below are step loads of infinite duration applied at time zero. Also, all of the initial velocities for the three problems discussed below are set equal to zero.

a. Parabolic Arch with Damping

In this problem, the interaction curves are determined for a parabolic shallow arch with velocity dependent damping.

The value of the damping used in this problem is $B_i = 0.001$, $i = 1, 2, 3$.

The buckling loads are listed in Table 5.2, and the interaction curves are presented in Figs. 5.5, 5.6, 5.7, and 5.8.

The P_2 vs. P_1 and the P_2 vs. P_3 interaction curves, given in Figs. 5.5 and 5.6, respectively, are convex toward the origin. The P_2 vs. $P_1 = P_3$ interaction curve, given in Fig. 5.7, is concave toward the origin. The P_1 vs. P_3 interaction curve is bounded (from above) by and can be approximated by the straight lines connecting the buckling load on the P_1 axis to the buckling load on the $P_1 = P_3$ axis and the buckling load on the P_3 axis to the buckling load on the $P_1 = P_3$ axis.

After buckling, the arch does not remain in the buckled region, but snaps back to the unbuckled region, with the motion oscillating between the two regions. The final shape of the arch for the given buckling loads is not determined in this study.

Finally, the change in the value of the buckling loads due to the use of different durations of time for the numerical integration is determined for a limited number of the buckling loads. For a duration of 200.0, the values of the buckling loads increase by up to 20% of the values listed in Table 5.2. For a duration of 400.0, the values of the buckling loads decrease by less than 1% of the values listed in Table 5.2. This verifies that the chosen duration of 300.0 for the numerical integration is appropriate.

TABLE 5.2

Non-Dimensional Buckling Loads for a
Parabolic Arch with Damping Under Step Loads

Axis or Ray	P_1 (x 10^{-4})	P_2 (x 10^{-4})	P_3 (x 10^{-4})
P_1 axis	5.46	0.0	0.0
P_2 axis	0.0	9.48	0.0
P_3 axis	0.0	0.0	5.47
P_1=P_3 axis	5.33	0.0	5.33
ray 1	4.26	1.76	0.0
ray 2	3.29	3.29	0.0
ray 3	2.61	5.21	0.0
ray 4	1.34	6.74	0.0
ray 5	0.0	1.77	4.27
ray 6	0.0	3.29	3.29
ray 7	0.0	5.21	2.16
ray 8	0.0	6.74	1.34
ray 9	5.00	2.07	5.00
ray 10	4.50	4.50	4.50
ray 11	2.87	6.93	2.87
ray 12	1.65	8.30	1.65
ray 13	1.07	0.0	5.39
ray 14	2.22	0.0	5.37
ray 15	3.59	0.0	5.38
ray 16	5.39	0.0	3.60
ray 17	5.36	0.0	2.22
ray 18	5.43	0.0	1.08
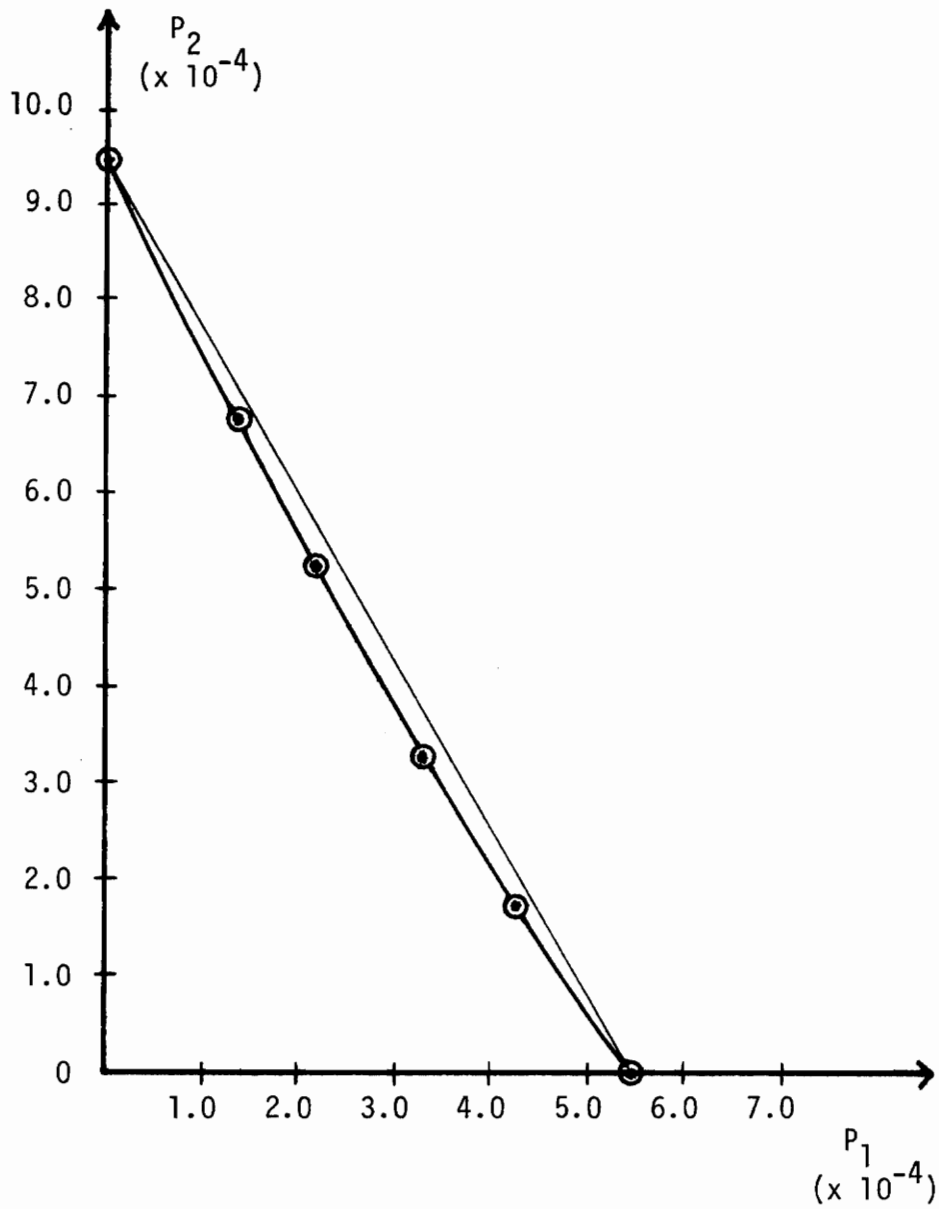
FIGURE 5.5: P_2 vs. P_1 Interaction Curve for a Parabolic Arch with Damping Under Step Loads

FIGURE 5.6: P_2 vs. P_3 Interaction Curve for a Parabolic
Arch with Damping Under Step Loads

FIGURE 5.7: P_2 vs. $P_1 = P_3$ Interaction Curve for a Parabolic Arch with Damping Under Step Loads

FIGURE 5.8: P_1 vs. P_3 Interaction Curve for a Parabolic
Arch with Damping Under Step Loads

b. <u>Parabolic Arch without Damping</u>

In this problem, the interaction curves are determined for a parabolic shallow arch with no velocity dependent damping.

The buckling loads are listed in Table 5.3, and the interaction curves are presented in Figs. 5.9, 5.10, 5.11, and 5.12.

The P_2 vs. P_1 and the P_2 vs. P_3 interaction curves, given in Figs. 5.9 and 5.10, respectively, can be approximated by a straight line connecting the buckling load on the P_2 axis to the buckling load on the P_1 axis and the buckling load on the P_2 axis to the buckling load on the P_3 axis, respectively. The P_2 vs. $P_1 = P_3$ interaction curve, given in Fig. 5.11, is concave toward the origin. The P_1 vs. P_3 interaction curve can be approximated by the straight lines connecting the buckling load on the P_1 axis to the buckling load on the $P_1 = P_3$ axis and the buckling load on the P_3 axis to the buckling load on the $P_1 = P_3$ axis.

After buckling, the arch does not remain in the buckled region, but snaps back to the unbuckled region, with the motion oscillating between the two regions.

The buckling load on the P_2 axis "bounces". "Bouncing of the buckling loads," as pertains to this study, is defined as the existence of loads larger than the buckling loads for which the arch does not buckle. This means that, as the loads increase, the arch buckles for some value, then does not buckle for a slightly higher value, and then buckles again for still a higher value. This cycle is repeated a number of times until a value is reached where

the arch buckles for all higher values. This phenomenon has also been found in the study by Johnson and McIvor [17].

The buckling loads of this problem are less than the static buckling loads determined by Welton [36] for the same parabolic arch, except for rays 10, 11, and 12. (See Fig. 5.11.) Also, the interaction curves of this problem do not have the same shape as the static interaction curves determined by Welton [36] for the same parabolic arch.

Finally, the change in the values of the buckling loads due to the use of different durations of time for the numerical integration is determined for a limited number of the buckling loads. For a duration of 200.0, the values of the buckling loads increase by up to 20% of the values listed in Table 5.3. For a duration of 400.0, the values of the buckling loads decrease by less than 5% of the values listed in Table 5.3. This verifies that the chosen duration of 300.0 for the numerical integration is appropriate.

TABLE 5.3

Non-Dimensional Buckling Loads for a
Parabolic Arch without Damping Under Step Loads

| Axis or Ray	P_1 $(\times 10^{-4})$	P_2 $(\times 10^{-4})$	P_3 $(\times 10^{-4})$
P_1 axis	5.32	0.0	0.0
P_2 axis	0.0	8.78	0.0
P_3 axis	0.0	0.0	5.33
$P_1 = P_3$ axis	5.15	0.0	5.15
ray 1	4.17	1.73	0.0
ray 2	3.22	3.22	0.0
ray 3	2.12	5.12	0.0
ray 4	1.32	6.64	0.0
ray 5	0.0	1.73	4.17
ray 6	0.0	3.22	3.22
ray 7	0.0	5.12	2.12
ray 8	0.0	6.64	1.32
ray 9	4.85	2.01	4.85
ray 10	4.41	4.41	4.41
ray 11	2.80	6.76	2.80
ray 12	1.60	8.04	1.60
ray 13	1.05	0.0	5.27
ray 14	2.17	0.0	5.24
ray 15	3.50	0.0	5.24
ray 16	5.24	0.0	3.50
ray 17	5.24	0.0	2.17
ray 18	5.28	0.0	1.05
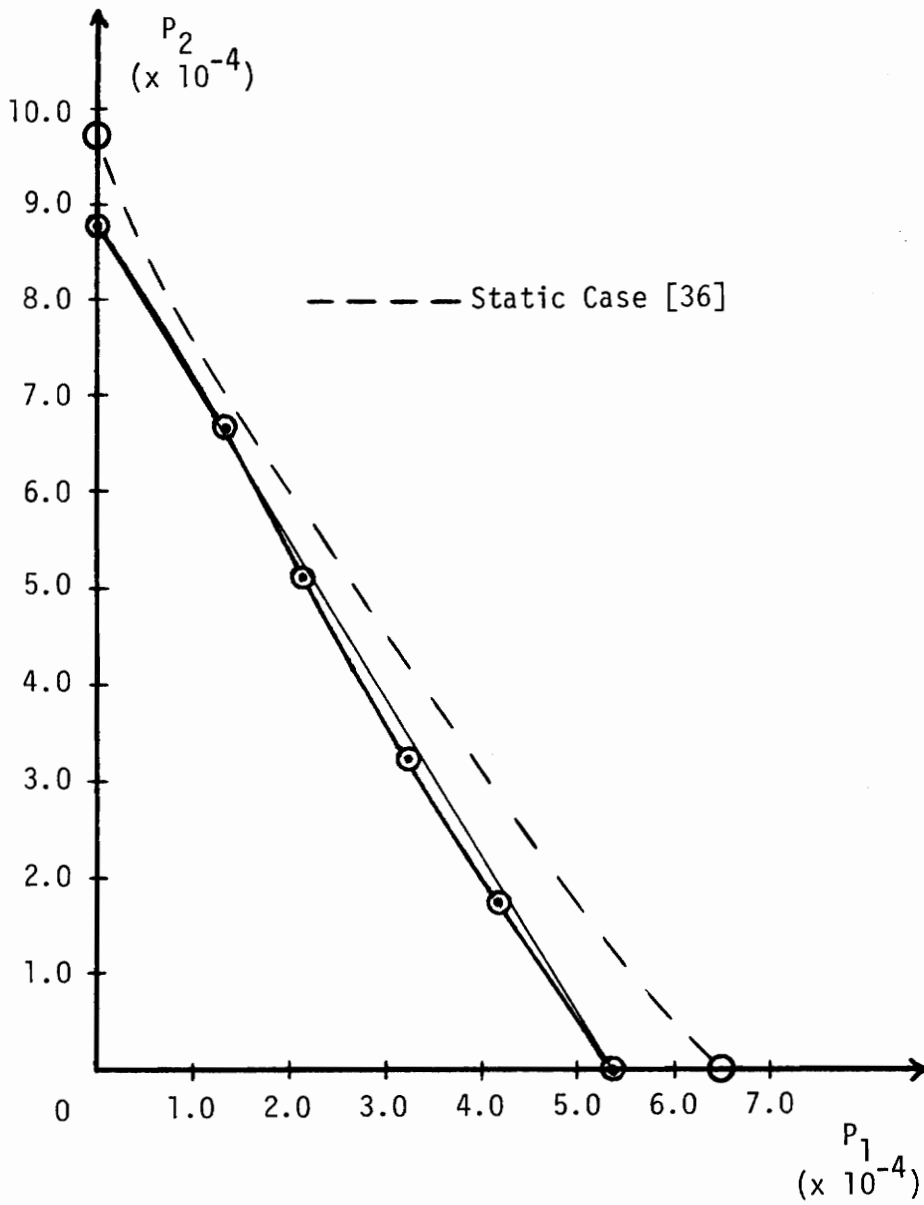
FIGURE 5.9: P_2 vs. P_1 Interaction Curve for a Parabolic
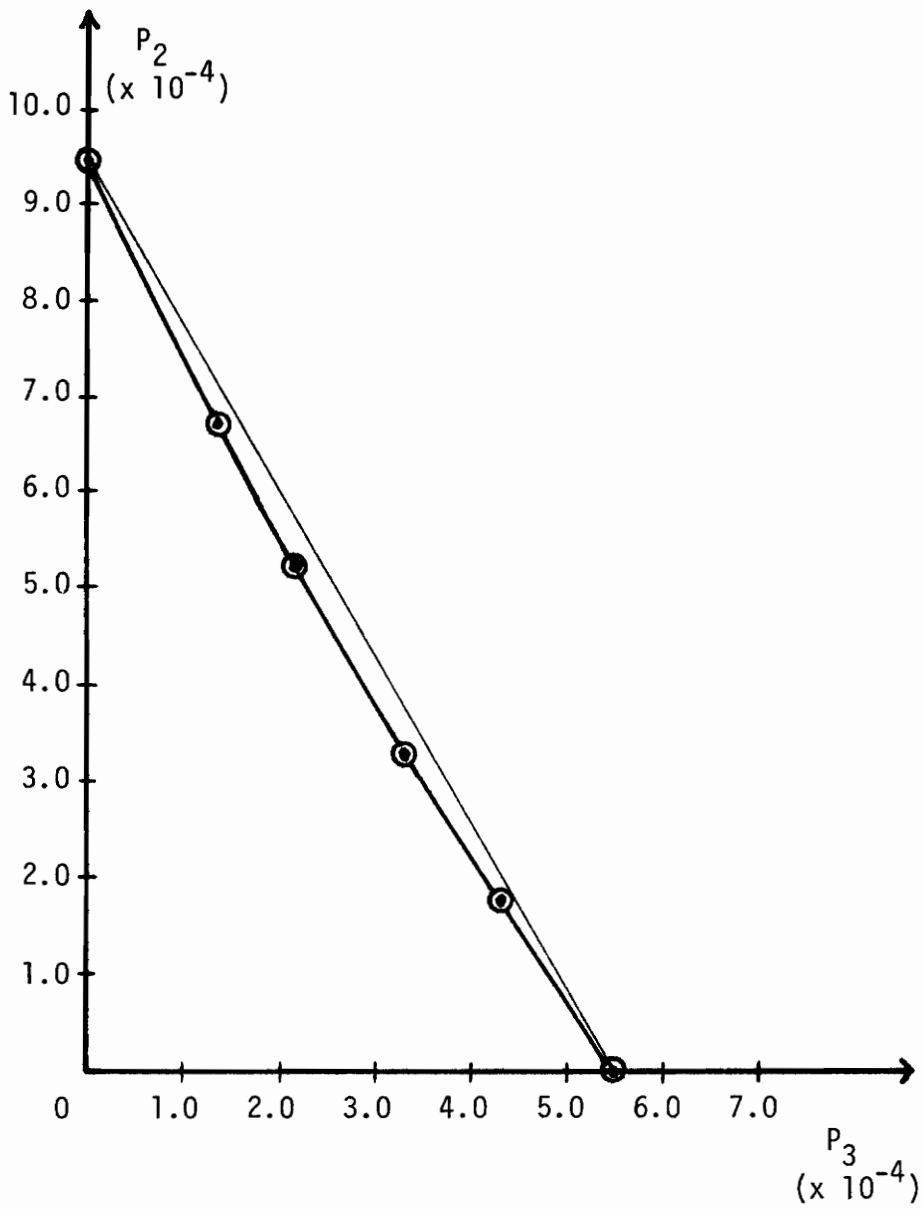Arch without Damping Under Step Loads

FIGURE 5.10: P_2 vs. P_3 Interaction Curve for a Parabolic Arch without Damping Under Step Loads
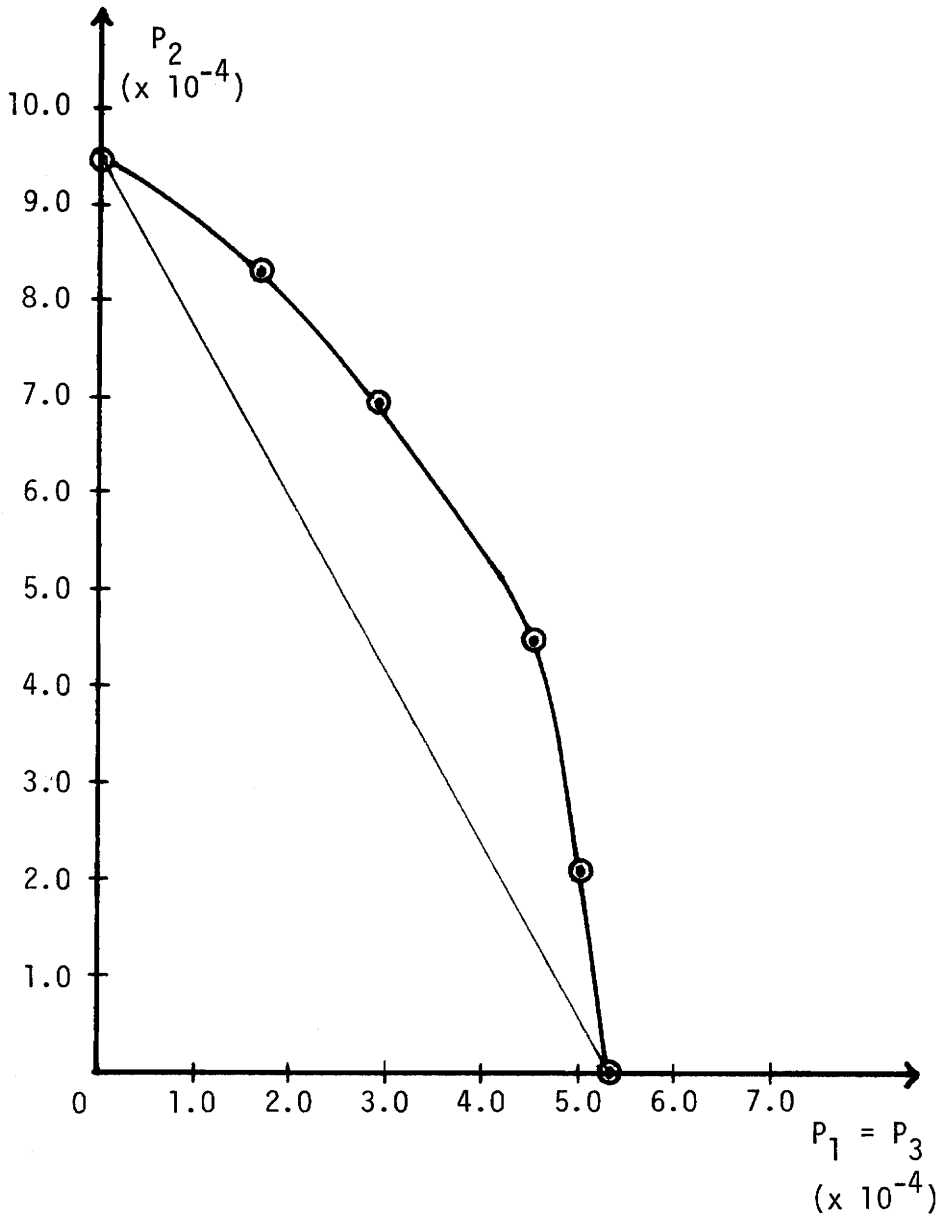
FIGURE 5.11: P_2 vs. $P_1 = P_3$ Interaction Curve for a Parabolic Arch without Damping Under Step Loads

FIGURE 5.12: P_1 vs. P_3 Interaction Curve for a Parabolic
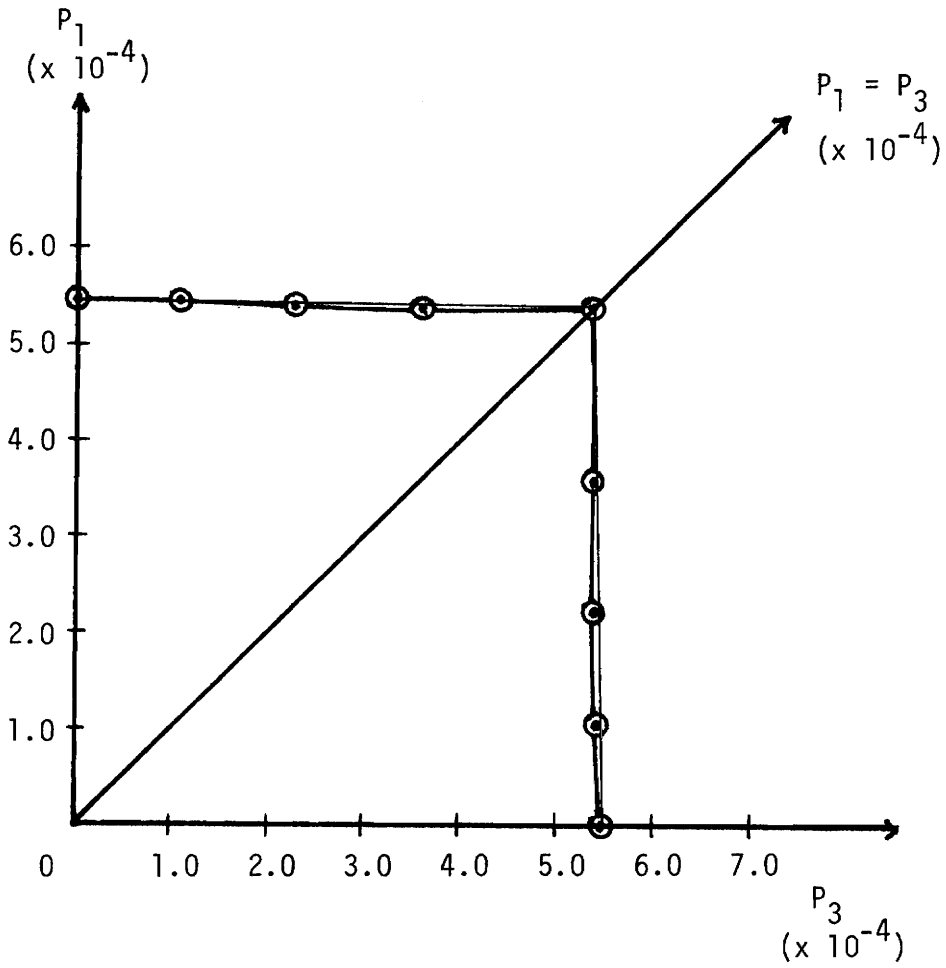Arch without Damping Under Step Loads

c. Eccentric Arch without Damping

In this problem, the interaction curves are determined for an eccentric shallow arch with no velocity dependent damping.

The buckling loads are listed in Table 5.4, and the interaction curves are presented in Figs. 5.13, 5.14, 5.15, and 5.16.

The P_2 vs. P_1 interaction curve, given in Fig. 5.13, is convex toward the origin. The P_2 vs. P_3 interaction curve, given in Fig. 5.14, can be approximated by a straight line connecting the buckling load on the P_2 axis to the buckling load on the P_3 axis. The P_2 vs. $P_1 = P_3$ interaction curve, given in Fig. 5.15, is concave toward the origin. The P_1 vs. P_3 interaction curve, given in Fig. 5.16, can be approximated by the straight lines connecting the buckling load on the P_1 axis to the buckling load on the $P_1 = P_3$ axis and the buckling load on the P_3 axis to the buckling load on the $P_1 = P_3$ axis.

After buckling, the arch does not remain in the buckled region, but snaps back to the unbuckled region, with the motion oscillating between the two regions.

The buckling load on the P_2 axis "bounces." Also, the buckling loads to the right of and near to the $P_1 = P_3$ axis of the P_1 vs. P_3 interaction curve "bounce."

The buckling loads of this problem are less than the static buckling loads determined by Welton [36] for the same eccentric arch, except for rays 10, 11, and 12. (See Fig. 5.15.) Also, the interaction curves of this problem, except for the P_1 vs. P_3 inter-

action curve, have a shape similar to the static interaction curves determined by Welton [36] for the same eccentric arch.

Finally, the change in the values of the buckling loads due to the use of different durations of time for the numerical integration is determined for a limited number of the buckling loads. For a duration of 200.0, the values of the buckling loads increase by up to 20% of the values listed in Table 5.4. For a duration of 400.0, the values of the buckling loads decrease by less than 3% of the values listed in Table 5.4. This verifies that the chosen duration of 300.0 for the numerical integration is appropriate.

TABLE 5.4

Non-Dimensional Buckling Loads for an
Eccentric Arch without Damping Under Step Loads

| Axis or Ray	P_1 $(\times 10^{-4})$	P_2 $(\times 10^{-4})$	P_3 $(\times 10^{-4})$
P_1 axis	5.32	0.0	0.0
P_2 axis	0.0	9.15	0.0
P_3 axis	0.0	0.0	5.55
$P_1 = P_3$ axis	5.19	0.0	5.19
ray 1	4.16	1.72	0.0
ray 2	3.21	3.21	0.0
ray 3	2.11	5.09	0.0
ray 4	1.31	6.59	0.0
ray 5	0.0	1.79	4.33
ray 6	0.0	3.34	3.34
ray 7	0.0	5.29	2.19
ray 8	0.0	6.84	1.36
ray 9	4.78	1.98	4.78
ray 10	4.02	4.02	4.02
ray 11	2.63	6.35	2.63
ray 12	1.60	8.04	1.60
ray 13	1.09	0.0	5.48
ray 14	2.26	0.0	5.46
ray 15	3.65	0.0	5.46
ray 16	5.25	0.0	3.51
ray 17	5.24	0.0	2.17
ray 18	5.28	0.0	1.05
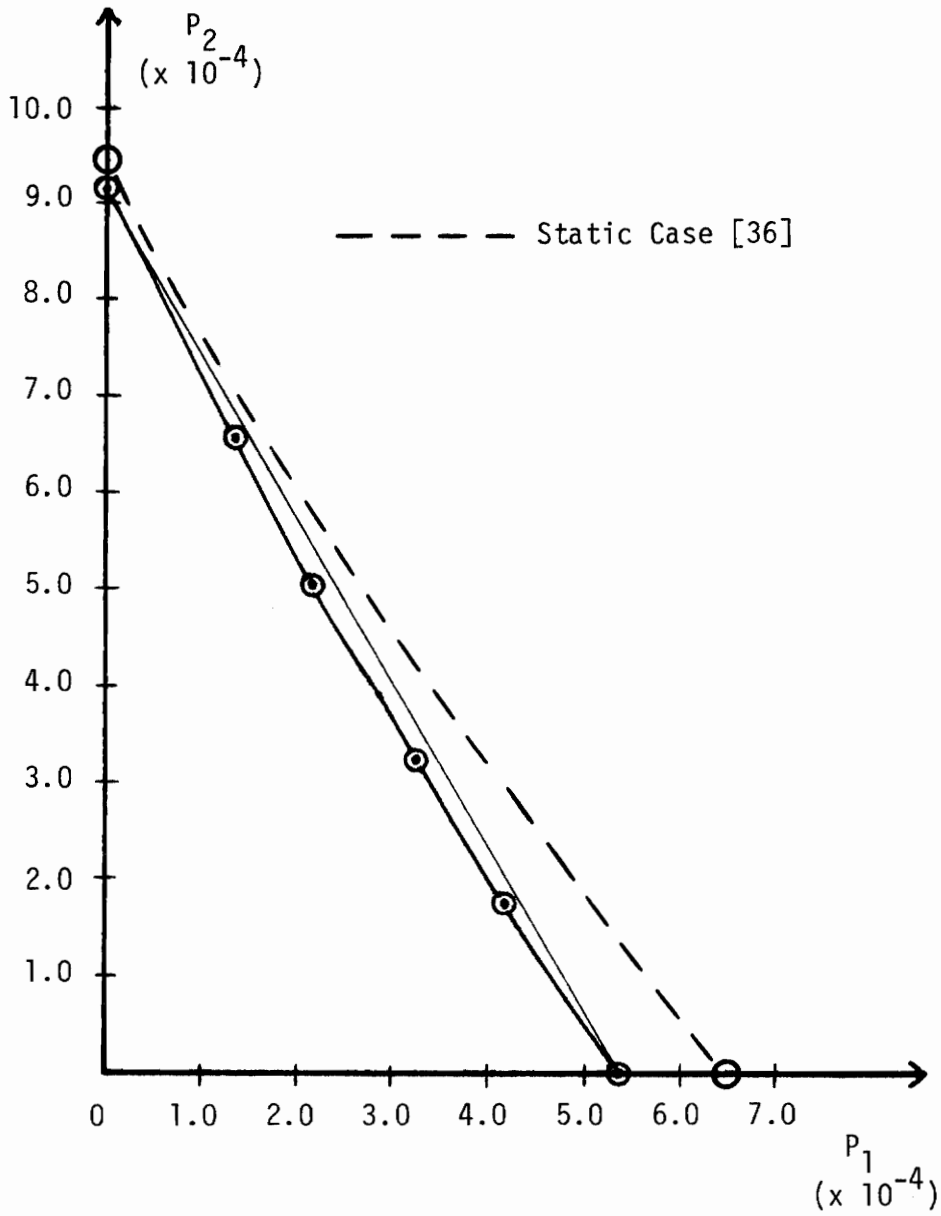
FIGURE 5.13: P_2 vs. P_1 Interaction Curve for an Eccentric Arch without Damping Under Step Loads
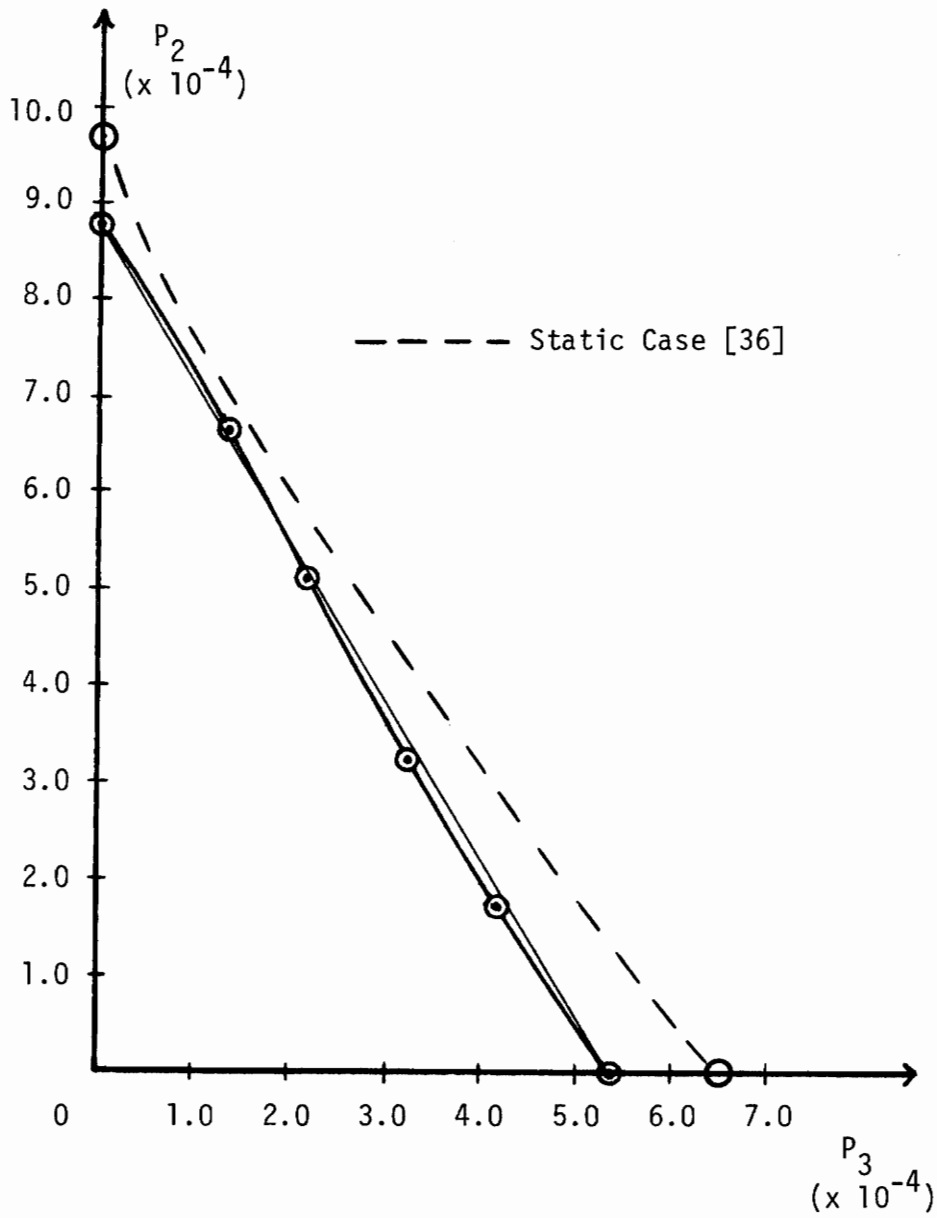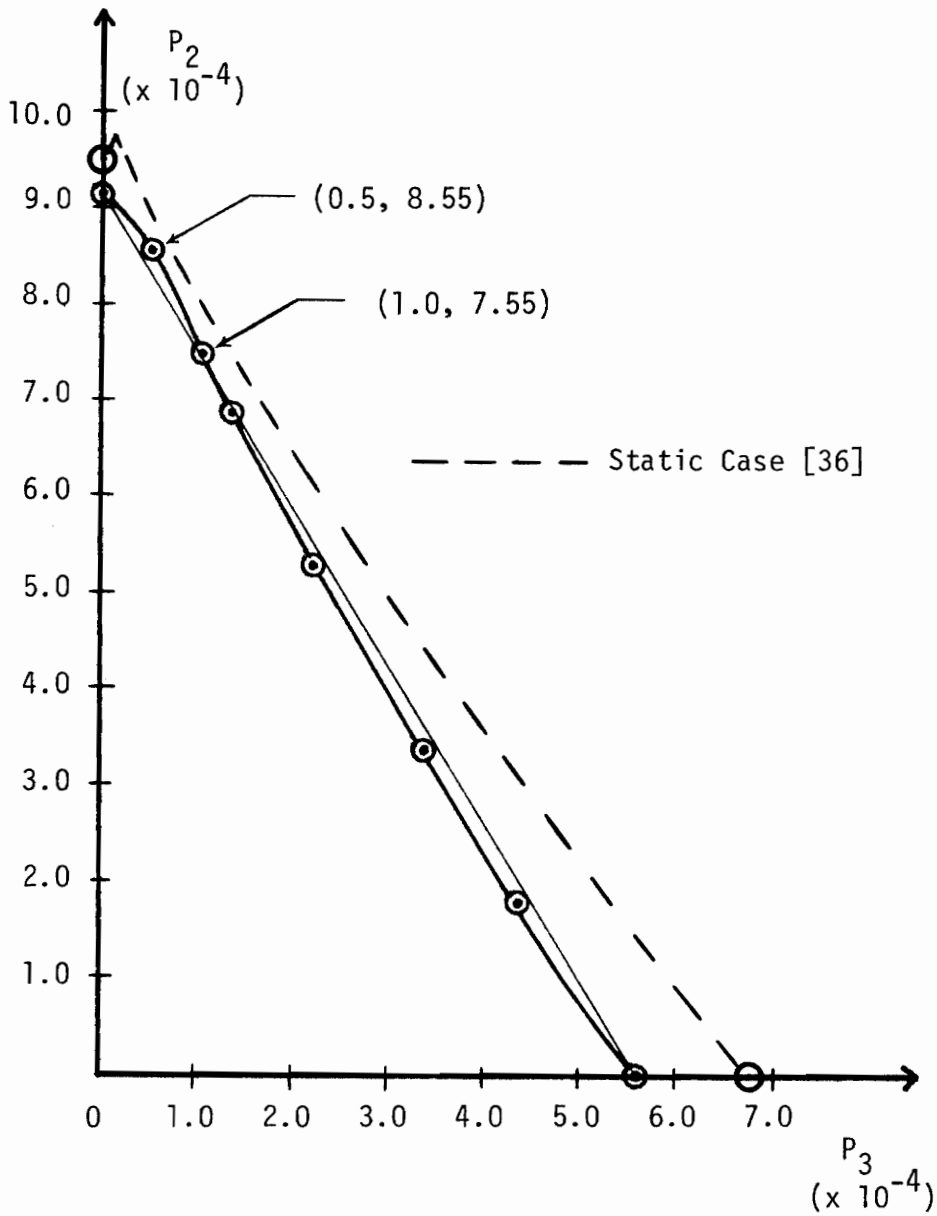
FIGURE 5.14: P_2 vs. P_3 Interaction Curve for an Eccentric
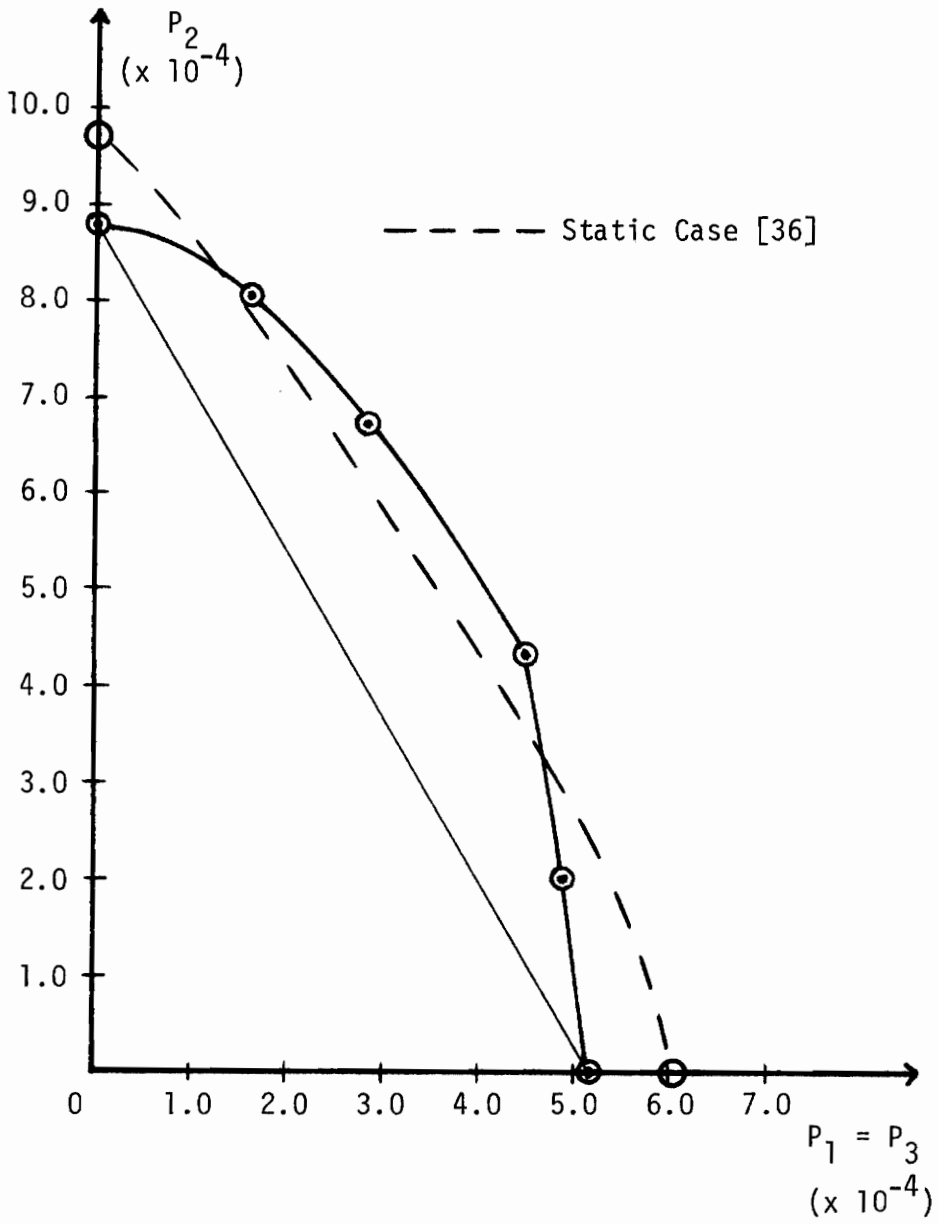Arch without Damping Under Step Loads

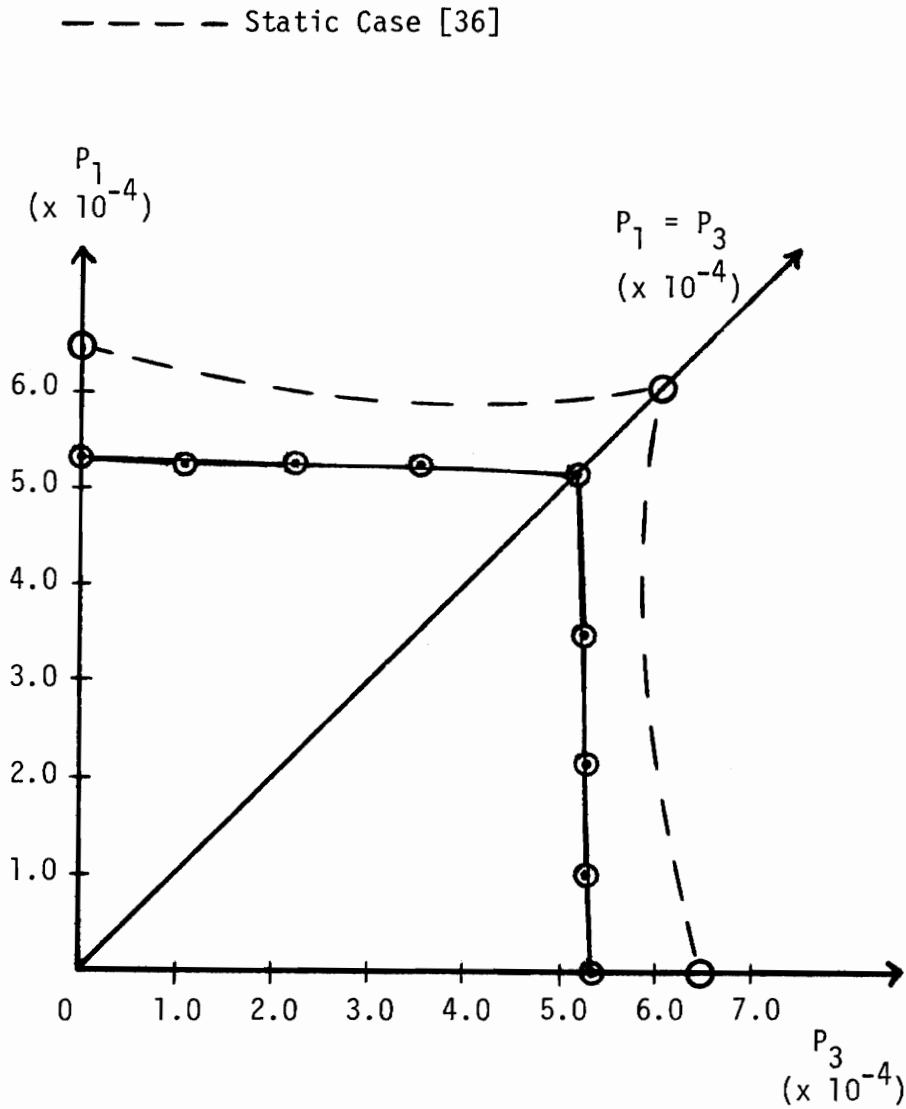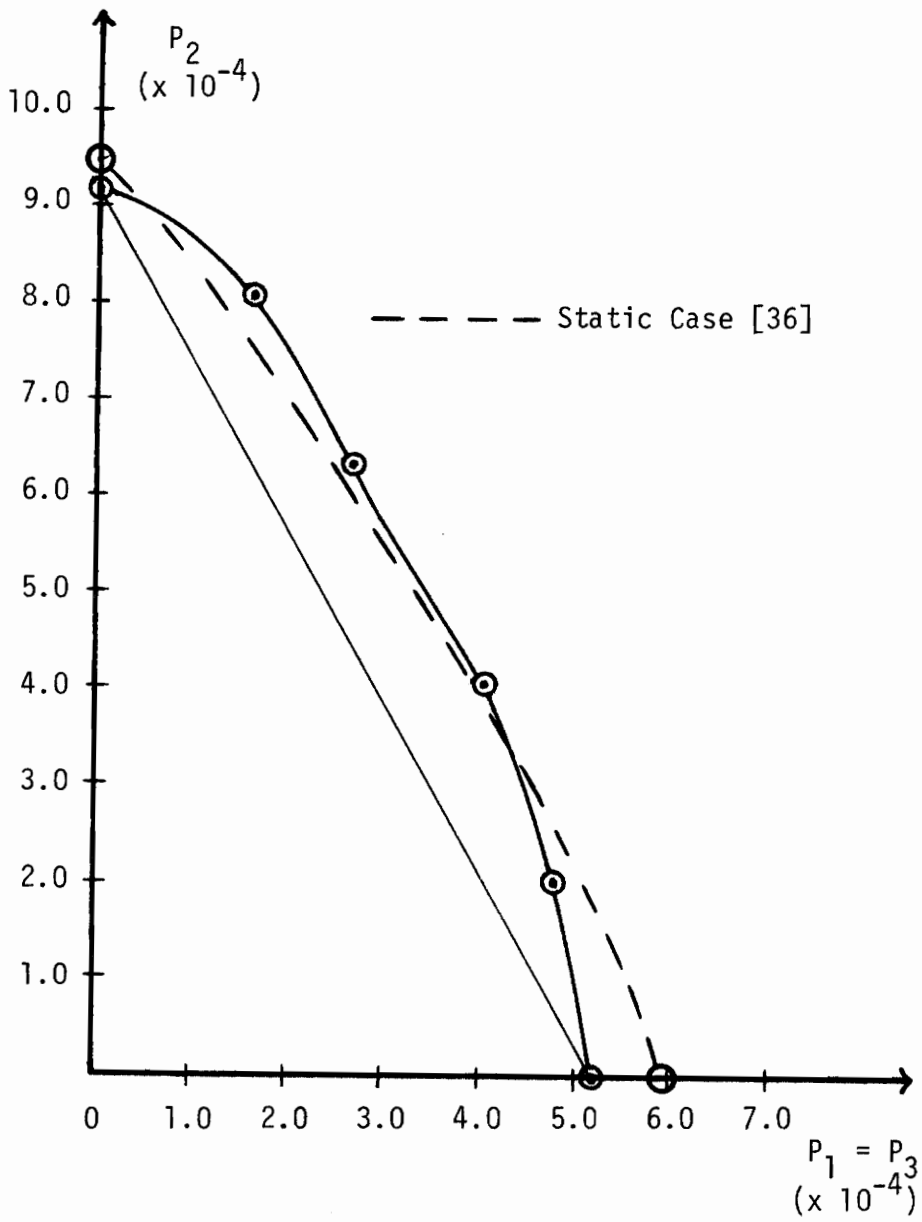FIGURE 5.15: P_2 vs. $P_1 = P_3$ Interaction Curve for an Eccentric Arch without Damping Under Step Loads
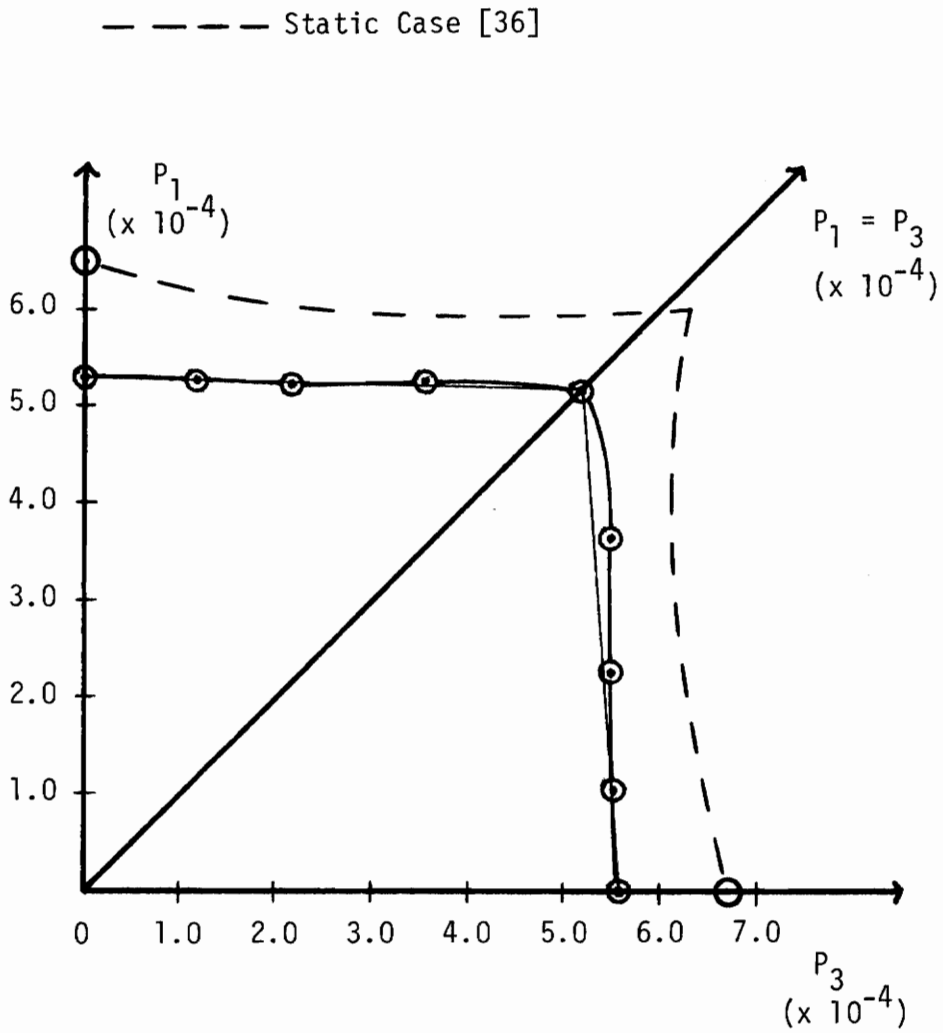
FIGURE 5.16: P_1 vs. P_3 Interaction Curve for an Eccentric
Arch without Damping Under Step Loads

5.3 Impulse Loads

All of the loads for the two problems discussed below are impulse loads, which impart initial velocities to the arch. The relationships between the impulse loads and the initial velocities are derived and listed in Appendix A-3. Thus, the numerical integration of the model's nondimensional nonlinear equations of motion is performed for no loads, but with the initial velocities imparted by the impulse loads.

a. Parabolic Arch without Damping

In this problem, the interaction curves are determined for a parabolic shallow arch with no velocity dependent damping.

The buckling loads are listed in Table 5.5, and the interaction curves are presented in Figs. 5.17, 5.18, 5.19, and 5.20.

All of the interaction curves, given in Figs. 5.17, 5.18, 5.19, and 5.20, are concave toward the origin.

After buckling, the arch does not remain in the buckled region, but snaps back to the unbuckled region, with the motion oscillating between the two regions.

All of the buckling loads, except those for rays 16, 17, and 18 of the $\hat{P}_1$ vs. $\hat{P}_3$ interaction curve, "bounce." The "bouncing" of the buckling loads does not appear until the last of the three digits of the buckling loads is determined. Because of this, the buckling loads listed in Table 5.5 are not the lowest buckling loads. Limited study, using incremental loading, shows that the value of the lowest buckling loads may be up to, if not more than, 5% less than the values listed

in Table 5.5. The lowest buckling loads are not determined in this
study, due to a lack of time. (See section 6.2.)

Finally, limited study, using incremental loading and a
duration of time of 400.0 for the numerical integration, shows that
the values of the buckling loads decrease by up to 5% of the values
listed in Table 5.5. Thus, for incremental loading, there is little
difference in the values of the buckling loads obtained by using
either a duration of 300.0 or 400.0. This verifies that the chosen
duration of 300.0 for the numerical integration is appropriate.

TABLE 5.5

Non-Dimensional Buckling Loads for a
Parabolic Arch without Damping Under Impulse Loads

Axis or Ray	$\hat{P}_1$ (x 10^{-2})	$\hat{P}_2$ (x 10^{-2})	$\hat{P}_3$ (x 10^{-2})
$\hat{P}_1$ axis	2.37	0.0	0.0
$\hat{P}_2$ axis	0.0	2.33	0.0
$\hat{P}_3$ axis	0.0	0.0	2.36
$\hat{P}_1=\hat{P}_3$ axis	1.51	0.0	1.51
ray 1	2.52	1.04	0.0
ray 2	2.01	2.01	0.0
ray 3	1.05	2.53	0.0
ray 4	0.53	2.66	0.0
ray 5	0.0	1.01	2.43
ray 6	0.0	1.85	1.85
ray 7	0.0	2.49	1.03
ray 8	0.0	2.51	0.50
ray 9	1.55	0.64	1.55
ray 10	1.61	1.61	1.61
ray 11	1.04	2.51	1.04
ray 12	0.52	2.61	0.52
ray 13	0.43	0.0	2.17
ray 14	0.89	0.0	2.14
ray 15	1.28	0.0	1.91
ray 16	1.95	0.0	1.30
ray 17	2.15	0.0	0.89
ray 18	2.31	0.0	0.46

FIGURE 5.17: $\hat{P}_2$ vs. $\hat{P}_1$ Interaction Curve for a Parabolic
Arch without Damping Under Impulse Loads

FIGURE 5.18: $\hat{P}_2$ vs. $\hat{P}_3$ Interaction Curve for a Parabolic Arch without Damping Under Impulse Loads

FIGURE 5.19: $\hat{P}_2$ vs. $\hat{P}_1 = \hat{P}_3$ Interaction Curve for a Parabolic Arch without Damping Under Impulse Loads
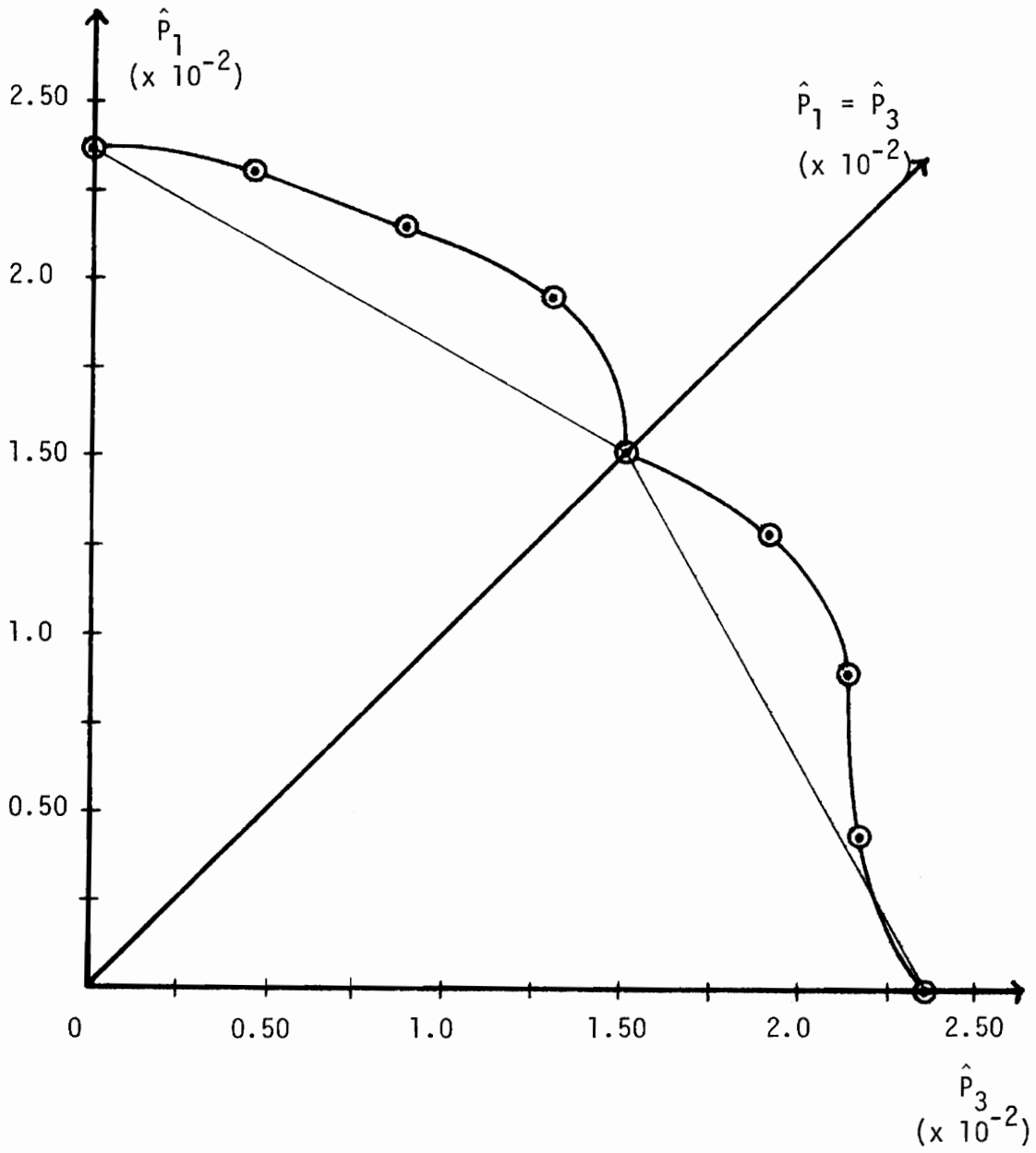
FIGURE 5.20: $\hat{P}_1$ vs. $\hat{P}_3$ Interaction Curve for a Parabolic Arch without Damping Under Impulse Loads

b. Eccentric Arch without Damping

In this problem, the interaction curves are determined for an eccentric shallow arch with no velocity dependent damping.

The buckling loads are listed in Table 5.6, and the interaction curves are presented in Figs. 5.21, 5.22, 5.23, and 5.24.

All of the interaction curves, given in Figs. 5.21, 5.22, 5.23, and 5.24, are concave toward the origin.

After buckling, the arch does not remain in the buckled region, but snaps back to the unbuckled region, with the motion oscillating between the two regions.

All of the buckling loads, except those for rays 16, 17, and 18 of the $\hat{P}_1$ vs. $\hat{P}_3$ interaction curve, "bounce." The "bouncing" of the buckling loads does not appear until the last of the three digits of the buckling loads is determined. Because of this, the buckling loads listed in Table 5.6 are not the lowest buckling loads. Limited study, using incremental loading, shows that the value of the lowest buckling loads may be up to, if not more than, 8% less than the values listed in Table 5.6. The lowest buckling loads are not determined in this study, due to a lack of time. (See section 6.2.)

Finally, limited study, using incremental loading and a duration of time of 400.0 for the numerical integration, shows that the values of the buckling loads decrease by up to 14% of the values listed in Table 5.6. Thus, for incremental loading, there is approximately a 6% decrease in the values of the buckling loads

obtained by using a duration of 400.0 instead of a duration of 300.0. This verifies that the chosen duration of 300.0 for the numerical integration is appropriate.

TABLE 5.6

Non-Dimensional Buckling Loads for an
Eccentric Arch without Damping Under Impulse Loads

Axis or Ray	$\hat{P}_1$ (x 10^{-2})	$\hat{P}_2$ (x 10^{-2})	$\hat{P}_3$ (x 10^{-2})
$\hat{P}_1$ axis	2.35	0.0	0.0
$\hat{P}_2$ axis	0.0	2.39	0.0
$\hat{P}_3$ axis	0.0	0.0	2.41
$\hat{P}_1=\hat{P}_3$ axis	1.55	0.0	1.55
ray 1	2.52	1.04	0.0
ray 2	1.96	1.96	0.0
ray 3	1.12	2.70	0.0
ray 4	0.50	2.51	0.0
ray 5	0.0	1.00	2.41
ray 6	0.0	1.95	1.95
ray 7	0.0	2.56	1.06
ray 8	0.0	2.77	0.55
ray 9	1.65	0.68	1.65
ray 10	1.71	1.71	1.71
ray 11	1.04	2.51	1.04
ray 12	0.51	2.56	0.51
ray 13	0.46	0.0	2.31
ray 14	0.92	0.0	2.21
ray 15	1.38	0.0	2.07
ray 16	1.96	0.0	1.31
ray 17	2.15	0.0	0.89
ray 18	2.31	0.0	0.46
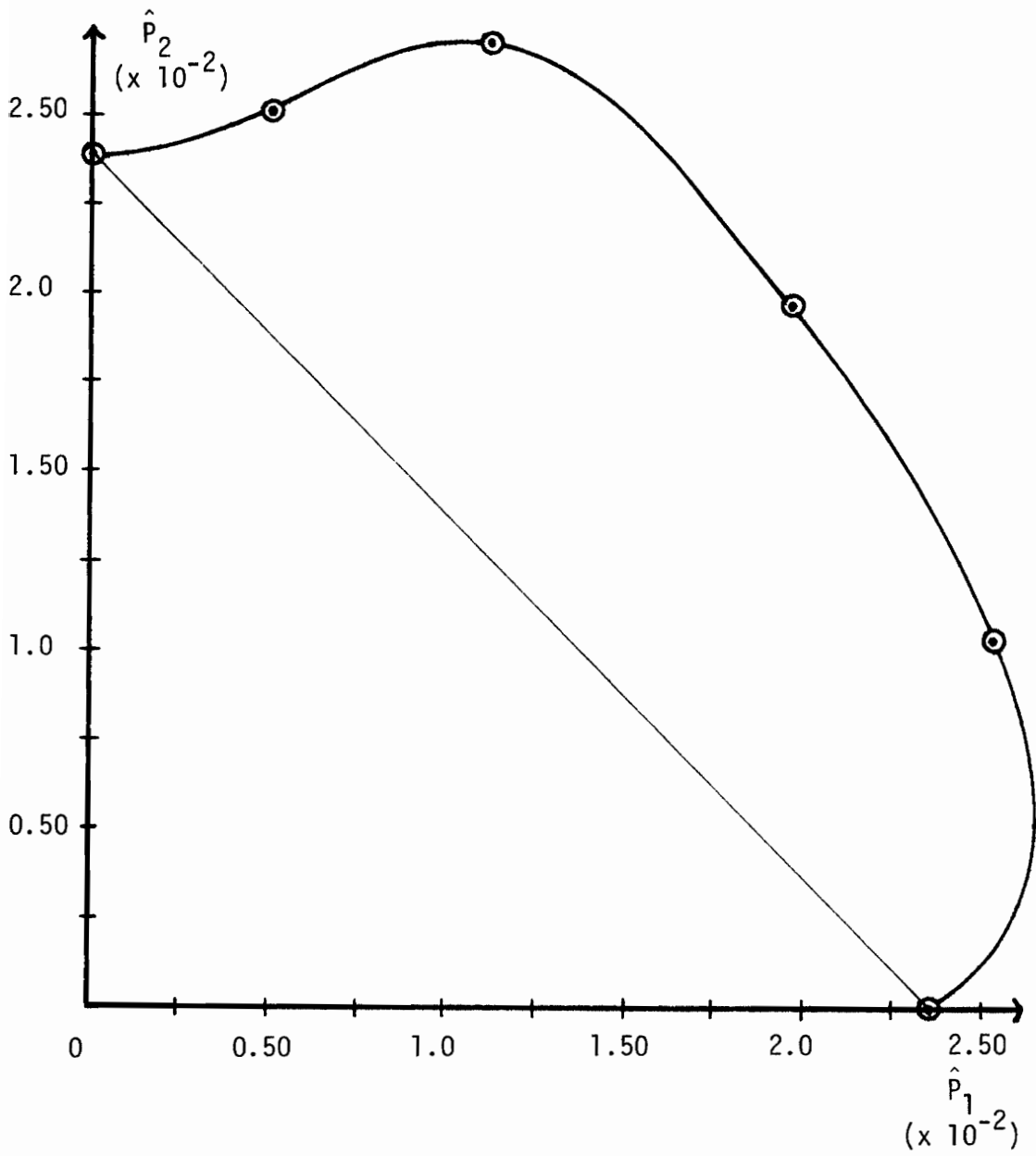
FIGURE 5.21: $\hat{P}_2$ vs. $\hat{P}_1$ Interaction Curve for an Eccentric Arch without Damping Under Impulse Loads
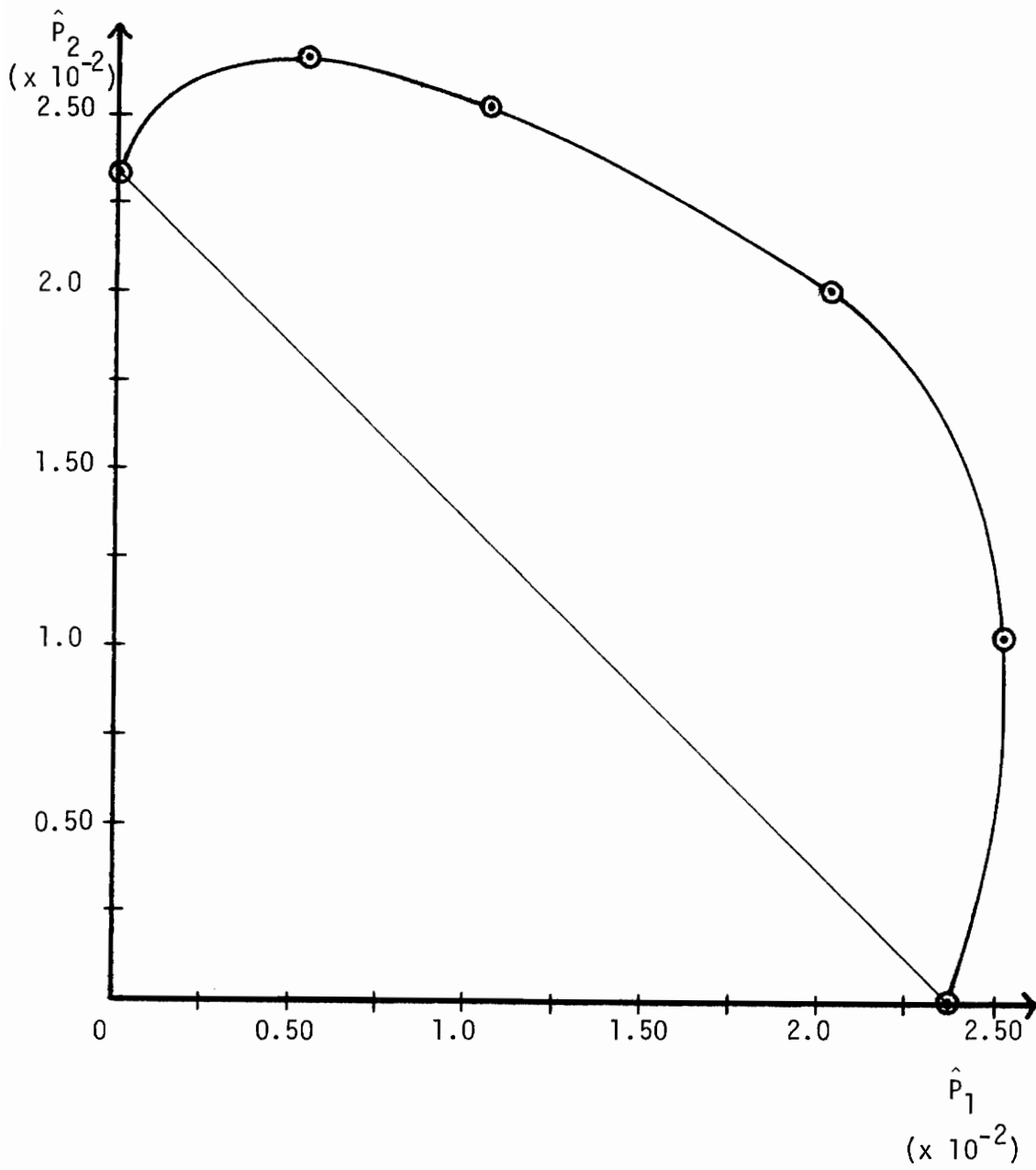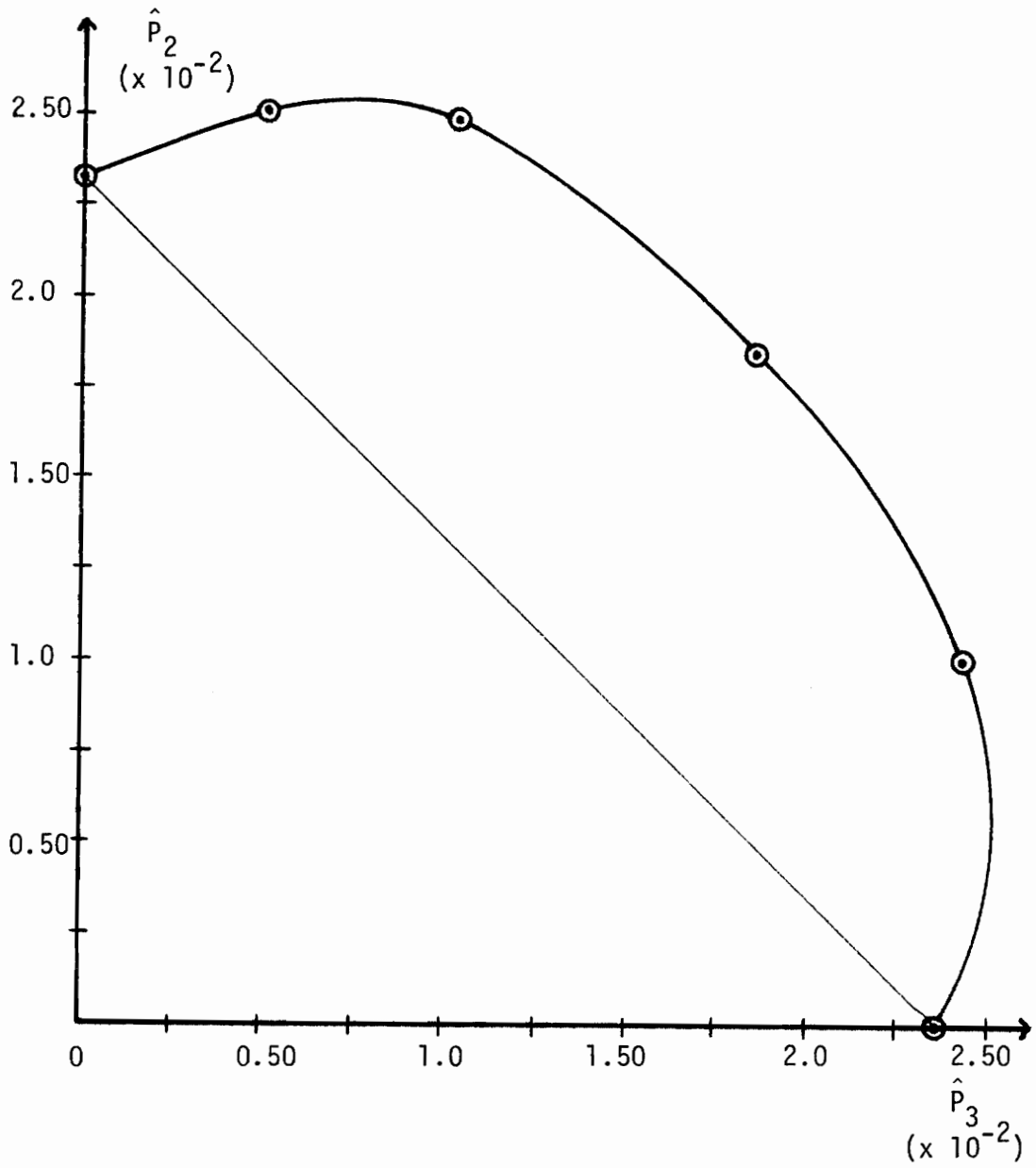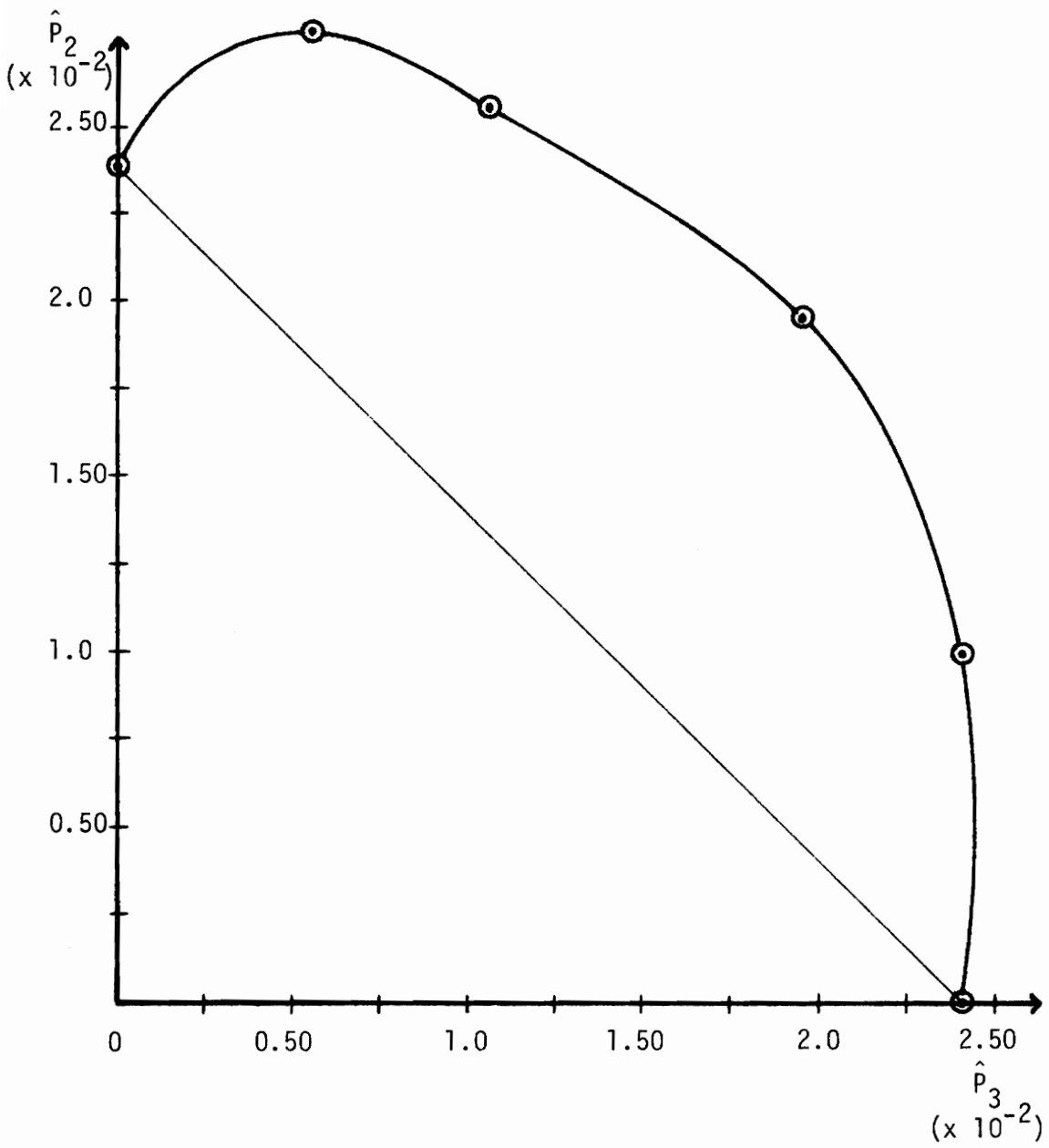
FIGURE 5.22: $\hat{P}_2$ vs. $\hat{P}_3$ Interaction Curve for an Eccentric
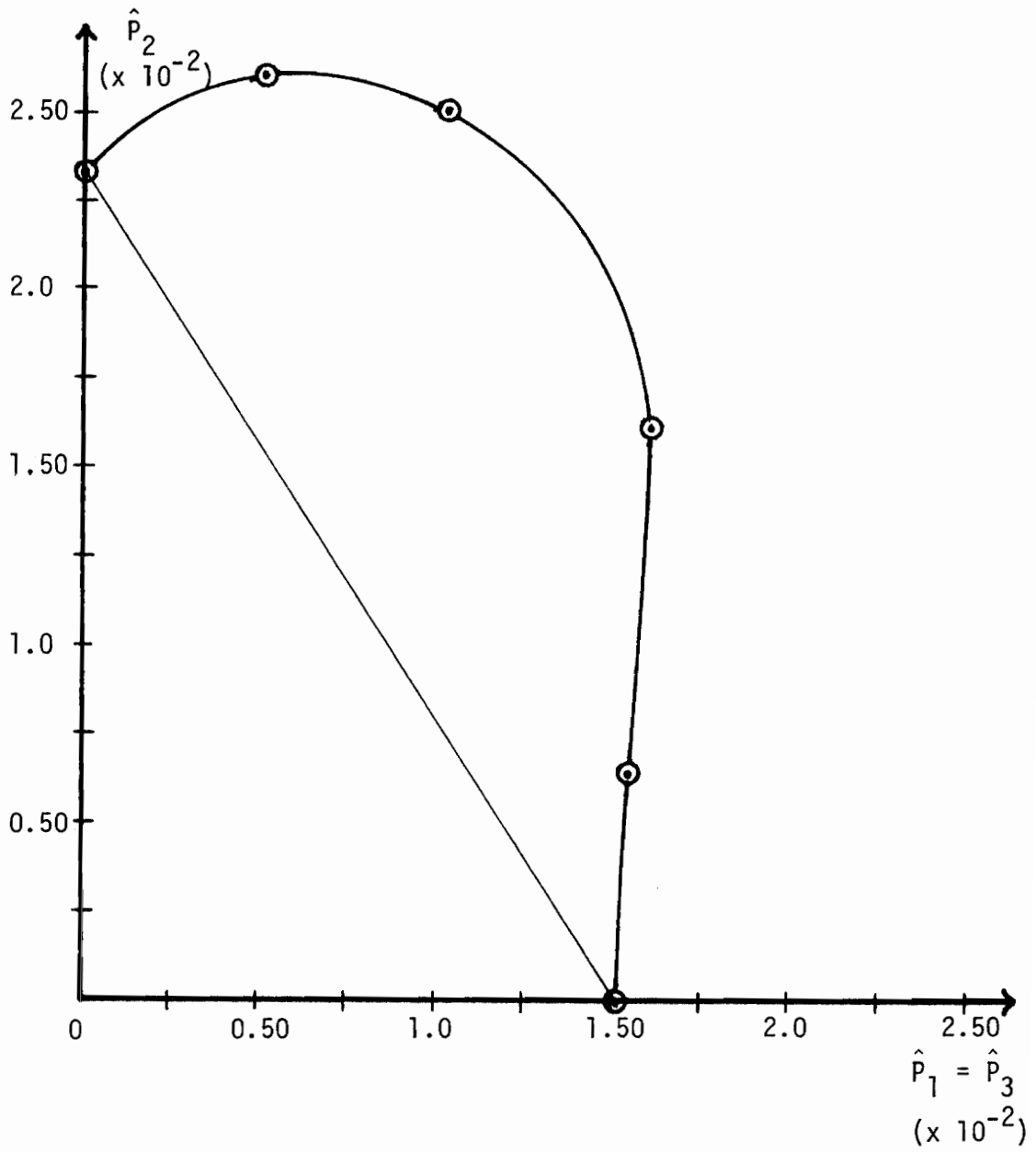Arch without Damping Under Impulse Loads
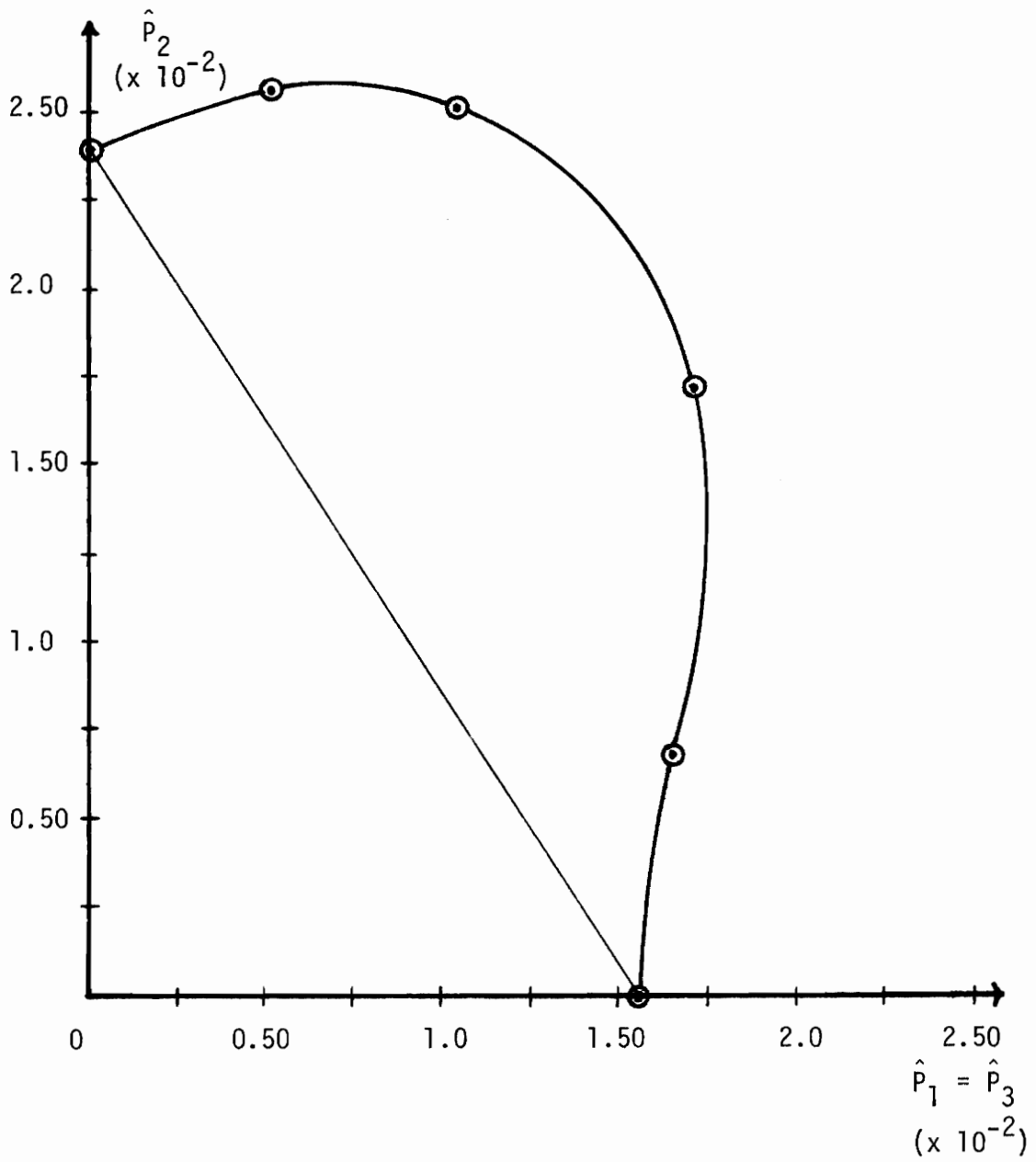
FIGURE 5.23: $\hat{P}_2$ vs. $\hat{P}_1 = \hat{P}_3$ Interaction Curve for an Eccentric Arch without Damping Under Impulse Loads
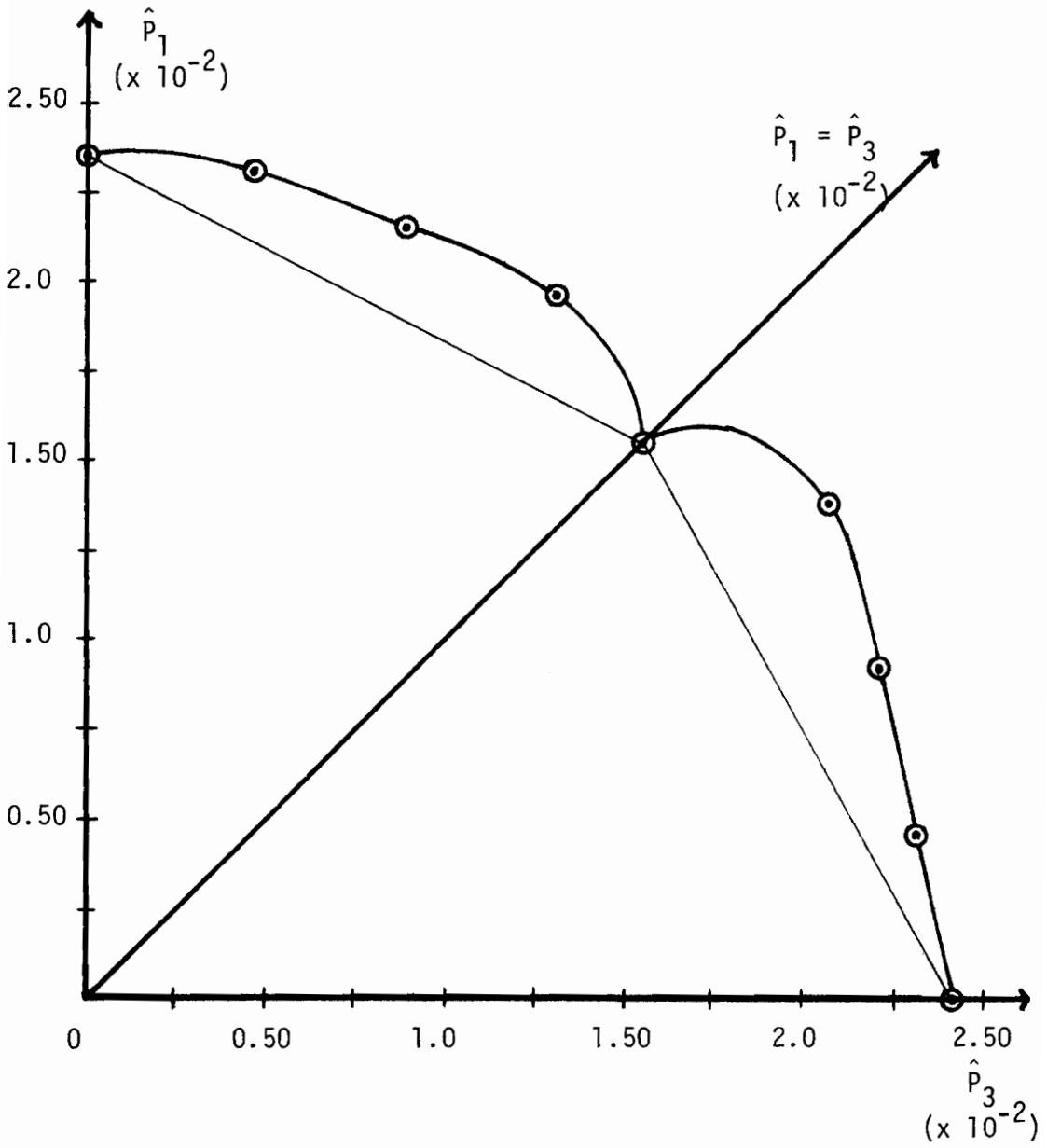
FIGURE 5.24: $\hat{P}_1$ vs. $\hat{P}_3$ Interaction Curve for an Eccentric Arch without Damping Under Impulse Loads

CHAPTER 6

SUMMARY

This chapter contains the conclusions of this study, which are drawn from the results presented. Also contained are the suggestions for further study, which are prompted by the results and conclusions of this study.

6.1 Conclusions

The conclusions drawn from the results of this study are enumerated and listed below.

1. For step loads with no damping, a comparison between the parabolic arch and the eccentric arch shows that the shapes of the P_2 vs. P_3 and P_2 vs. $P_1 = P_3$ interaction curves are similar, while the shapes of the P_2 vs. P_1 and P_1 vs. P_3 interaction curves differ slightly. Also, a comparison between the values of the buckling loads (Tables 5.3 and 5.4) shows that they differ only slightly.

   For impulse loads with no damping, a comparison between the parabolic arch and the eccentric arch shows that the shapes of the $\hat{P}_2$ vs. $\hat{P}_3$ and $\hat{P}_2$ vs. $\hat{P}_1 = \hat{P}_3$ interaction curves are similar, while the shapes of the $\hat{P}_2$ vs. $\hat{P}_1$ and $\hat{P}_1$ vs. $\hat{P}_3$ interaction curves differ slightly. Also, a comparison between the values of the buckling loads (Tables 5.5 and 5.6) shows that they differ only slightly.

81

2. For the parabolic arch with no damping, a comparison between the step loads and the impulse loads shows that the shapes of the interaction curves are completely dissimilar, except that the P_2 vs. $P_1 = P_3$ and $\hat{P}_2$ vs. $\hat{P}_1 = \hat{P}_3$ interaction curves are concave toward the origin.

    For the eccentric arch with no damping, a comparison between the step loads and the impulse loads shows that the shapes of the interaction curves are completely dissimilar, except that the P_2 vs. $P_1 = P_3$ and $\hat{P}_2$ vs. $\hat{P}_1 = \hat{P}_3$ interaction curves are concave toward the origin.

3. For the parabolic arch, a comparison between the static case [36] and the dynamic case (step loads with no damping) shows that the shapes of the interaction curves differ slightly. Also, a comparison between the values of the buckling loads shows that the static buckling loads are larger than the dynamic buckling loads by 25% or less along an axis or ray, except for rays 10, 11, and 12 (Fig. 5.11), where the dynamic buckling loads are larger than the static buckling loads by 12% or less along a ray.

    For the eccentric arch, a comparison between the static case [36] and the dynamic case (step loads with no damping) shows that the shapes of the interaction curves differ slightly. Also, a comparison between the values of the buckling loads shows that the static buckling loads are larger than the dynamic buckling loads by 25% or less along an axis or ray, except for rays 10, 11, and 12 (Fig. 5.15), where the dynamic buckling loads are

larger than the static buckling loads by 7% or less along a ray.

4. For the parabolic arch under step loads, a comparison between damping and no damping shows that the shapes of the P_2 vs. $P_1 = P_3$ and P_1 vs. P_3 interaction curves are similar, while the shapes of the P_2 vs. P_1 and P_2 vs. P_3 interaction curves differ slightly. Also, a comparison between the values of the buckling loads (Tables 5.2 and 5.3) shows that they differ only slightly, with the damping producing larger loads.

5. For both the parabolic and eccentric arches with no damping under impulse loads, the values of the buckling loads (Tables 5.5 and 5.6) are unreliable because of the "bouncing" phenomenon in combination with the loading procedure used. (See sections 5.2.b and 5.1.)

6.2 Suggestions for Further Study

The suggestions for further study prompted by the results and conclusions of this study are enumerated and listed below.

1. For the parabolic arch with no damping under impulse loads, use incremental loading (incrementing the third digit by 1 from zero) to determine reliable values of the buckling loads and the extent of the "bouncing."

2. Because there was little difference between the parabolic arch and the eccentric arch for both step and impulse loads with no damping, increase the amount of eccentricity (shorten bar ④)

for the eccentric arch and determine if the shapes of the inter-
action curves are affected.

3. Increase the height of the parabolic arch (increase the value of
    α_1) and determine if the shapes of the interaction curves are
    affected. Also for the parabolic arch, vary the ratio of α_1 to
    α_2 for constant height and determine if the shapes of the inter-
    action curves are affected.

4. For the parabolic arch under impulse loads, apply damping to
    determine if the "bouncing" can be either eliminated or reduced.

5. Compare the results from the Newmark-Beta method to the results
    from a Runge-Kutta method, a Gear variable order method, or other
    methods to verify that the Newmark-Beta method is the most accurate
    for least execution time. (This was not done in this study because
    the two methods mentioned above were not available for use.)

APPENDIX A-1

BIBLIOGRAPHY

BIBLIOGRAPHY

1. Adeli, H., Gere, J. M., and Weaver, W., Jr., "Algorithms for Nonlinear Structural Dynamics," Journal of the Structural Division, ASCE, Vol. 104, No. ST2, Proc. Paper 13538, February, 1978, pp. 263-280.

2. Bathe, K. J., and Wilson, E. L., "Stability and Accuracy Analysis of Direct Integration Methods," International Journal of Earthquake Engineering and Structural Dynamics, Vol. 1, No. 3, January-March, 1973, pp. 283-291.

3. Bathe, K., and Wilson, E. L., Numerical Methods in Finite Element Analysis, Prentice-Hall, Inc., Englewood Cliffs, New Jersey, 1976.

4. Budiansky, B., and Roth, R. S., "Axisymmetric Dynamic Buckling of Clamped Shallow Spherical Shells," NASA TN D-1510, December, 1962, pp. 597-606.

5. Cheung, M. C., and Babcock, C. D., Jr., "An Energy Approach to the Dynamic Stability of Arches," Journal of Applied Mechanics, ASME, Vol. 37, No. 4, December, 1970, pp. 1012-1018.

6. Fulton, R. E., and Barton, F. W., "Dynamic Buckling of Shallow Arches," Journal of the Engineering Mechanics Division, ASCE, Vol. 97, No. EM3, Proc. Paper 8214, June, 1971, pp. 865-877.

7. Hegemier, G. A., and Tzung, F., "Influence of Damping on the Snapping of a Shallow Arch Under a Step Pressure Load," AIAA Journal, Vol. 7, No. 8, August, 1969, pp. 1494-1499.

8. Hoff, N. J., and Bruce, V. G., "Dynamic Analysis of the Buckling of Laterally Loaded Flat Arches," Journal of Mathematics and Physics, Vol. 32, No. 4, January, 1954, pp. 276-288.

9. Holzer, S. M., "Lecture Notes on CE 6020 - Dynamics of Structures," Virginia Polytechnic Institute and State University, Spring Quarter, 1977, Blacksburg, Virginia.

10. Horne, D. B., "Objective Functions for Nonlinear Structural Analysis," thesis submitted to the Graduate Faculty of the Virginia Polytechnic Institute and State University in partial fulfillment of the requirements for the degree of Master of Science in Civil Engineering, July, 1978, Blacksburg, Virginia.

11. Hsu, C. S., "On Dynamic Stability of Elastic Bodies with Prescribed Initial Conditions," International Journal of Engineering Science, Vol. 4, No. 1, March, 1966, pp. 1-21.

12. Hsu, C. S., "The Effects of Various Parameters on the Dynamic Stability of a Shallow Arch," Journal of Applied Mechanics, ASME, Vol. 34, No. 2, June, 1967, pp. 349-358.

13. Hsu, C. S., "Stability of Shallow Arches Against Snap-Through Under Timewise Step Loads," Journal of Applied Mechanics, ASME, Vol. 35, No. 1, March, 1968, pp. 31-39.

14. Hsu, C. S. "Equilibrium Configurations of a Shallow Arch of Arbitrary Shape and Their Dynamic Stability Character," International Journal of Non-Linear Mechanics, Vol. 3, No. 2, June, 1968, pp. 113-136.

15. Hsu, C. S., Kuo, C. T., and Plaut, R. H., "Dynamic Stability Criteria for Clamped Shallow Arches Under Timewise Step Loads," AIAA Journal, Vol. 7, No. 10, October, 1969, pp. 1925-1931.

16. Humphreys, J. S., "On Dynamic Snap Buckling of Shallow Arches," AIAA Journal, Vol. 4, No. 5, May, 1966, pp. 878-886.

17. Johnson, E. R., and McIvor, I. K., "The Effect of Spatial Distribution on Dynamic Snap-Through," Journal of Applied Mechanics, ASME, to appear.

18. Langhaar, H. L., Energy Methods in Applied Mechanics, John Wiley and Sons, Inc., New York, 1962.

19. Lo, D. L. C., and Masur, E. F., "Dynamic Buckling of Shallow Arches," Journal of the Engineering Mechanics Division, ASCE, Vol. 102, No. EM5, Proc. Paper 12493, October, 1976, pp. 901-917.

20. Lock, M. H., "Snapping of a Shallow Sinusoidal Arch Under a Step Pressure Load," AIAA Journal, Vol. 4, No. 7, July, 1966, pp. 1249-1256.

21. Lock, M. H., "Effect of Rise Time on Critical Dynamic Load," AIAA Journal, Vol. 6, No. 1, January, 1968, pp. 162-164.

22. McIvor, I. K., "Dynamic Buckling of Shallow Arches," Journal of the Engineering Mechanics Division, ASCE, Vol. 98, No. EM2, Discussion, April, 1972, pp. 478-481.

23. Meirovitch, L., Methods of Analytical Dynamics, McGraw-Hill Book Company, New York, 1970.

24. Meirovitch, L., Elements of Vibration Analysis, McGraw-Hill Book Company, New York, 1975.

25. Newmark, N. M., "A Method of Computation for Structural Dynamics," Journal of the Engineering Mechanics Division, ASCE, Vol. 85, No. EM3, Proc. Paper 2094, July, 1959, pp. 67-94.

26. Nickell, R. E., "Direct Integration Methods in Structural Dynamics," Journal of the Engineering Mechanics Division, ASCE, Vol. 99, No. EM2, Proc. Paper 9652, April, 1973, pp. 303-317.

27. Ovenshire, L. J., and McIvor, I. K., "On the Dynamic Snap-Through of a Shallow Cylindrical Shell Subject to Nearly Symmetric Impulsive Loading," International Journal of Solids and Structures, Vol. 7, No. 6, June, 1971, pp. 585-601.

28. Ovenshire, L. J., and McIvor, I. K., "Conditions for the Existence of Dynamic Snap-Through of a Shallow Cylindrical Shell Under Impulsive Loading," International Journal of Non-Linear Mechanics, Vol. 7, No. 1, February, 1972, pp. 19-29.

29. Plaut, R. H., "Stability of Shallow Arches Under Multiple Loads," Journal of the Engineering Mechanics Division, ASCE, to appear.

30. Popelar, C. H., and Abraham, G. M., "A Comparison of Initial Velocities for Dynamic Instability of a Shallow Arch," Developments in Theoretical and Applied Mechanics, Vol. 5, Proceedings of the Fifth Southeastern Conference on Theoretical and Applied Mechanics held in Raleigh-Durham, North Carolina, April 16-17, 1970, pp. 745-762.

31. Rapp, I. H., Smith, C. V., Jr., and Simitses, G. J., "Dynamic Snap-Through Buckling of Shallow Arches with Nonuniform Stiffness," ASME Paper No. 75-DET-41.

32. Reed, R. R., and Broyles, R. W., "Dynamic Buckling of a Two-Degree-of-Freedom Mechanism," International Journal of Mechanical Sciences, Vol. 12, No. 3, March, 1970, pp. 209-229.

33. Spiegel, M. R., Theory and Problems of Theoretical Mechanics, Schaum's Outline Series, McGraw-Hill Book Company, New York, 1967.

34. Sundararajan, V., and Kumani, D. S., "Dynamic Snap-Buckling of Shallow Arches Under Inclined Loads," AIAA Journal, Vol. 10, No. 8, August, 1972, pp. 1090-1091.

35. Wells, D. A., Theory and Problems of Lagrangian Dynamics, Schaum's Outline Series, McGraw-Hill Book Company, New York, 1967.

36. Welton, R. H. B., III, "Stability Analysis of Arch Models Under Multiple Loads," thesis submitted to the Graduate Faculty of the Virginia Polytechnic Institute and State University in partial fulfillment of the requirements for the degree of Master of Science in Civil Engineering, May, 1977, Blacksburg, Virginia.

APPENDIX A-2

EQUATIONS OF MOTION

EQUATIONS OF MOTION

Definitions

$$L_1 \sin \theta_1 + L_2 \sin \theta_2 = L_3 \sin \theta_3 + L_4 \sin \theta_4$$

$$\theta_4 = \sin^{-1} \left[\frac{L_1}{L_4} \sin \theta_1 + \frac{L_2}{L_4} \sin \theta_2 - \frac{L_3}{L_4} \sin \theta_3 \right]$$

$$\dot{\theta}_4 = \frac{1}{\cos \theta_4} \left[\frac{L_1}{L_4} \dot{\theta}_1 \cos \theta_1 + \frac{L_2}{L_4} \dot{\theta}_2 \cos \theta_2 - \frac{L_3}{L_4} \dot{\theta}_3 \cos \theta_3 \right]$$

$$\ddot{\theta}_4 = \frac{1}{\cos \theta_4} \left[\frac{L_1}{L_4} \ddot{\theta}_1 \cos \theta_1 + \frac{L_2}{L_4} \ddot{\theta}_2 \cos \theta_2 - \frac{L_3}{L_4} \ddot{\theta}_3 \cos \theta_3 \right.$$

$$- \frac{L_1}{L_4} \dot{\theta}_1^2 \sin \theta_1 - \frac{L_2}{L_4} \dot{\theta}_2^2 \sin \theta_2 + \frac{L_3}{L_4} \dot{\theta}_3^2 \sin \theta_3$$

$$\left. + \dot{\theta}_4^2 \sin \theta_4 \right]$$

Definitions

$$\frac{\partial \theta_4}{\partial \theta_1} = \frac{\partial \dot{\theta}_4}{\partial \dot{\theta}_1} = \frac{L_1}{L_4} \frac{\cos \theta_1}{\cos \theta_4}$$

$$\frac{\partial \theta_4}{\partial \theta_2} = \frac{\partial \dot{\theta}_4}{\partial \dot{\theta}_2} = \frac{L_2}{L_4} \frac{\cos \theta_2}{\cos \theta_4}$$

$$\frac{\partial \theta_4}{\partial \theta_3} = \frac{\partial \dot{\theta}_4}{\partial \dot{\theta}_3} = - \frac{L_3}{L_4} \frac{\cos \theta_3}{\cos \theta_4}$$

$$\frac{\partial \dot{\theta}_4}{\partial \theta_1} = \frac{d}{dt} \left[\frac{\partial \dot{\theta}_4}{\partial \dot{\theta}_1} \right] = - \frac{L_1}{L_4} \dot{\theta}_1 \frac{\sin \theta_1}{\cos \theta_4}$$
$$+ \frac{L_1}{L_4} \frac{\cos \theta_1}{(\cos \theta_4)^2} \dot{\theta}_4 \sin \theta_4$$

$$\frac{\partial \dot{\theta}_4}{\partial \theta_2} = \frac{d}{dt} \left[\frac{\partial \dot{\theta}_4}{\partial \dot{\theta}_2} \right] = - \frac{L_2}{L_4} \dot{\theta}_2 \frac{\sin \theta_2}{\cos \theta_4}$$
$$+ \frac{L_2}{L_4} \frac{\cos \theta_2}{(\cos \theta_4)^2} \dot{\theta}_4 \sin \theta_4$$

$$\frac{\partial \dot{\theta}_4}{\partial \theta_3} = \frac{d}{dt} \left[\frac{\partial \dot{\theta}_4}{\partial \dot{\theta}_3} \right] = \frac{L_3}{L_4} \dot{\theta}_3 \frac{\sin \theta_3}{\cos \theta_4}$$
$$- \frac{L_3}{L_4} \frac{\cos \theta_3}{(\cos \theta_4)^2} \dot{\theta}_4 \sin \theta_4$$

Kinetic Energy and Its Derivatives

Definitions

(note: refer to Eqs. 3.19 thru 3.23, pp. 19-20)

$$v_{x_i} = \frac{d}{dt}(S_{x_i}) \, , \qquad i = 1, 2, 3, 4$$

$$v_{y_i} = \frac{d}{dt}(S_{y_i}) \, , \qquad i = 1, 2, 3, 4$$

$$v_i^2 = v_{x_i}^2 + v_{y_i}^2 \, , \qquad i = 1, 2, 3, 4$$

$$I_i = \frac{1}{12} m_i L_i^2 \, , \qquad i = 1, 2, 3, 4$$

$$\omega_i = \dot{\theta}_i \, , \qquad i = 1, 2, 3, 4$$

$$T = T_1 + T_2 + T_3 + T_4$$

$$\frac{\partial T}{\partial \theta_i} = \frac{\partial T_1}{\partial \theta_i} + \frac{\partial T_2}{\partial \theta_i} + \frac{\partial T_3}{\partial \theta_i} + \frac{\partial T_4}{\partial \theta_i} \, , \qquad i = 1, 2, 3$$

$$\frac{d}{dt}[\frac{\partial T}{\partial \dot{\theta}_i}] = \frac{d}{dt}[\frac{\partial T_1}{\partial \dot{\theta}_i}] + \frac{d}{dt}[\frac{\partial T_2}{\partial \dot{\theta}_i}] + \frac{d}{dt}[\frac{\partial T_3}{\partial \dot{\theta}_i}] + \frac{d}{dt}[\frac{\partial T_4}{\partial \dot{\theta}_i}] \, ,$$

$$i = 1, 2, 3$$

<u>Member 1</u>

$$S_{x_1} = \frac{L_1}{2} \cos \theta_1$$

$$S_{y_1} = \frac{L_1}{2} \sin \theta_1$$

$$v_{x_1} = -\frac{L_1}{2} \dot{\theta}_1 \sin \theta_1$$

$$v_{y_1} = \frac{L_1}{2} \dot{\theta}_1 \cos \theta_1$$

$$T_1 = \frac{1}{6} m_1 L_1^2 \dot{\theta}_1^2$$

$$\frac{\partial T_1}{\partial \theta_1} = \frac{\partial T_1}{\partial \theta_2} = \frac{\partial T_1}{\partial \theta_3} = 0$$

$$\frac{d}{dt} \left[\frac{\partial T_1}{\partial \dot{\theta}_1} \right] = \frac{1}{3} m_1 L_1^2 \ddot{\theta}_1$$

$$\frac{d}{dt} \left[\frac{\partial T_1}{\partial \dot{\theta}_2} \right] = \frac{d}{dt} \left[\frac{\partial T_1}{\partial \dot{\theta}_3} \right] = 0$$

Member 2

$$S_{x_2} = L_1 \cos \theta_1 + \frac{L_2}{2} \cos \theta_2$$

$$S_{y_2} = L_1 \sin \theta_1 + \frac{L_2}{2} \sin \theta_2$$

$$v_{x_2} = -L_1 \dot{\theta}_1 \sin \theta_1 - \frac{L_2}{2} \dot{\theta}_2 \sin \theta_2$$

$$v_{y_2} = L_1 \dot{\theta}_1 \cos \theta_1 + \frac{L_2}{2} \dot{\theta}_2 \cos \theta_2$$

$$T_2 = \frac{1}{2} m_2 L_1^2 \dot{\theta}_1^2 + \frac{1}{2} m_2 L_1 L_2 \dot{\theta}_1 \dot{\theta}_2 \cos (\theta_1 - \theta_2)$$

$$+ \frac{1}{6} m_2 L_2^2 \dot{\theta}_2^2$$

$$\frac{\partial T_2}{\partial \theta_1} = - \frac{1}{2} m_2 L_1 L_2 \dot{\theta}_1 \dot{\theta}_2 \sin (\theta_1 - \theta_2)$$

$$\frac{\partial T_2}{\partial \theta_2} = \frac{1}{2} m_2 L_1 L_2 \dot{\theta}_1 \dot{\theta}_2 \sin (\theta_1 - \theta_2)$$

$$\frac{\partial T_2}{\partial \theta_3} = 0$$

$$\frac{d}{dt} \left[\frac{\partial T_2}{\partial \dot{\theta}_1} \right] = m_2 L_1^2 \ddot{\theta}_1$$

$$+ \frac{1}{2} m_2 L_1 L_2 \ddot{\theta}_2 \cos (\theta_1 - \theta_2)$$

$$+ \frac{1}{2} m_2 L_1 L_2 \dot{\theta}_2^2 \sin (\theta_1 - \theta_2)$$

$$- \frac{1}{2} m_2 L_1 L_2 \dot{\theta}_1 \dot{\theta}_2 \sin (\theta_1 - \theta_2)$$

$$\frac{d}{dt} \left[\frac{\partial T_2}{\partial \dot{\theta}_2}\right] = \frac{1}{2} m_2 L_1 L_2 \ddot{\theta}_1 \cos(\theta_1 - \theta_2)$$

$$- \frac{1}{2} m_2 L_1 L_2 \dot{\theta}_1^2 \sin(\theta_1 - \theta_2)$$

$$+ \frac{1}{2} m_2 L_1 L_2 \dot{\theta}_1 \dot{\theta}_2 \sin(\theta_1 - \theta_2)$$

$$+ \frac{1}{3} m_2 L_2^2 \ddot{\theta}_2$$

$$\frac{d}{dt} \left[\frac{\partial T_2}{\partial \dot{\theta}_3}\right] = 0$$

Member 3

$$S_{x_3} = L_1 \cos \theta_1 + L_2 \cos \theta_2 + \frac{L_3}{2} \cos \theta_3$$

$$S_{y_3} = L_1 \sin \theta_1 + L_2 \sin \theta_2 - \frac{L_3}{2} \sin \theta_3$$

$$V_{x_3} = - L_1 \dot{\theta}_1 \sin \theta_1 - L_2 \dot{\theta}_2 \sin \theta_2 - \frac{L_3}{2} \dot{\theta}_3 \sin \theta_3$$

$$V_{y_3} = L_1 \dot{\theta}_1 \cos \theta_1 + L_2 \dot{\theta}_2 \cos \theta_2 - \frac{L_3}{2} \dot{\theta}_3 \cos \theta_3$$

$$T_3 = \frac{1}{2} m_3 L_1^2 \dot{\theta}_1^2 + m_3 L_1 L_2 \dot{\theta}_1 \dot{\theta}_2 \cos (\theta_1 - \theta_2)$$

$$- \frac{1}{2} m_3 L_1 L_3 \dot{\theta}_1 \dot{\theta}_3 \cos (\theta_1 + \theta_3)$$

$$+ \frac{1}{2} m_3 L_2^2 \dot{\theta}_2^2 - \frac{1}{2} m_3 L_2 L_3 \dot{\theta}_2 \dot{\theta}_3 \cos (\theta_2 + \theta_3)$$

$$+ \frac{1}{6} m_3 L_3^2 \dot{\theta}_3^2$$

$$\frac{\partial T_3}{\partial \theta_1} = - m_3 L_1 L_2 \dot{\theta}_1 \dot{\theta}_2 \sin (\theta_1 - \theta_2)$$

$$+ \frac{1}{2} m_3 L_1 L_3 \dot{\theta}_1 \dot{\theta}_3 \sin (\theta_1 + \theta_3)$$

$$\frac{\partial T_3}{\partial \theta_2} = m_3 L_1 L_2 \dot{\theta}_1 \dot{\theta}_2 \sin (\theta_1 - \theta_2)$$

$$+ \frac{1}{2} m_3 L_2 L_3 \dot{\theta}_2 \dot{\theta}_3 \sin (\theta_2 + \theta_3)$$

$$\frac{\partial T_3}{\partial \theta_3} = \frac{1}{2} m_3 L_1 L_3 \dot{\theta}_1 \dot{\theta}_3 \sin(\theta_1 + \theta_3)$$

$$+ \frac{1}{2} m_3 L_2 L_3 \dot{\theta}_2 \dot{\theta}_3 \sin(\theta_2 + \theta_3)$$

$$\frac{d}{dt}\left[\frac{\partial T_3}{\partial \dot{\theta}_1}\right] = m_3 L_1^2 \ddot{\theta}_1 + m_3 L_1 L_2 \ddot{\theta}_2 \cos(\theta_1 - \theta_2)$$

$$- m_3 L_1 L_2 \dot{\theta}_1 \dot{\theta}_2 \sin(\theta_1 - \theta_2)$$

$$+ m_3 L_1 L_2 \dot{\theta}_2^2 \sin(\theta_1 - \theta_2)$$

$$- \frac{1}{2} m_3 L_1 L_3 \ddot{\theta}_3 \cos(\theta_1 + \theta_3)$$

$$+ \frac{1}{2} m_3 L_1 L_3 \dot{\theta}_1 \dot{\theta}_3 \sin(\theta_1 + \theta_3)$$

$$+ \frac{1}{2} m_3 L_1 L_3 \dot{\theta}_3^2 \sin(\theta_1 + \theta_3)$$

$$\frac{d}{dt}\left[\frac{\partial T_3}{\partial \dot{\theta}_2}\right] = m_3 L_1 L_2 \ddot{\theta}_1 \cos(\theta_1 - \theta_2)$$

$$- m_3 L_1 L_2 \dot{\theta}_1^2 \sin(\theta_1 - \theta_2)$$

$$+ m_3 L_1 L_2 \dot{\theta}_1 \dot{\theta}_2 \sin(\theta_1 - \theta_2)$$

$$+ m_3 L_2^2 \ddot{\theta}_2$$

$$- \frac{1}{2} m_3 L_2 L_3 \ddot{\theta}_3 \cos(\theta_2 + \theta_3)$$

$$+ \frac{1}{2} m_3 L_2 L_3 \dot{\theta}_3^2 \sin(\theta_2 + \theta_3)$$

$$+ \frac{1}{2} m_3 L_2 L_3 \dot{\theta}_2 \dot{\theta}_3 \sin(\theta_2 + \theta_3)$$

$$\frac{d}{dt} \left[\frac{\partial T_3}{\partial \dot{\theta}_3} \right] = -\frac{1}{2} m_3 L_1 L_3 \ddot{\theta}_1 \cos(\theta_1 + \theta_3)$$

$$+ \frac{1}{2} m_3 L_1 L_3 \dot{\theta}_1^2 \sin(\theta_1 + \theta_3)$$

$$+ \frac{1}{2} m_3 L_1 L_3 \dot{\theta}_1 \dot{\theta}_3 \sin(\theta_1 + \theta_3)$$

$$- \frac{1}{2} m_3 L_2 L_3 \ddot{\theta}_2 \cos(\theta_2 + \theta_3)$$

$$+ \frac{1}{2} m_3 L_2 L_3 \dot{\theta}_2^2 \sin(\theta_2 + \theta_3)$$

$$+ \frac{1}{2} m_3 L_2 L_3 \dot{\theta}_2 \dot{\theta}_3 \sin(\theta_2 + \theta_3)$$

$$+ \frac{1}{3} m_3 L_3^2 \ddot{\theta}_3$$

Member 4

$$S_{x_4} = L_1 \cos \theta_1 + L_2 \cos \theta_2 + L_3 \cos \theta_3 + \frac{L_4}{2} \cos \theta_4$$

$$S_{y_4} = L_1 \sin \theta_1 + L_2 \sin \theta_2 - L_3 \sin \theta_3 - \frac{L_4}{2} \sin \theta_4$$

$$v_{x_4} = - L_1 \dot{\theta}_1 \sin \theta_1 - L_2 \dot{\theta}_2 \sin \theta_2 - L_3 \dot{\theta}_3 \sin \theta_3 - \frac{L_4}{2} \dot{\theta}_4 \sin \theta_4$$

$$v_{y_4} = L_1 \dot{\theta}_1 \cos \theta_1 + L_2 \dot{\theta}_2 \cos \theta_2 - L_3 \dot{\theta}_3 \cos \theta_3 - \frac{L_4}{2} \dot{\theta}_4 \cos \theta_4$$

$$T_4 = \frac{1}{2} m_4 L_1^2 \dot{\theta}_1^2 + m_4 L_1 L_2 \dot{\theta}_1 \dot{\theta}_2 \cos (\theta_1 - \theta_2)$$

$$- m_4 L_1 L_3 \dot{\theta}_1 \dot{\theta}_3 \cos (\theta_1 + \theta_3)$$

$$- \frac{1}{2} m_4 L_1 L_4 \dot{\theta}_1 \dot{\theta}_4 \cos (\theta_1 + \theta_4)$$

$$+ \frac{1}{2} m_4 L_2^2 \dot{\theta}_2^2 - m_4 L_2 L_3 \dot{\theta}_2 \dot{\theta}_3 \cos (\theta_2 + \theta_3)$$

$$- \frac{1}{2} m_4 L_2 L_4 \dot{\theta}_2 \dot{\theta}_4 \cos (\theta_2 + \theta_4)$$

$$+ \frac{1}{2} m_4 L_3^2 \dot{\theta}_3^2 + \frac{1}{2} m_4 L_3 L_4 \dot{\theta}_3 \dot{\theta}_4 \cos (\theta_3 - \theta_4)$$

$$+ \frac{1}{6} m_4 L_4^2 \dot{\theta}_4^2$$

$$\frac{\partial T_4}{\partial \theta_1} = - m_4 L_1 L_2 \dot{\theta}_1 \dot{\theta}_2 \sin(\theta_1 - \theta_2)$$

$$+ m_4 L_1 L_3 \dot{\theta}_1 \dot{\theta}_3 \sin(\theta_1 + \theta_3)$$

$$- \frac{1}{2} m_4 L_1 L_4 \dot{\theta}_1 \frac{\partial \dot{\theta}_4}{\partial \theta_1} \cos(\theta_1 + \theta_4)$$

$$+ \frac{1}{2} m_4 L_1 L_4 \dot{\theta}_1 \dot{\theta}_4 (1 + \frac{\partial \theta_4}{\partial \theta_1}) \sin(\theta_1 + \theta_4)$$

$$- \frac{1}{2} m_4 L_2 L_4 \dot{\theta}_2 \frac{\partial \dot{\theta}_4}{\partial \theta_1} \cos(\theta_2 + \theta_4)$$

$$+ \frac{1}{2} m_4 L_2 L_4 \dot{\theta}_2 \dot{\theta}_4 \frac{\partial \theta_4}{\partial \theta_1} \sin(\theta_2 + \theta_4)$$

$$+ \frac{1}{2} m_4 L_3 L_4 \dot{\theta}_3 \frac{\partial \dot{\theta}_4}{\partial \theta_1} \cos(\theta_3 - \theta_4)$$

$$+ \frac{1}{2} m_4 L_3 L_4 \dot{\theta}_3 \dot{\theta}_4 \frac{\partial \theta_4}{\partial \theta_3} \sin(\theta_3 - \theta_4)$$

$$+ \frac{1}{3} m_4 L_4^2 \dot{\theta}_4 \frac{\partial \dot{\theta}_4}{\partial \theta_1}$$

$$\frac{\partial T_4}{\partial \theta_2} = m_4 L_1 L_2 \dot{\theta}_1 \dot{\theta}_2 \sin(\theta_1 - \theta_2)$$

$$- \frac{1}{2} m_4 L_1 L_4 \dot{\theta}_1 \frac{\partial \dot{\theta}_4}{\partial \theta_2} \cos(\theta_1 + \theta_4)$$

$$+ \frac{1}{2} m_4 L_1 L_4 \dot{\theta}_1 \dot{\theta}_4 \frac{\partial \theta_4}{\partial \theta_2} \sin(\theta_1 + \theta_4)$$

$$+ m_4 L_2 L_3 \dot{\theta}_2 \dot{\theta}_3 \sin(\theta_2 + \theta_3)$$

$$- \frac{1}{2} m_4 L_2 L_4 \dot{\theta}_2 \frac{\partial \dot{\theta}_4}{\partial \theta_2} \cos(\theta_2 + \theta_4)$$

$$+ \frac{1}{2} m_4 L_2 L_4 \dot{\theta}_2 \dot{\theta}_4 (1 + \frac{\partial \theta_4}{\partial \theta_2}) \sin(\theta_2 + \theta_4)$$

$$+ \frac{1}{2} m_4 L_3 L_4 \dot{\theta}_3 \frac{\partial \dot{\theta}_4}{\partial \theta_2} \cos(\theta_3 - \theta_4)$$

$$+ \frac{1}{2} m_4 L_3 L_4 \dot{\theta}_3 \dot{\theta}_4 \frac{\partial \theta_4}{\partial \theta_2} \sin(\theta_3 - \theta_4)$$

$$+ \frac{1}{3} m_4 L_4{}^2 \dot{\theta}_4 \frac{\partial \dot{\theta}_4}{\partial \theta_2}$$

$$\frac{\partial T_4}{\partial \theta_3} = m_4 L_1 L_3 \dot{\theta}_1 \dot{\theta}_3 \sin(\theta_1 + \theta_3)$$

$$- \frac{1}{2} m_4 L_1 L_4 \dot{\theta}_1 \frac{\partial \dot{\theta}_4}{\partial \theta_3} \cos(\theta_1 + \theta_4)$$

$$+ \frac{1}{2} m_4 L_1 L_4 \dot{\theta}_1 \dot{\theta}_4 \frac{\partial \theta_4}{\partial \theta_3} \sin(\theta_1 + \theta_4)$$

$$+ m_4 L_2 L_3 \dot{\theta}_2 \dot{\theta}_3 \sin(\theta_2 + \theta_3)$$

$$- \frac{1}{2} m_4 L_2 L_4 \dot{\theta}_2 \frac{\partial \dot{\theta}_4}{\partial \theta_3} \cos(\theta_2 + \theta_4)$$

$$+ \frac{1}{2} m_4 L_2 L_4 \dot{\theta}_2 \dot{\theta}_4 \frac{\partial \theta_4}{\partial \theta_3} \sin(\theta_2 + \theta_4)$$

$$+ \frac{1}{2} m_4 L_3 L_4 \dot{\theta}_3 \frac{\partial \dot{\theta}_4}{\partial \theta_3} \cos(\theta_3 - \theta_4)$$

$$- \frac{1}{2} m_4 L_3 L_4 \dot{\theta}_3 \dot{\theta}_4 (1 - \frac{\partial \theta_4}{\partial \theta_3}) \sin(\theta_3 - \theta_4)$$

$$+ \frac{1}{3} m_4 L_4{}^2 \dot{\theta}_4 \frac{\partial \dot{\theta}_4}{\partial \theta_3}$$

$$\frac{d}{dt} \left[\frac{\partial T_4}{\partial \dot{\theta}_1} \right] = m_4 L_1^2 \ddot{\theta}_1 + m_4 L_1 L_2 \ddot{\theta}_2 \cos(\theta_1 - \theta_2)$$

$$- m_4 L_1 L_2 \dot{\theta}_1 \dot{\theta}_2 \sin(\theta_1 - \theta_2)$$

$$+ m_4 L_1 L_2 \dot{\theta}_2^2 \sin(\theta_1 - \theta_2)$$

$$- m_4 L_1 L_3 \ddot{\theta}_3 \cos(\theta_1 + \theta_3)$$

$$+ m_4 L_1 L_3 \dot{\theta}_1 \dot{\theta}_3 \sin(\theta_1 + \theta_3)$$

$$+ m_4 L_1 L_3 \dot{\theta}_3^2 \sin(\theta_1 + \theta_3)$$

$$- \frac{1}{2} m_4 L_1 L_4 \ddot{\theta}_4 \cos(\theta_1 + \theta_4)$$

$$+ \frac{1}{2} m_4 L_1 L_4 \dot{\theta}_1 \dot{\theta}_4 \sin(\theta_1 + \theta_4)$$

$$+ \frac{1}{2} m_4 L_1 L_4 \dot{\theta}_4^2 \sin(\theta_1 + \theta_4)$$

$$- \frac{1}{2} m_4 L_1 L_4 \ddot{\theta}_1 \frac{\partial \dot{\theta}_4}{\partial \dot{\theta}_1} \cos(\theta_1 + \theta_4)$$

$$- \frac{1}{2} m_4 L_1 L_4 \dot{\theta}_1 \frac{d}{dt} \left[\frac{\partial \dot{\theta}_4}{\partial \dot{\theta}_1} \right] \cos(\theta_1 + \theta_4)$$

$$+ \frac{1}{2} m_4 L_1 L_4 \dot{\theta}_1^2 \frac{\partial \dot{\theta}_4}{\partial \dot{\theta}_1} \sin(\theta_1 + \theta_4)$$

$$+ \frac{1}{2} m_4 L_1 L_4 \dot{\theta}_1 \dot{\theta}_4 \frac{\partial \dot{\theta}_4}{\partial \dot{\theta}_1} \sin(\theta_1 + \theta_4)$$

$$- \frac{1}{2} m_4 L_2 L_4 \ddot{\theta}_2 \frac{\partial \dot{\theta}_4}{\partial \dot{\theta}_1} \cos (\theta_2 + \theta_4)$$

$$- \frac{1}{2} m_4 L_2 L_4 \dot{\theta}_2 \frac{d}{dt} [\frac{\partial \dot{\theta}_4}{\partial \dot{\theta}_1}] \cos (\theta_2 + \theta_4)$$

$$+ \frac{1}{2} m_4 L_2 L_4 \dot{\theta}_2^2 \frac{\partial \dot{\theta}_4}{\partial \dot{\theta}_1} \sin (\theta_2 + \theta_4)$$

$$+ \frac{1}{2} m_4 L_2 L_4 \dot{\theta}_2 \dot{\theta}_4 \frac{\partial \dot{\theta}_4}{\partial \dot{\theta}_1} \sin (\theta_2 + \theta_4)$$

$$+ \frac{1}{2} m_4 L_3 L_4 \ddot{\theta}_3 \frac{\partial \dot{\theta}_4}{\partial \dot{\theta}_1} \cos (\theta_3 - \theta_4)$$

$$+ \frac{1}{2} m_4 L_3 L_4 \dot{\theta}_3 \frac{d}{dt} [\frac{\partial \dot{\theta}_4}{\partial \dot{\theta}_1}] \cos (\theta_3 - \theta_4)$$

$$- \frac{1}{2} m_4 L_3 L_4 \dot{\theta}_3^2 \frac{\partial \dot{\theta}_4}{\partial \dot{\theta}_1} \sin (\theta_3 - \theta_4)$$

$$+ \frac{1}{2} m_4 L_3 L_4 \dot{\theta}_3 \dot{\theta}_4 \frac{\partial \dot{\theta}_4}{\partial \dot{\theta}_1} \sin (\theta_3 - \theta_4)$$

$$+ \frac{1}{3} m_4 L_4^2 \ddot{\theta}_4 \frac{\partial \dot{\theta}_4}{\partial \dot{\theta}_1}$$

$$+ \frac{1}{3} m_4 L_4^2 \dot{\theta}_4 \frac{d}{dt} [\frac{\partial \dot{\theta}_4}{\partial \dot{\theta}_1}]$$

$$\frac{d}{dt} [\frac{\partial T_4}{\partial \dot{\theta}_2}] = m_4 L_1 L_2 \ddot{\theta}_1 \cos (\theta_1 - \theta_2)$$

$$- m_4 L_1 L_2 \dot{\theta}_1^2 \sin (\theta_1 - \theta_2)$$

$$+ m_4 L_1 L_2 \dot{\theta}_1 \dot{\theta}_2 \sin(\theta_1 - \theta_2)$$

$$- \frac{1}{2} m_4 L_1 L_4 \ddot{\theta}_1 \frac{\partial \dot{\theta}_4}{\partial \dot{\theta}_2} \cos(\theta_1 + \theta_4)$$

$$- \frac{1}{2} m_4 L_1 L_4 \dot{\theta}_1 \frac{d}{dt} \left[\frac{\partial \dot{\theta}_4}{\partial \dot{\theta}_2} \right] \cos(\theta_1 + \theta_4)$$

$$+ \frac{1}{2} m_4 L_1 L_4 \dot{\theta}_1^2 \frac{\partial \dot{\theta}_4}{\partial \dot{\theta}_2} \sin(\theta_1 + \theta_4)$$

$$+ \frac{1}{2} m_4 L_1 L_4 \dot{\theta}_1 \dot{\theta}_4 \frac{\partial \dot{\theta}_4}{\partial \dot{\theta}_2} \sin(\theta_1 + \theta_4)$$

$$+ m_4 L_2^2 \ddot{\theta}_2 - m_4 L_2 L_3 \ddot{\theta}_3 \cos(\theta_2 + \theta_3)$$

$$+ m_4 L_2 L_3 \dot{\theta}_2 \dot{\theta}_3 \sin(\theta_2 + \theta_3)$$

$$+ m_4 L_2 L_3 \dot{\theta}_3^2 \sin(\theta_2 + \theta_3)$$

$$- \frac{1}{2} m_4 L_2 L_4 \ddot{\theta}_4 \cos(\theta_2 + \theta_4)$$

$$+ \frac{1}{2} m_4 L_2 L_4 \dot{\theta}_2 \dot{\theta}_4 \sin(\theta_2 + \theta_4)$$

$$+ \frac{1}{2} m_4 L_2 L_4 \dot{\theta}_4^2 \sin(\theta_2 + \theta_4)$$

$$- \frac{1}{2} m_4 L_2 L_4 \ddot{\theta}_2 \frac{\partial \dot{\theta}_4}{\partial \dot{\theta}_2} \cos(\theta_2 + \theta_4)$$

$$- \frac{1}{2} m_4 \, L_2 \, L_4 \, \dot{\theta}_2 \, \frac{d}{dt} \, [\frac{\partial \dot{\theta}_4}{\partial \dot{\theta}_2}] \, \cos \, (\theta_2 + \theta_4)$$

$$+ \frac{1}{2} m_4 \, L_2 \, L_4 \, \dot{\theta}_2^{\,2} \, \frac{\partial \dot{\theta}_4}{\partial \dot{\theta}_2} \, \sin \, (\theta_2 + \theta_4)$$

$$+ \frac{1}{2} m_4 \, L_2 \, L_4 \, \dot{\theta}_2 \, \dot{\theta}_4 \, \frac{\partial \dot{\theta}_4}{\partial \dot{\theta}_2} \, \sin \, (\theta_2 + \theta_4)$$

$$+ \frac{1}{2} m_4 \, L_3 \, L_4 \, \ddot{\theta}_3 \, \frac{\partial \dot{\theta}_4}{\partial \dot{\theta}_2} \, \cos \, (\theta_3 - \theta_4)$$

$$+ \frac{1}{2} m_4 \, L_3 \, L_4 \, \dot{\theta}_3 \, \frac{d}{dt} \, [\frac{\partial \dot{\theta}_4}{\partial \dot{\theta}_2}] \, \cos \, (\theta_3 - \theta_4)$$

$$- \frac{1}{2} m_4 \, L_3 \, L_4 \, \dot{\theta}_3^{\,2} \, \frac{\partial \dot{\theta}_4}{\partial \dot{\theta}_2} \, \sin \, (\theta_3 - \theta_4)$$

$$+ \frac{1}{2} m_4 \, L_3 \, L_4 \, \dot{\theta}_3 \, \dot{\theta}_4 \, \frac{\partial \dot{\theta}_4}{\partial \dot{\theta}_2} \, \sin \, (\theta_3 - \theta_4)$$

$$+ \frac{1}{3} m_4 \, L_4^{\,2} \, \ddot{\theta}_4 \, \frac{\partial \dot{\theta}_4}{\partial \dot{\theta}_2}$$

$$+ \frac{1}{3} m_4 \, L_4^{\,2} \, \dot{\theta}_4 \, \frac{d}{dt} \, [\frac{\partial \dot{\theta}_4}{\partial \dot{\theta}_2}]$$

$$\frac{d}{dt} \, [\frac{\partial T_4}{\partial \dot{\theta}_3}] = - \, m_4 \, L_1 \, L_3 \, \ddot{\theta}_1 \, \cos \, (\theta_1 + \theta_3)$$

$$+ m_4 \, L_1 \, L_3 \, \dot{\theta}_1^{\,2} \, \sin \, (\theta_1 + \theta_3)$$

$$+ m_4 \, L_1 \, L_3 \, \dot{\theta}_1 \, \dot{\theta}_3 \, \sin \, (\theta_1 + \theta_3)$$

$$- \frac{1}{2} m_4 L_1 L_4 \ddot{\theta}_1 \frac{\partial \dot{\theta}_4}{\partial \dot{\theta}_3} \cos (\theta_1 + \theta_4)$$

$$- \frac{1}{2} m_4 L_1 L_4 \dot{\theta}_1 \frac{d}{dt} [\frac{\partial \dot{\theta}_4}{\partial \dot{\theta}_3}] \cos (\theta_1 + \theta_4)$$

$$+ \frac{1}{2} m_4 L_1 L_4 \dot{\theta}_1^2 \frac{\partial \dot{\theta}_4}{\partial \dot{\theta}_3} \sin (\theta_1 + \theta_4)$$

$$+ \frac{1}{2} m_4 L_1 L_4 \dot{\theta}_1 \dot{\theta}_4 \frac{\partial \dot{\theta}_4}{\partial \dot{\theta}_3} \sin (\theta_1 + \theta_4)$$

$$- m_4 L_2 L_3 \ddot{\theta}_2 \cos (\theta_2 + \theta_3)$$

$$+ m_4 L_2 L_3 \dot{\theta}_2^2 \sin (\theta_2 + \theta_3)$$

$$+ m_4 L_2 L_3 \dot{\theta}_2 \dot{\theta}_3 \sin (\theta_2 + \theta_3)$$

$$- \frac{1}{2} m_4 L_2 L_4 \ddot{\theta}_2 \frac{\partial \dot{\theta}_4}{\partial \dot{\theta}_3} \cos (\theta_2 + \theta_4)$$

$$- \frac{1}{2} m_4 L_2 L_4 \dot{\theta}_2 \frac{d}{dt} [\frac{\partial \dot{\theta}_4}{\partial \dot{\theta}_3}] \cos (\theta_2 + \theta_4)$$

$$+ \frac{1}{2} m_4 L_2 L_4 \dot{\theta}_2^2 \frac{\partial \dot{\theta}_4}{\partial \dot{\theta}_3} \sin (\theta_2 + \theta_4)$$

$$+ \frac{1}{2} m_4 L_2 L_4 \dot{\theta}_2 \dot{\theta}_4 \frac{\partial \dot{\theta}_4}{\partial \dot{\theta}_3} \sin (\theta_2 + \theta_4)$$

$$+ m_4 L_3^2 \ddot{\theta}_3 + \frac{1}{2} m_4 L_3 L_4 \ddot{\theta}_4 \cos (\theta_3 - \theta_4)$$

$$- \frac{1}{2} m_4 L_3 L_4 \dot{\theta}_3 \dot{\theta}_4 \sin(\theta_3 - \theta_4)$$

$$+ \frac{1}{2} m_4 L_3 L_4 \dot{\theta}_4^2 \sin(\theta_3 - \theta_4)$$

$$+ \frac{1}{2} m_4 L_3 L_4 \ddot{\theta}_3 \frac{\partial \dot{\theta}_4}{\partial \dot{\theta}_3} \cos(\theta_3 - \theta_4)$$

$$+ \frac{1}{2} m_4 L_3 L_4 \dot{\theta}_3 \frac{d}{dt} [\frac{\partial \dot{\theta}_4}{\partial \dot{\theta}_3}] \cos(\theta_3 - \theta_4)$$

$$- \frac{1}{2} m_4 L_3 L_4 \dot{\theta}_3^2 \frac{\partial \dot{\theta}_4}{\partial \dot{\theta}_3} \sin(\theta_3 - \theta_4)$$

$$+ \frac{1}{2} m_4 L_3 L_4 \dot{\theta}_3 \dot{\theta}_4 \frac{\partial \dot{\theta}_4}{\partial \dot{\theta}_3} \sin(\theta_3 - \theta_4)$$

$$+ \frac{1}{3} m_4 L_4^2 \ddot{\theta}_4 \frac{\partial \dot{\theta}_4}{\partial \dot{\theta}_3}$$

$$+ \frac{1}{3} m_4 L_4^2 \dot{\theta}_4 \frac{d}{dt} [\frac{\partial \dot{\theta}_4}{\partial \dot{\theta}_3}]$$

Derivatives of the Potential Energy

$$\frac{\partial V}{\partial \theta_1} = - C_1 \left[(\alpha_1 - \alpha_2) - (\theta_1 - \theta_2) \right]$$

$$- C_3 \left[(\alpha_4 - \alpha_3) - (\theta_4 - \theta_3) \right] \frac{\partial \theta_4}{\partial \theta_1}$$

$$- K \left[L_1 \cos \theta_1 + L_2 \cos \theta_2 \right.$$

$$+ L_3 \cos \theta_3 + L_4 \cos \theta_4$$

$$- L_1 \cos \alpha_1 - L_2 \cos \alpha_2$$

$$\left. - L_3 \cos \alpha_3 - L_4 \cos \alpha_4 \right] \quad .$$

$$\left[L_1 \sin \theta_1 + L_4 \frac{\partial \theta_4}{\partial \theta_1} \sin \theta_4 \right]$$

$$+ (P_1 + P_2 + P_3) L_1 \cos \theta_1$$

$$\frac{\partial V}{\partial \theta_2} = C_1 \left[(\alpha_1 - \alpha_2) - (\theta_1 - \theta_2) \right]$$

$$- C_2 \left[(\alpha_3 + \alpha_2) - (\theta_3 + \theta_2) \right]$$

$$- C_3 \left[(\alpha_4 - \alpha_3) - (\theta_4 - \theta_3) \right] \frac{\partial \theta_4}{\partial \theta_2}$$

$$- K \left[L_1 \cos \theta_1 + L_2 \cos \theta_2 \right.$$

$$+ L_3 \cos \theta_3 + L_4 \cos \theta_4$$

$$- L_1 \cos \alpha_1 - L_2 \cos \alpha_2$$

$$\left. - L_3 \cos \alpha_3 - L_4 \cos \alpha_4 \right] \quad .$$

$$\left[L_2 \sin \theta_2 + L_4 \frac{\partial \theta_4}{\partial \theta_2} \sin \theta_4 \right]$$

$$+ (P_2 + P_3) L_2 \cos \theta_2$$

$$\frac{\partial V}{\partial \theta_3} = - C_2 \left[(\alpha_3 + \alpha_2) - (\theta_3 + \theta_2) \right]$$

$$+ C_3 \left[(\alpha_4 - \alpha_3) - (\theta_4 - \theta_3) \right] \left[1 - \frac{\partial \theta_4}{\partial \theta_3} \right]$$

$$- K \left[L_1 \cos \theta_1 + L_2 \cos \theta_2 \right.$$

$$+ L_3 \cos \theta_3 + L_4 \cos \theta_4$$

$$- L_1 \cos \alpha_1 - L_2 \cos \alpha_2$$

$$\left. - L_3 \cos \alpha_3 - L_4 \cos \alpha_4 \right] \quad .$$

$$\left[L_3 \sin \theta_3 + L_4 \frac{\partial \theta_4}{\partial \theta_3} \sin \theta_4 \right]$$

$$- P_3 L_3 \cos \theta_3$$

Derivatives of Rayleigh's Dissipation Function

$$\frac{\partial F}{\partial \dot{\theta}_1} = B_1 \, [\dot{\theta}_1 - \dot{\theta}_2]$$
$$+ B_3 \, [\dot{\theta}_4 - \dot{\theta}_3] \, \frac{\partial \dot{\theta}_4}{\partial \dot{\theta}_1}$$

$$\frac{\partial F}{\partial \dot{\theta}_2} = -B_1 \, [\dot{\theta}_1 - \dot{\theta}_2]$$
$$+ B_2 \, [\dot{\theta}_3 + \dot{\theta}_2]$$
$$+ B_3 \, [\dot{\theta}_4 - \dot{\theta}_3] \, \frac{\partial \dot{\theta}_4}{\partial \dot{\theta}_2}$$

$$\frac{\partial F}{\partial \dot{\theta}_3} = B_2 \, [\dot{\theta}_3 + \dot{\theta}_2]$$
$$+ B_3 \, [\dot{\theta}_4 - \dot{\theta}_3] \, [\frac{\partial \dot{\theta}_4}{\partial \dot{\theta}_3} - 1]$$

Definitions

$$TA = \cos \theta_4$$

$$TB = - \frac{1}{TA} \left[\frac{L_1}{L_4} \dot{\theta}_1^2 \sin \theta_1 + \frac{L_2}{L_4} \dot{\theta}_2^2 \sin \theta_2 - \frac{L_3}{L_4} \dot{\theta}_3^2 \sin \theta_3 \right]$$

$$TC = \frac{1}{TA^3} \left[\frac{L_1}{L_4} \dot{\theta}_1 \cos \theta_1 + \frac{L_2}{L_4} \dot{\theta}_2 \cos \theta_2 - \frac{L_3}{L_4} \dot{\theta}_3 \cos \theta_3 \right]^2$$

$$\left[\frac{L_1}{L_4} \sin \theta_1 + \frac{L_2}{L_4} \sin \theta_2 - \frac{L_3}{L_4} \sin \theta_3 \right] = \frac{1}{TA} \dot{\theta}_4^2 \sin \theta_4$$

[A] matrix

$$A_{11} = [\frac{1}{3} m_1 + m_2 + m_3 + m_4] L_1^2$$

$$+ m_4 L_1 [- \frac{L_1}{2} \frac{\cos \theta_1}{\cos \theta_4} \cos (\theta_1 + \theta_4)$$

$$+ \frac{L_4}{3} \frac{\cos \theta_1}{\cos \theta_4} \frac{\partial \dot{\theta}_4}{\partial \dot{\theta}_1}$$

$$- \frac{L_4}{2} \cos (\theta_1 + \theta_4) \frac{\partial \dot{\theta}_4}{\partial \dot{\theta}_1}]$$

$$A_{12} = \{[\frac{1}{2} m_2 + m_3 + m_4] L_1 L_2\} \cos (\theta_1 - \theta_2)$$

$$+ m_4 L_2 [- \frac{L_1}{2} \frac{\cos \theta_2}{\cos \theta_4} \cos (\theta_1 + \theta_4)$$

$$+ \frac{L_4}{3} \frac{\cos \theta_2}{\cos \theta_4} \frac{\partial \dot{\theta}_4}{\partial \dot{\theta}_1}$$

$$- \frac{L_4}{2} \cos (\theta_2 + \theta_4) \frac{\partial \dot{\theta}_4}{\partial \dot{\theta}_1}]$$

$$A_{13} = -\{[\frac{1}{2} m_3 + m_4] L_1 L_3\} \cos (\theta_1 + \theta_3)$$

$$+ m_4 L_3 [\frac{L_1}{2} \frac{\cos \theta_3}{\cos \theta_4} \cos (\theta_1 + \theta_4)$$

$$- \frac{L_4}{3} \frac{\cos \theta_3}{\cos \theta_4} \frac{\partial \dot{\theta}_4}{\partial \dot{\theta}_1}$$

$$+ \frac{L_4}{2} \cos (\theta_3 - \theta_4) \frac{\partial \dot{\theta}_4}{\partial \dot{\theta}_1}]$$

$$A_{21} = \{[\tfrac{1}{2} m_2 + m_3 + m_4] L_1 L_2\} \cos(\theta_1 - \theta_2)$$

$$+ m_4 L_1 [- \frac{L_2}{2} \frac{\cos \theta_1}{\cos \theta_4} \cos(\theta_2 + \theta_4)$$

$$+ \frac{L_4}{3} \frac{\cos \theta_1}{\cos \theta_4} \frac{\partial \dot{\theta}_4}{\partial \dot{\theta}_2}$$

$$- \frac{L_4}{2} \cos(\theta_1 + \theta_4) \frac{\partial \dot{\theta}_4}{\partial \dot{\theta}_2}]$$

$$A_{22} = [\tfrac{1}{3} m_2 + m_3 + m_4] L_2^2$$

$$+ m_4 L_2 [- \frac{L_2}{2} \frac{\cos \theta_2}{\cos \theta_4} \cos(\theta_2 + \theta_4)$$

$$+ \frac{L_4}{3} \frac{\cos \theta_2}{\cos \theta_4} \frac{\partial \dot{\theta}_4}{\partial \dot{\theta}_2}$$

$$- \frac{L_4}{2} \cos(\theta_2 + \theta_4) \frac{\partial \dot{\theta}_4}{\partial \dot{\theta}_2}]$$

$$A_{23} = -\{[\tfrac{1}{2} m_3 + m_4] L_2 L_3\} \cos(\theta_2 + \theta_3)$$

$$+ m_4 L_3 [\frac{L_2}{2} \frac{\cos \theta_3}{\cos \theta_4} \cos(\theta_2 + \theta_4)$$

$$- \frac{L_4}{3} \frac{\cos \theta_3}{\cos \theta_4} \frac{\partial \dot{\theta}_4}{\partial \dot{\theta}_2}$$

$$+ \frac{L_4}{2} \cos(\theta_3 - \theta_4) \frac{\partial \dot{\theta}_4}{\partial \dot{\theta}_2}]$$

$$A_{31} = -\left\{\left[\tfrac{1}{2} m_3 + m_4\right] L_1 L_3\right\} \cos(\theta_1 + \theta_3)$$

$$+ m_4 L_1 \left[\frac{L_3}{2} \frac{\cos\theta_1}{\cos\theta_4} \cos(\theta_3 - \theta_4)\right.$$

$$+ \frac{L_4}{3} \frac{\cos\theta_1}{\cos\theta_4} \frac{\partial\dot\theta_4}{\partial\dot\theta_3}$$

$$\left. - \frac{L_4}{2} \cos(\theta_1 + \theta_4) \frac{\partial\dot\theta_4}{\partial\dot\theta_3}\right]$$

$$A_{32} = -\left\{\left[\tfrac{1}{2} m_3 + m_4\right] L_2 L_3\right\} \cos(\theta_2 + \theta_3)$$

$$+ m_4 L_2 \left[\frac{L_3}{2} \frac{\cos\theta_2}{\cos\theta_4} \cos(\theta_3 - \theta_4)\right.$$

$$+ \frac{L_4}{3} \frac{\cos\theta_2}{\cos\theta_4} \frac{\partial\dot\theta_4}{\partial\dot\theta_3}$$

$$\left. - \frac{L_4}{2} \cos(\theta_2 + \theta_4) \frac{\partial\dot\theta_4}{\partial\dot\theta_3}\right]$$

$$A_{33} = \left[\tfrac{1}{3} m_3 + m_4\right] L_3^{\,2}$$

$$+ m_4 L_3 \left[- \frac{L_3}{2} \frac{\cos\theta_3}{\cos\theta_4} \cos(\theta_3 - \theta_4)\right.$$

$$- \frac{L_4}{3} \frac{\cos\theta_3}{\cos\theta_4} \frac{\partial\dot\theta_4}{\partial\dot\theta_3}$$

$$\left. + \frac{L_4}{2} \cos(\theta_3 - \theta_4) \frac{\partial\dot\theta_4}{\partial\dot\theta_3}\right]$$

{D} vector

$$D_1 = -\{[\tfrac{1}{2} m_2 + m_3 + m_4] L_1 L_2\} \cdot$$

$$\dot{\theta}_2^{\,2} \sin(\theta_1 - \theta_2)$$

$$-\{[\tfrac{1}{2} m_3 + m_4] L_1 L_3\} \cdot$$

$$\dot{\theta}_3^{\,2} \sin(\theta_1 + \theta_3)$$

$$+ [\tfrac{1}{2} m_4 L_1 L_4] \sin(\theta_1 + \theta_4) \cdot$$

$$[-\dot{\theta}_4^{\,2} - \dot{\theta}_1^{\,2} \frac{\partial \dot{\theta}_4}{\partial \dot{\theta}_1}]$$

$$+ [\tfrac{1}{2} m_4 L_2 L_4] \sin(\theta_2 + \theta_4) \cdot$$

$$[-\dot{\theta}_2^{\,2} \frac{\partial \dot{\theta}_4}{\partial \dot{\theta}_1}]$$

$$+ [\tfrac{1}{2} m_4 L_3 L_4] \sin(\theta_3 - \theta_4) \cdot$$

$$[\dot{\theta}_3^{\,2} \frac{\partial \dot{\theta}_4}{\partial \dot{\theta}_1}]$$

$$+ [\tfrac{1}{2} m_4 L_1 L_4] \cos(\theta_1 + \theta_4) \cdot$$

$$[TB + TC]$$

$$- [\tfrac{1}{3} m_4 L_4^{\,2}] [-\frac{\partial \dot{\theta}_4}{\partial \dot{\theta}_1} (TB + TC)]$$

$$+ C_1 [(\alpha_1 - \alpha_2) - (\theta_1 - \theta_2)]$$

$$+ C_3 [(\alpha_4 - \alpha_3) - (\theta_4 - \theta_3)] \frac{\partial \theta_4}{\partial \theta_1}$$

$$+ K [L_1 \cos \theta_1 + L_2 \cos \theta_2 + L_3 \cos \theta_3$$

$$+ L_4 \cos \theta_4 - L_1 \cos \alpha_1 - L_2 \cos \alpha_2$$

$$- L_3 \cos \alpha_3 - L_4 \cos \alpha_4] \cdot$$

$$[L_1 \sin \theta_1 + L_4 \frac{\partial \theta_4}{\partial \theta_1} \sin \theta_4]$$

$$- (P_1 + P_2 + P_3) L_1 \cos \theta_1$$

$$- B_1 (\dot{\theta}_1 - \dot{\theta}_2)$$

$$- B_3 (\dot{\theta}_4 - \dot{\theta}_3) \frac{\partial \dot{\theta}_4}{\partial \dot{\theta}_1}$$

$$D_2 = \{[\tfrac{1}{2} m_2 + m_3 + m_4] L_1 L_2\} \cdot$$

$$\dot{\theta}_1^2 \sin(\theta_1 - \theta_2)$$

$$-\{[\tfrac{1}{2} m_3 + m_4] L_2 L_3\} \cdot$$

$$\dot{\theta}_3^2 \sin(\theta_2 + \theta_3)$$

$$+ [\tfrac{1}{2} m_4 L_1 L_4] \sin(\theta_1 + \theta_4) \cdot$$

$$[-\dot{\theta}_1^2 \frac{\partial \dot{\theta}_4}{\partial \dot{\theta}_2}]$$

$$+ [\tfrac{1}{2} m_4 L_2 L_4] \sin(\theta_2 + \theta_4) \cdot$$

$$[-\dot{\theta}_4^2 - \dot{\theta}_2^2 \frac{\partial \dot{\theta}_4}{\partial \dot{\theta}_2}]$$

$$+ [\tfrac{1}{2} m_4 L_3 L_4] \sin(\theta_3 - \theta_4) \cdot$$

$$[\dot{\theta}_3^2 \frac{\partial \dot{\theta}_4}{\partial \dot{\theta}_2}]$$

$$+ [\tfrac{1}{2} m_4 L_2 L_4] \cos(\theta_2 + \theta_4) \cdot$$

$$[TB + TC]$$

$$- [\tfrac{1}{3} m_4 L_4^2] [\frac{\partial \dot{\theta}_4}{\partial \dot{\theta}_2} (TB + TC)]$$

$$- C_1 [(\alpha_1 - \alpha_2) - (\theta_1 - \theta_2)]$$

$$+ C_2 [(\alpha_3 + \alpha_2) - (\theta_3 + \theta_2)]$$

$$+ C_3 [(\alpha_4 - \alpha_3) - (\theta_4 - \theta_3)] \frac{\partial \theta_4}{\partial \theta_2}$$

$$+ K [L_1 \cos \theta_1 + L_2 \cos \theta_2 + L_3 \cos \theta_3$$

$$+ L_4 \cos \theta_4 - L_1 \cos \alpha_1 - L_2 \cos \alpha_2$$

$$- L_3 \cos \alpha_3 - L_4 \cos \alpha_4] \cdot$$

$$[L_2 \sin \theta_2 + L_4 \frac{\partial \theta_4}{\partial \theta_2} \sin \theta_4]$$

$$- (P_2 + P_3) L_2 \cos \theta_2$$

$$+ B_1 (\dot{\theta}_1 - \dot{\theta}_2)$$

$$- B_2 (\dot{\theta}_3 + \dot{\theta}_2)$$

$$- B_3 (\dot{\theta}_4 - \dot{\theta}_3) \frac{\partial \dot{\theta}_4}{\partial \dot{\theta}_2}$$

$$D_3 = -\{[\tfrac{1}{2} m_3 + m_4] L_1 L_3\} \cdot$$

$$\dot{\theta}_1^{\,2} \sin(\theta_1 + \theta_3)$$

$$-\{[\tfrac{1}{2} m_3 + m_4] L_2 L_3\} \cdot$$

$$\dot{\theta}_2^{\,2} \sin(\theta_2 + \theta_3)$$

$$+ [\tfrac{1}{2} m_4 L_1 L_4] \sin(\theta_1 + \theta_4) \cdot$$

$$[-\dot{\theta}_1^{\,2} \frac{\partial \dot{\theta}_4}{\partial \dot{\theta}_3}]$$

$$+ [\tfrac{1}{2} m_4 L_2 L_4] \sin(\theta_2 + \theta_4) \cdot$$

$$[-\dot{\theta}_2^{\,2} \frac{\partial \dot{\theta}_4}{\partial \dot{\theta}_3}]$$

$$+ [\tfrac{1}{2} m_4 L_3 L_4] \sin(\theta_3 - \theta_4) \cdot$$

$$[-\dot{\theta}_4^{\,2} + \dot{\theta}_3^{\,2} \frac{\partial \dot{\theta}_4}{\partial \dot{\theta}_3}]$$

$$+ [\tfrac{1}{2} m_4 L_3 L_4] \cos(\theta_3 - \theta_4) \cdot$$

$$[-TB - TC]$$

$$- [\tfrac{1}{3} m_4 L_4^{\,2}] [\frac{\partial \dot{\theta}_4}{\partial \dot{\theta}_3} (TB + TC)]$$

$$+ C_2 [(\alpha_3 + \alpha_2) - (\theta_3 + \theta_2)]$$

$$- C_3 [(\alpha_4 - \alpha_3) - (\theta_4 - \theta_3)] [1 - \frac{\partial \theta_4}{\partial \theta_3}]$$

$$+ K [L_1 \cos \theta_1 + L_2 \cos \theta_2 + L_3 \cos \theta_3$$

$$+ L_4 \cos \theta_4 - L_1 \cos \alpha_1 - L_2 \cos \alpha_2$$

$$- L_3 \cos \alpha_3 - L_4 \cos \alpha_4] \cdot$$

$$[L_3 \sin \theta_3 + L_4 \frac{\partial \theta_4}{\partial \theta_3} \sin \theta_4]$$

$$+ P_3 L_3 \cos \theta_3$$

$$- B_2 (\dot{\theta}_3 + \dot{\theta}_2)$$

$$- B_3 (\dot{\theta}_4 - \dot{\theta}_3) [\frac{\partial \dot{\theta}4}{\partial \dot{\theta}_3} - 1]$$

APPENDIX A-3

INITIAL VELOCITIES FOR IMPULSE LOADS

INITIAL VELOCITIES FOR IMPULSE LOADS

The initial velocities, $\dot{\theta}_1$, $\dot{\theta}_2$, and $\dot{\theta}_3$, imparted to the model by the impulse loads, $\hat{P}_1$, $\hat{P}_2$, and $\hat{P}_3$, (applied at joints $\boxed{2}$, $\boxed{3}$, and $\boxed{4}$, respectively,) are derived from the equation

$$\Delta p_k = \hat{Q}_k , \quad k = 1, 2, \ldots, n , \tag{A-3.1}$$

where

$$\Delta p_k = \lim_{\varepsilon \to 0} \left. \frac{\partial T}{\partial \dot{q}_k} \right|_{t}^{t+\varepsilon} \tag{A-3.2}$$

and

$$\hat{Q}_k = \sum_{j=1}^{P} \vec{F}_j \cdot \frac{\partial \vec{r}_j}{\partial q_k} . \tag{A-3.3}$$

As can be seen, Eqs. A-3.1 are a set of n simultaneous equations, where Δp_k are the changes in the generalized momenta p_k of the system, and $\hat{Q}_k$ are the generalized impulses of the system. In Eqs. A-3.1, A-3.2, and A-3.3, $\vec{F}_j$ are the impulse force vectors of the system, $\vec{r}_j$ are the position vectors corresponding to the impulse force vectors $\vec{F}_j$ of the system, and n, T, q_k, and $\dot{q}_k$ are as defined in section 3.1.

Now, applying Eqs. 3.6, 3.7, 3.8, and 3.9 to Eqs. A-3.1, A-3.2, and A-3.3, and remembering that there is no generalized momentum before the impulse loads are applied, yields a set of 3 simultaneous equations, which are

$$\frac{\partial T}{\partial \dot{\theta}_1} = \hat{Q}_1 , \tag{A-3.4}$$

$$\frac{\partial T}{\partial \dot{\theta}_2} = \hat{Q}_2 \quad , \tag{A-3.5}$$

$$\frac{\partial T}{\partial \dot{\theta}_3} = \hat{Q}_3 \quad . \tag{A-3.6}$$

In the above equations, T is given by Eq. 3.22, and

$$\hat{Q}_1 = - (\hat{P}_1 + \hat{P}_2 + \hat{P}_3) \; L_1 \cos \theta_1 \quad , \tag{A-3.7}$$

$$\hat{Q}_2 = - (\hat{P}_2 + \hat{P}_3) \; L_2 \cos \theta_2 \quad , \tag{A-3.8}$$

$$\hat{Q}_3 = \hat{P}_3 \; L_3 \cos \theta_3 \quad . \tag{A-3.9}$$

Finally, applying Eqs. 3.22, A-3.7, A-3.8, and A-3.9 to Eqs. A-3.4, A-3.5, and A-3.6, rearranging terms, and expressing in matrix form yields

$$[A] \; \{\dot{\theta}\} = [D] \; \{\hat{P}\} \quad , \tag{A-3.10}$$

where $[A]$ is a 3 x 3 matrix given in Eq. 3.26 (and Appendix A-2), $\{\dot{\theta}\}$ is a 3 x 1 "velocity" vector with $\dot{\theta}_1$, $\dot{\theta}_2$, and $\dot{\theta}_3$ as its members, $[D]$ is a 3 x 3 matrix given below, and $\{\hat{P}\}$ is a 3 x 1 "impulse load" vector with $\hat{P}_1$, $\hat{P}_2$, and $\hat{P}_3$ as its members. The terms of the $[D]$ matrix are

$$D_{11} = D_{12} = D_{13} = -L_1 \cos \theta_1 \quad , \tag{A-3.11}$$

$$D_{21} = D_{31} = D_{32} = 0 \quad , \tag{A-3.12}$$

$$D_{22} = D_{23} = -L_2 \cos \theta_2 \quad , \tag{A-3.13}$$

$$D_{33} = L_3 \cos \theta_3 \ . \tag{A-3.14}$$

For our model, the impulse loads are applied at time zero, and thus impart initial velocities to the model. Because of this, all of the θ's in the [A] and [D] matrices should be replaced by α's, since θ_i equals α_i at time zero.

To non-dimensionalize Eq. A-3.10, apply Eqs. 3.27 thru 3.35 and

$$\hat{P}_i = \frac{\hat{P}_i}{L_1 \sqrt{Km_1}} \ , \quad i = 1, 2, 3 \ , \tag{A-3.15}$$

where the left hand side of Eq. A-3.15 represents the non-dimensional impulse loads, and the right hand side of Eq. A-3.15 represents the model's dimensional parameters and impulse loads.

APPENDIX A-4

COMPUTER CODE LISTING AND USER'S GUIDE

The computer code, which is listed after this user's guide, is written in the WATFIV computer language, and consists of four sections. The first section, the main program, reads in and writes out all of the program's controlling parameters, and calls all of the subroutines so that the numerical integration of the model's equations of motion can be performed. The second section, subroutine EQCONS, reads in and writes out all of the model's parameters, and calculates all of the constants in the [A] matrix and {D} vector of Eq. 3.26. The third section, subroutine NMBETA, performs the numerical integration of the model's equations of motion using the procedure described in section 4.2.c of this study. Finally, the last section, subroutine FITZEQ, calculates the {R} vector of Eq. 4.13, and also calculates the initial velocities for the impulse loads using the equations listed in Appendix A-3.

The order of the input data and the format for the punching of the input data onto the data cards is listed below.

Cards

1   NPROTY
            (I5)

repeat the following cards NPROTY times

2   XM1, XM2, XM3, XM4
            (4D10.7)

3   XL1, XL2, XL3, XL4
            (4D10.7)

4	ALPHA1, ALPHA2, ALPHA3, ALPHA4 (4D10.7)
5	C1, C2, C3, XK (4D10.7)
6	B1, B2, B3 (3D10.7)
7	A, B, C, D (4D10.6)
8	EPSILO, DELTIM, TIMMAX (D8.5, 2D8.3)
9	ICOUNT (I5)
10	LDUMMY, NOPT (I1, 8X, I1)
11 to 11+ICOUNT	P1, P2, P3 (3D10.7)

The definitions of the input parameters listed above are listed below.

Parameter	Definition
NPROTY	number of problem types to be run at one time, each problem type having different model parameter values and/or initial conditions
XMi	mass of bar i, i = 1, 2, 3, 4
XLi	length of bar i, i = 1, 2, 3, 4
ALPHAi	initial angle of bar i, i = 1, 2, 3, 4
Ci	rotational spring coefficient i, i = 1, 2, 3
XK	translational spring coefficient
Bi	damping coefficient i, i = 1, 2, 3

A, B, C, D   initial velocity of bars 1, 2, 3, 4, respectively

EPSILO   error tolerance for use in the Newmark-Beta Method

DELTIM   time step used in the Newmark-Beta Method

TIMMAX   maximum time for which the Newmark-Beta method will be used on a problem

ICOUNT   number of problems for each problem type to be run at one time

LDTYOP   describes the loading; 0 - step; 1 - impulse (read in under LDUMMY)

NOPT   describes how the output will be printed; 1 - all time steps will be printed; 2 - every five time steps will be printed; 3 - only the failure step will be printed

P1, P2, P3   loads P_1, P_2, P_3, respectively ($\hat{P}_1$, $\hat{P}_2$, $\hat{P}_3$, respectively for impulse problems)

COMPUTER CODE LISTING

```
      IMPLICIT REAL*8 (A-H,O-Z)
      COMMON /CONSTA/XL1,XL2,XL3,XL4,ALPHA1,ALPHA2,ALPHA3,ALPHA4,B1,B2,B
     13,C1,C2,C3,XK,T1,T2,T3,T4,T5,T6,T7,T8,T9,T10,T11,T12,T13,T14,T15,T
     216,T17,T18,T19,T20,T21,T22,XL14,XL24,XL34
      COMMON /ERRTIM/ EPSILO,DELTIM,TIMMAX
      COMMON /OPTIOS/LDTYOP,NOPT
      COMMON /PSTORE/P1,P2,P3
      COMMON /VARSTO/R(3),THETA(3),DTHETA(3),DDTHET(3),THETA4,DTHETA4,DDT
     1HE4
C *******************************************************************
C   NPROTY - NUMBER OF PROBLEM TYPES TO BE RUN AT ONE TIME; EACH
C            PROBLEM TYPE HAS DIFFERENT INITIAL CONDITIONS, WHICH
C            REQUIRE GOING THROUGH EQCONS BEFORE RUNNING EACH PROBLEM
C            TYPE
C   A,B,C,D - INITIAL VELOCITIES OF THE FOUR BARS
C   EPSILO - ERROR TOLERANCE FOR USE IN THE NEWMARK BETA METHOD
C   DELTIM - TIME STEP USED IN THE NEWMARK BETA METHOD
C   TIMMAX - MAXIMUM TIME FOR WHICH THE NEWMARK BETA METHOD WILL BE
C            USED ON A PROBLEM
C   ICOUNT - NUMBER OF PROBLEMS FOR EACH PROBLEM TYPE TO BE RUN AT ONE
C            TIME
C   LDTYOP - DESCRIBES THE TYPE OF LOADING : 0 - STEP ; 1 - IMPULSE
C            (READ IN UNDER LDUMMY)
C   NOPT - DESCRIBES HOW THE OUTPUT WILL BE PRINTED : 1 - ALL TIME
C            STEPS WILL BE PRINTED; 2 - EVERY FIVE TIME STEPS WILL BE
C            PRINTED; 3 - ONLY THE FAILURE TIME STEP WILL BE PRINTED
C   THETA1 - ANGLE OF BAR 1 AT ANY TIME
C   THETA2 - ANGLE OF BAR 2 AT ANY TIME
C   THETA3 - ANGLE OF BAR 3 AT ANY TIME
C   THETA4 - ANGLE OF BAR 4 AT ANY TIME
C   DTHET1 - VELOCITY OF BAR 1 AT ANY TIME
C   DTHET2 - VELOCITY OF BAR 2 AT ANY TIME
```

```
C     DTHET3  -  VELOCITY OF BAR 3 AT ANY TIME
C     DTHET4  -  VELOCITY OF BAR 4 AT ANY TIME
C
C     DDTHE1  -  ACCELERATION OF BAR 1 AT ANY TIME
C     DDTHE2  -  ACCELERATION OF BAR 2 AT ANY TIME
C     DDTHE3  -  ACCELERATION OF BAR 3 AT ANY TIME
C     DDTHE4  -  ACCELERATION OF BAR 4 AT ANY TIME
C     THETA   -  DEGREE OF FREEDOM VECTOR ( ANGLE OF BAR AT ANY TIME )
C     DTHETA  -  VELOCITY VECTOR OF THETA
C     DDTHET  -  ACCELERATION VECTOR OF THETA
C     P1  -  LOAD AT JOINT 2
C     P2  -  LOAD AT JOINT 3
C     P3  -  LOAD AT JOINT 4
C     ****************************************************************
      READ(5,10) NPROTY
   10 FORMAT(I5)
      DO 150 JMF=1,NPROTY
      CALL EQCONS
      READ(5,20) A,B,C,D
   20 FORMAT(4D10.6)
      WRITE(6,30) A,B,C,D
   30 FORMAT(////5X,'LISTED BELOW ARE THE GIVEN INITIAL VELOCITIES OF T
     1HE FOUR BARS FOR ALL THE PROBLEMS.'////10X,'DTHETA 1 = ',F10.7//1
     20X,'DTHETA 2 = ',F10.7//10X,'DTHETA 3 = ',F10.7//10X,'DTHETA 4 = '
     3,F10.7)
      READ(5,40) EPSILO,DELTIM,TIMMAX
   40 FORMAT(D8.5,2D8.3)
      WRITE(6,50) DELTIM,TIMMAX
   50 FORMAT(////5X,'LISTED BELOW ARE THE TIME STEP AND THE MAXIMUM TIM
     1E FOR THIS PROBLEM TYPE.'////10X,'DELTIM = ',F8.3//10X,'TIMMAX =
     2 ',F8.3)
      READ(5,60) ICOUNT
   60 FORMAT(I5)
```

```
      READ(5,70) LDUMMY,NOPT
70    FORMAT(I1,8X,I1)
      NCOUNT = 0
80    NCOUNT = NCOUNT+1
      LDTYOP = LDUMMY
      THETA(1) = ALPHA1
      THETA(2) = ALPHA2
      THETA(3) = ALPHA3
      DTHETA(1) = A
      DTHETA(2) = B
      DTHETA(3) = C
      DTHET4 = D
      READ(5,90) P1,P2,P3
90    FORMAT(3D10.7)
      IF(LDTYOP.EQ.1) GO TO 110
      WRITE(6,100) P1,P2,P3
100   FORMAT('1',4X,'LISTED BELOW ARE THE GIVEN LOADS APPLIED TO THE SYS
     1TEM.'////10X,'P1 = ',F10.7//10X,'P2 = ',F10.7//10X,'P3 = ',F10.7)
      GO TO 140
110   WRITE(6,120) P1,P2,P3
120   FORMAT('1',4X,'THIS IS AN IMPULSE PROBLEM. LISTED BELOW ARE THE IN
     1ITIAL VELOCITIES AND THE LOADS WHICH PRODUCED THOSE VELOCITIES.'//
     210X,'THE RESULTS BELOW ARE FOR A PROBLEM WITH INITIAL VELOCITIES A
     3S LISTED BELOW AND WITH NO LOADS APPLIED.'////10X,'P1 = ',F10.7//
     410X,'P2 = ',F10.7//10X,'P3 = ',F10.7)
      CALL FITZEQ
      WRITE(6,130) (I,DTHETA(I),I=1,3)
130   FORMAT(///3(10X,'DTHETA',I2,' = ',F10.7))
140   CALL NMBETA
      IF(NCOUNT.LT.ICOUNT) GO TO 80
150   CONTINUE
      STOP
```

END

```
      SUBROUTINE EQCONS
      IMPLICIT REAL*8 (A-H,O-Z)
      COMMON /CONSTA/XL1,XL2,XL3,XL4,ALPHA1,ALPHA2,ALPHA3,ALPHA4,B1,B2,B
     13,C1,C2,C3,XK,T1,T2,T3,T4,T5,T6,T7,T8,T9,T10,T11,T12,T13,T14,T15,T
     216,T17,T18,T19,T20,T21,T22,XL14,XL24,XL34
C     ************************************************************
C     THIS SUBROUTINE READS IN ALL THE MEMBER AND MODEL PROPERTIES, AND
C     CALCULATES ALL OF THE CONSTANTS IN THE EQUATIONS FOR R(I).
C     ************************************************************
C     ALPHA1 -  INITIAL ANGLE OF BAR 1
C     ALPHA2 -  INITIAL ANGLE OF BAR 2
C     ALPHA3 -  INITIAL ANGLE OF BAR 3
C     ALPHA4 -  INITIAL ANGLE OF BAR 4
C     XM1 -  MASS OF BAR 1
C     XM2 -  MASS OF BAR 2
C     XM3 -  MASS OF BAR 3
C     XM4 -  MASS OF BAR 4
C     XL1 -  LENGTH OF BAR 1
C     XL2 -  LENGTH OF BAR 2
C     XL3 -  LENGTH OF BAR 3
C     XL4 -  LENGTH OF BAR 4
C     B1 -  DAMPING COEFFICIENT AT JOINT 2
C     B2 -  DAMPING COEFFICIENT AT JOINT 3
C     B3 -  DAMPING COEFFICIENT AT JCINT 4
C     C1 -  ROTATIONAL SPRING COEFFICIENT AT JOINT 2
C     C2 -  ROTATIONAL SPRING COEFFICIENT AT JOINT 3
C     C3 -  ROTATIONAL SPRING COEFFICIENT AT JOINT 4
C     XK -  LINEAR SPRING COEFFICIENT
C     ************************************************************
      READ(5,10) XM1,XM2,XM3,XM4
   10 FORMAT(4D10.7)
      READ(5,20) XL1,XL2,XL3,XL4
```

```fortran
   20 FORMAT(4D10.7)
      READ(5,30) ALPHA1,ALPHA2,ALPHA3,ALPHA4
   30 FORMAT(4D10.7)
      READ(5,40) C1,C2,C3,XK
   40 FORMAT(4D10.7)
      READ(5,50) B1,B2,B3
   50 FORMAT(3D10.7)
      WRITE(6,60) XM1,XL1,ALPHA1,XM2,XL2,ALPHA2,XM3,XL3,ALPHA3,XM4,XL4,A
     1LPHA4
   60 FORMAT('1',4X,'LISTED BELOW ARE THE MEMBER PROPERTIES AND THE INIT
     1IAL SHAPE PROPERTIES OF THE MODEL.'//10X,'ALL OF WHICH HAVE BEEN N
     2ON DIMENSIONALIZED.'/////10X,'MASS 1 = ',F10.7,10X,'LENGTH 1 = ',F
     310.7,10X,'ALPHA 1 = ',F10.7//10X,'MASS 2 = ',F10.7,10X,'LENGTH 2 =
     4 ',F10.7,10X,'ALPHA 2 = ',F10.7//10X,'MASS 3 = ',F10.7,10X,'LENGTH
     5 3 = ',F10.7,10X,'ALPHA 3 = ',F10.7//10X,'MASS 4 = ',F10.7,10X,'LE
     6NGTH 4 = ',F10.7,10X,'ALPHA 4 = ',F10.7)
      WRITE(6,70) B1,C1,XK,B2,C2,B3,C3
   70 FORMAT(///10X,'B1 = ',F10.7,10X,'C1 = ',F10.7,10X,'XK = ',F10.7//
     110X,'B2 = ',F10.7,10X,'C2 = ',F10.7,10X,'B3 = ',F10.7,10X,'C3 = '
     2,F10.7)
      CALPH1 = DCOS(ALPHA1)
      CALPH2 = DCOS(ALPHA2)
      CALPH3 = DCOS(ALPHA3)
      CALPH4 = DCOS(ALPHA4)
      XL14 = XL1/XL4
      XL24 = XL2/XL4
      XL34 = XL3/XL4
C     ***************************************************************
C     T - CONSTANTS IN THE A MATRIX AND THE D VECTOR
C     ***************************************************************
      T1 = ((1.0D0/3.0D0)*XM1+XM2+XM3+XM4)*XL1**2
      T2 = (0.5D0*XM2+XM3+XM4)*XL1*XL2
```

```
T3  = (0.5D0*XM3+XM4)*XL1*XL3
T4  = ((1.0D0/3.0D0)*XM2+XM3+XM4)*XL2**2
T5  = (0.5D0*XM3+XM4)*XL2*XL3
T6  = ((1.0D0/3.0D0)*XM3+XM4)*XL3**2
T7  = 0.5D0*XM4*XL1*XL4
T8  = 0.5D0*XM4*XL2*XL4
T9  = 0.5D0*XM4*XL3*XL4
T10 = (1.0D0/3.0D0)*XM4*XL4**2
T11 = XM4*XL1
T12 = XM4*XL2
T13 = XM4*XL3
T14 = XL1/2.0D0
T15 = XL2/2.0D0
T16 = XL3/2.0D0
T17 = XL4/2.0D0
T18 = XL4/3.0D0
T19 = XL1*CALPH1+XL2*CALPH2+XL3*CALPH3+XL4*CALPH4
T20 = ALPHA1-ALPHA2
T21 = ALPHA3+ALPHA2
T22 = ALPHA4-ALPHA3
RETURN
END
```

```
      SUBROUTINE NMBETA
      IMPLICIT REAL*8 (A-H,O-Z)
      COMMON /CONSTA/XL1,XL2,XL3,XL4,ALPHA1,ALPHA2,ALPHA3,ALPHA4,B1,B2,B
     13,C1,C2,C3,XK,T1,T2,T3,T4,T5,T6,T7,T8,T9,T10,T11,T12,T13,T14,T15,T
     216,T17,T18,T19,T20,T21,T22,XL14,XL24,XL34
      COMMON /ERRTIM/ EPSILO,DELTIM,TIMMAX
      COMMON /OPTIOS/LOIYOP,NOPT
      COMMON /VARSTO/R(3),THETA(3),DTHETA(3),DDTHET(3),THETA4,DTHET4,DDT
     1HE4
      DIMENSION D(3),V(3),DIFF(3)
C     ***************************************************************
C     THIS SUBROUTINE USES NEWMARKS-BETA METHOD OF DIRECT INTEGRATION TO
C     SOLVE OUR DIFFERENTIAL EQUATIONS.
C     ***************************************************************
      WRITE(6,10) EPSILO
   10 FORMAT(////5X,"THESE ARE THE RESULTS FROM NMBETA, MY OWN CODING O
     1F THE NEWMARK-BETA METHOD OF DIRECT INTEGRATION SOLUTION TO THIS P
     2ROBLEM."////10X,"THE TOLERANCE IS ",D8.1////12X,"TIME",7X,"ITERA
     3TIONS",10X,"THETA 1",15X,"THETA 2",15X,"THETA 3",15X,"THETA 4"///)
C     ***************************************************************
C     IF THE FOLLOWING CARDS ARE USED IN THE PROGRAM INSTEAD OF THEIR
C     COUNTERPARTS THAT ARE PRESENTLY IN THE PROGRAM, THEN YOU CAN GET
C     THE PRINT OUT OF THE DISPLACEMENTS, THE VELOCITIES, AND THE
C     ACCELERATIONS FOR ALL FOUR BARS.
C     **********
C     PUT THE COMMON /VARCON/ CARD IN THE COMMON LIST FOR NMBETA AND
C     FITZEQ
C     **********
C     COMMON /VARCON/CTHET1,CTHET2,CTHET3,TA,TB,TC
C  10 FORMAT(////5X,"THESE ARE THE RESULTS FROM NMBETA, MY OWN CODING O
C    1F THE NEWMARK-BETA METHOD OF DIRECT INTEGRATION SOLUTION TO THIS P
C    2ROBLEM."////10X,"THE TOLERANCE IS ",D8.1////12X,"TIME",8X,"ITERA
```

```
C     3TIONS',11X,'THETA',17X,'DTHETA',16X,'DDTHET')
C     **********
C     PUT THE DDTHE4 CARD RIGHT BEFORE THE 90 WRITE(6,100) CARD
C     **********
      DDTHE4 = XL14*DDTHET(1)*CTHET1/TA+XL24*DDTHET(2)*CTHET2/TA-XL34*DD
     1THET(3)*CTHET3/TA+TB+TC
   90 WRITE(6,100) TIME,K,(THETA(I),DTHETA(I),DDTHET(I),I=1,3),THETA4,DT
     1HET4,DDTHE4
  100 FORMAT(////10X,F7.3,10X,I4,10X,D17.10,2(10X,D17.10)//2(41X,D17.10
     1,2(10X,D17.10)//),41X,D17.10,2(10X,D17.10))
C     *****************************************************************
      TIME = 0.0D0
      CALL FITZEQ
      DO 20 I=1,3
      DDTHET(I) = R(I)
   20 CONTINUE
      K = 0
      IF(NOPT.EQ.2) NPROUT = 5
      GO TO 70
   30 K =0
   40 K = K+1
      DO 50 I=1,3
      THETA(I) = D(I)+0.25D0*DELTIM**2*DDTHET(I)
      DTHETA(I) = V(I)+0.5D0*DELTIM*DDTHET(I)
   50 CONTINUE
      J = 0
      CALL FITZEQ
      DO 60 I=1,3
      DIFF(I) = DABS(DDTHET(I)-R(I))
      IF(DIFF(I).LE.EPSILO) GO TO 60
      DDTHET(I) = R(I)
      J = J+1
```

```
   60 CONTINUE
      IF(J.GT.0) GO TO 40
      IF(NOPT.EQ.2) NPROUT = NPROUT+1
   70 DO 80 I=1,3
      D(I) = THETA(I)+DELTIM*DTHETA(I)+0.2500*DELTIM**2*DDTHET(I)
      V(I) = DTHETA(I)+0.5D0*DELTIM*DDTHET(I)
   80 CONTINUE
      GO TO (90,110,120),NOPT
   90 WRITE(6,100) TIME,K,(THETA(I),I=1,3),THETA4
  100 FORMAT(10X,F8.3,8X,I4,3X,4(5X,D17.10)//)
      NOPTFN = 2
      GO TO (140,140,130),NOPT
  110 IF(NPROUT.LT.5) GO TO 140
      NPROUT = 0
      GO TO 90
  120 IF(THETA(I).LT.0.0D0.AND.THETA4.LT.0.0D0) GO TO 90
      NOPTFN = 1
      GO TO 140
  130 TIME = 2.0D0*TIMMAX
  140 CONTINUE
      TIME = TIME+DELTIM
      IF(TIME.LE.TIMMAX) GO TO 30
      IF(NOPTFN.EQ.1.AND.NOPT.EQ.3) WRITE(6,150) TIMMAX,K,(THETA(I),I=1,
     13),THETA4
  150 FORMAT(10X,F8.3,8X,I4,3X,4(5X,D17.10)////38X,'FROM TIME = 0.000 T
     10 THE GIVEN TIME,'//39X,'THETA 1 AND THETA 4 ARE NEVER NEGATIVE SI
     2MULTANEOUSLY.')
      RETURN
      END
```

```
      SUBROUTINE FITZEQ
      IMPLICIT REAL*8 (A-H,O-Z)
      COMMON /CONSTA/XL1,XL2,XL3,XL4,ALPHA1,ALPHA2,ALPHA3,ALPHA4,B1,B2,B
     13,C1,C2,C3,XK,T1,T2,T3,T4,T5,T6,T7,T8,T9,T10,T11,T12,T13,T14,T15,T
     216,T17,T18,T19,T20,T21,T22,XL14,XL24,XL34
      COMMON /OPTIOS/LDIYOP,NOPT
      COMMON /PSTORE/P1,P2,P3
      COMMON /VARSTO/R(3),THETA1,THETA2,THETA3,DTHET1,DTHET2,DTHET3,DDTH
     1ET(3),THETA4,DTHET4,DDTHE4
C     ***************************************************************
C        THIS SUBROUTINE CALCULATES R(I).
C     ***************************************************************
      STHET1 = DSIN(THETA1)
      STHET2 = DSIN(THETA2)
      STHET3 = DSIN(THETA3)
      CTHET1 = DCOS(THETA1)
      CTHET2 = DCOS(THETA2)
      CTHET3 = DCOS(THETA3)
      TC1 = XL14*DTHET1*CTHET1+XL24*DTHET2*CTHET2-XL34*DTHET3*CTHET3
      TA1 = XL14*STHET1+XL24*STHET2-XL34*STHET3
      THETA4 = DARSIN(TA1)
      STHET4 = DSIN(THETA4)
      CTHET4 = DCOS(THETA4)
      TA = CTHET4
      TA3 = TA**3
      DTHET4 = TC1/TA
      TB = (-XL14*DTHET1**2*STHET1-XL24*DTHET2**2*STHET2+XL34*DTHET3**2*
     1STHET3)/TA
      TC = TA1*TC1**2/TA3
C     ***************************************************************
C        PDIJ - PARTIAL DERIVATIVE OF I WITH RESPECT TO J
C     ***************************************************************
```

```
      RP1 = R11*P1+R12*P2+R13*P3
      RP2 = R21*P1+R22*P2+R23*P3
      RP3 = R31*P1+R32*P2+R33*P3
      DTHET1 = RP1
      DTHET2 = RP2
      DTHET3 = RP3
      P1 = 0.0D0
      P2 = 0.0D0
      P3 = 0.0D0
      LDTYOP = 2
      GO TO 20
   10 CONTINUE
      DT1SQ = DTHET1**2
      DT2SQ = DTHET2**2
      DT3SQ = DTHET3**2
      DT4SQ = DTHET4**2
C *********************************************************************
C     TV - REPEATED VARIABLE TERMS IN THE D VECTOR
C *********************************************************************
      TV1 = XL1*CTHET1+XL2*CTHET2+XL3*CTHET3+XL4*CTHET4
      TV2 = T20-(THETA1-THETA2)
      TV3 = T21-(THETA3+THETA2)
      TV4 = T22-(THETA4-THETA3)
      TV5 = DTHET1-DTHET2
      TV6 = DTHET3+DTHET2
      TV7 = DTHET4-DTHET3
      D1 = -T2*DT2SQ*SN12-T3*DT3SQ*SN13+T7*SN14*(-DT4SQ-DT1SQ*PDD4D1)+T8
     1*SN24*(-DT2SQ*PDD4D1)+T9*SN34*(DT3SQ*PDD4D1)+T7*CS14*(TB+TC)-T10*P
     2DD4D1*(TB+TC)+C1*TV2+C3*TV4*PD41+XK*(TV1-T19)*(XL1*STHET1+XL4*STHE
     3T4*PD41)-(P1+P2+P3)*XL1*CTHET1-B1*TV5-B3*TV7*PDD4D1
      D2 = T2*DT1SQ*SN12-T5*DT3SQ*SN23+T7*SN14*(-DT1SQ*PDD4D2)+T8*SN24*(
     1-DT4SQ-DT2SQ*PDD4D2)+T9*SN34*(DT3SQ*PDD4D2)+T8*CS24*(TB+TC)-T10*PD
```

```
2D4D2*(TB+TC)-C1*TV2+C2*TV3+C3*TV4*PD42+XK*(TV1-T19)*(XL2*STHET2+XL
34*STHET4*PD42)-(P2+P3)*XL2*CTHET2+B1*TV5-B2*TV6-B3*TV7*PDD4D2
      D3 = -T3*DT1SQ*SN13-T5*DT2SQ*SN23+T7*SN14*(-DT1SQ*PDD4D3)+T8*SN24*
1(-DT2SQ*PDD4D3)+T9*SN34*(-DT4SQ+DT3SQ*PDD4D3)-T9*CS34*(TB+TC)-T10*
2PDD4D3*(TB+TC)+C2*TV3-C3*TV4*(1.0D0-PD43)+XK*(TV1-T19)*(XL3*STHET3
3+XL4*STHET4*PD43)+P3*XL3*CTHET3-B2*TV6-B3*TV7*(PDD4D3-1.0D0)
      R(1) = BMAT11*D1+BMAT12*D2+BMAT13*D3
      R(2) = BMAT21*D1+BMAT22*D2+BMAT23*D3
      R(3) = BMAT31*D1+BMAT32*D2+BMAT33*D3
   20 CONTINUE
      RETURN
      END
```
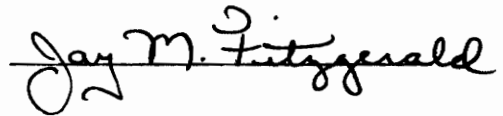
VITA

Jay Michael Fitzgerald was born on March 18, 1954, in Arlington, Virginia. He attended Bishop Dennis J. O'Connell High School and graduated in June, 1972. He entered Virginia Polytechnic Institute and State University in September, 1972, studying for a degree in Civil Engineering. He graduated in June, 1976 with a Bachelor of Science Degree in Civil Engineering, specializing in Structures.

The author began his graduate studies at Virginia Polytechnic Institute and State University in September, 1976, as a recipient of a Graduate Teaching Assistantship, studying for a Master of Science Degree in Civil Engineering (Structural).

The author is an associate member of the American Society of Civil Engineers.

DETERMINATION OF INTERACTION CURVES
FOR THE STABILITY OF A THREE DEGREE OF FREEDOM,
SHALLOW ARCH MODEL UNDER MULTIPLE DYNAMIC LOADS

by

Jay M. Fitzgerald

(ABSTRACT)

The primary purpose of this study is to determine stability boundaries (interaction curves) for a three degree of freedom, shallow arch model under multiple dynamic loads. The model consists of four rigid bars connected by frictionless pins, with rotational springs and dashpots at the three interior joints, and a translational spring at the right hand exterior joint. Three independent loads (P_1, P_2, P_3) are applied to the model, one at each of the three interior joints.

The model's equations of motion, which are derived from Lagrange's equations of motion, are numerically integrated, using the Newmark-Beta method ($\beta = 1/4$), to determine the buckling loads. The buckling loads are those loads for which the buckling criterion, the end bars simultaneously below the horizontal, is satisfied.

The interaction curves and buckling loads are determined for a parabolic arch with damping under step loads, a parabolic arch without damping under step loads, an eccentric arch without damping under step loads, a parabolic arch without damping under impulse loads, and an